Properties and use of SO_2 for the Hybrid Sulfur Process

Andries J. Krüger

2011

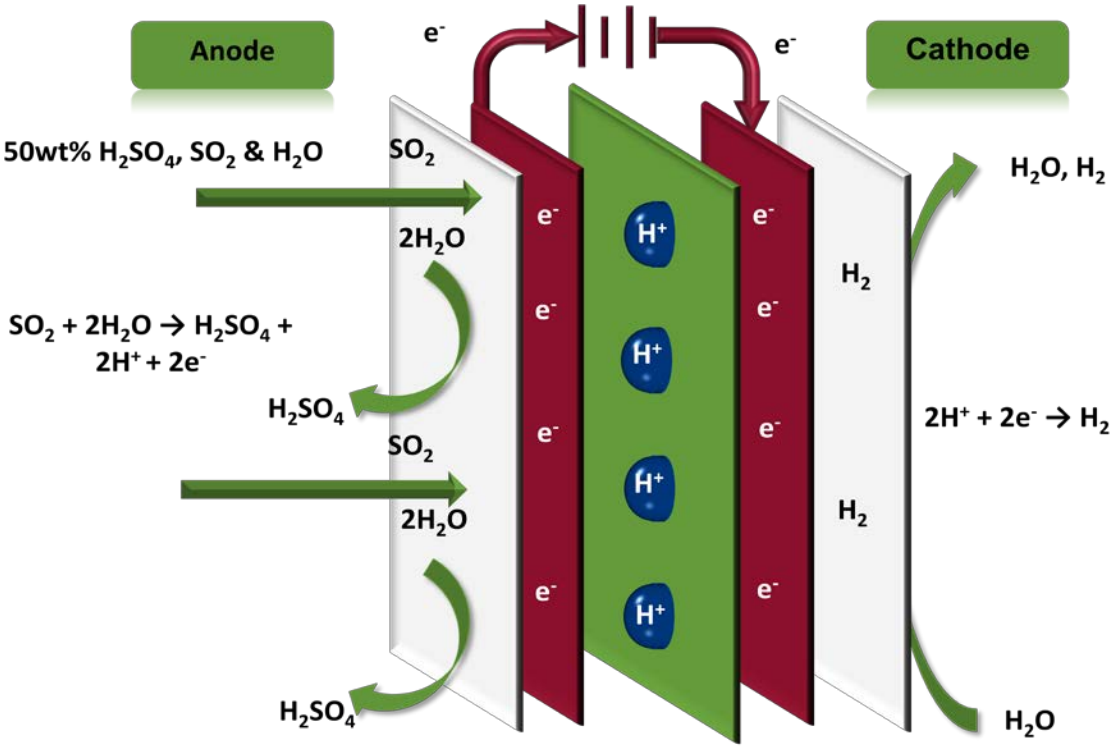

Supervisor: Professor Henning M. Krieg

Assistant Supervisor: Dr Cobus J. Kriek

HySA Infrastructure Hydrogen South Africa
science & technology Department Science and Technology REPUBLIC OF SOUTH AFRICA
CRB CHEMICAL RESOURCE BENEFICIATION CHEMIESE HULPBRONVEREDELING
NORTH-WEST UNIVERSITY YUNIBESITI YA BOKONE-BOPHIRIMA NOORDWES-UNIVERSITEIT POTCHEFSTROOM CAMPUS

Properties and use of SO_2 for the Hybrid Sulfur Process

Andries J Krüger

13061631

Dissertation submitted in partial fulfilment of the requirements for the degree Master of Science in chemistry at the Potchefstroom campus of the North-West University

Supervisor: Prof. H. M. Krieg

Assistant-Supervisor: Dr. R.J. Kriek

May 2011

NORTH-WEST UNIVERSITY
YUNIBESITI YA BOKONE-BOPHIRIMA
NOORDWES-UNIVERSITEIT
POTCHEFSTROOM CAMPUS

Acknowledgements

I would like to express my sincerest gratitude towards:

- My Heavenly Father for giving me the ability, patience and determination to complete this research.

- My wife, Annike Krüger, for keeping me motivated for the entire duration of my studies, and for showing love and understanding the late nights and early mornings spent in the laboratory to complete experimental work.

- My parents for giving me the opportunity to further my academic career and for the continuous support and motivational talks.

- Professor Henning M. Krieg, Membrane Technology, for the tireless work helping me put my newly acquired knowledge to paper. The moral support and talks on everything other than chemistry were greatly appreciated.

- Dr. R. J. Kriek, Platinum Research Group, for helping me define my experimental work as well as all the fruitful discussion.

- Simon G. Stone, Project Manager at Giner Electrochemical Systems, LLC (USA), for the constant and intensive guidance with regards to almost each and every aspects pertaining to the electrolysis setup and other fields which made my learning curve much shorter.

- Professor Hein Neomagus, Chemical Engineering Department at North-West University, for always finding time to help with the detailed work needed for the solubility part of my research.

- Dr. Jochen A. Kerres and Andreas Chromick, University of Stuttgart – Germany, for hosting us over a two week period while discussing possible future collaborations and supplying us with their latest PBI based membranes (not added in this study due to time constrains).

- Dr. L. R. Tiedt at the Laboratory of Electron Microscopy, North-West University, for helping with SEM images and EDX analysis.

- Mr. Jan Kroeze and Adrian Brock, Technicians of the Engineering Department – North-West University, for helping me build the solubility setup, the early morning coffee and talks ensured a great start to each day.

- Johan Broodryk, Instrument-making – North West University, for building the electrolysis setup and making all the extra alterations over the course of this study.

- Mrs Linda Mey, secretary at Chemical Research Beneficiation – North-West University, for doing my administration regarding payments and deliveries with great enthusiasm.

- HySA Infrastructure Centre of Competence, Department of Science and Technology, for the funding of this project and making it possible for me to attend the *Advances in Polymer Electrolyte Membrane Fuel Cell Systems 2009, Asilomar Conference Grounds, USA* conference.

- Chemical Research Beneficiation, North West University, Potchefstroom Campus for the use for the use of their laboratories (Membrane Technology hall) for both the solubility and electrolyser setups.

- DFG/NRF Research cooperation programme (UID: 70720) for the much appreciated financial support regarding visits to the University of Stuttgart, Germany.

- My colleagues and thus friends for all the interesting times spent in the labs, much needed coffee breaks, social gatherings and advice when my work was getting the better of me.

Abstract

An increased pressure on non-pollutant renewable energy supplies has driven research on alternative energy sources and production methods. Within the H_2 economy one of the favourite alternative processes is the sulfur-based thermochemical cycles producing oxygen and hydrogen from water. The Hybrid Sulfur process (HyS) is one such process and uses an external heat source to thermally decompose H_2SO_4 into SO_2, O_2 and H_2O. The O_2 is removed while the SO_2 and H_2O are chemically converted to H_2SO_4, protons and electrons using a Pt based catalyst coated onto a proton exchange membrane (PEM). The protons diffuse through the membrane and recombine with the electrons supplied by an electrical circuit to produce H_2. This electrolysis step theoretically needs only 0.158V, which is significantly less than that needed by conventional water electrolysis (1.23V). The initial feed composition for the HyS electrolysis step was 50wt% H_2SO_4 saturated with SO_2.

To establish the HyS technology in SA, this study entailed i) the design, building and characterization of a setup for the experimental determination of the SO_2 solubility in 50wt% H_2SO_4 at elevated temperatures and pressures and ii) the building of a working SO_2 electrolysis setup with subsequent initial testing of commercially available membrane electrode assemblies consisting of a PEM covered with suitable catalyst.

SO_2 solubility in 50wt% H_2SO_4 was measured as a function of temperature and pressure ranging from 30 – 80^{o}C and 0 – 10 bar. From the SO_2 solubility measurements, it became clear that the maximum amount of SO_2 soluble in 50wt% H_2SO_4 decreased with increased temperature, from 12.8 gSO_2/100g H_2SO_4 at 30^{o}C to 8gSO_2/100g H_2SO_4 at 80^{o}C. Increased system pressure at 80^{o}C had no noticeable advantage over lower pressures obtained at 30^{o}C with regards to the solubility. As a control, the SO_2 solubility in water was determined, which yielded results that were comparable to literature data, which verified the suitability of the designed setup to measure SO_2 gas solubility in liquids.

The SO_2 electrolysis was performed by supplying the anode of the cell with SO_2 gas, while the water was fed to the cathode using graphite plates as flow fields. Initial experimental work was done at ambient pressures on the anode (SO_2 gas-fed) and cathode (water-fed) after which the water pressure was increased from ambient to 1 bar. Various parameters were evaluated for SO_2 electrolysis at ambient conditions, including operating temperature, membrane thickness and catalyst loading. The operating temperature was increased from 50°C to 80°C which resulted in a significant voltage improvement from 0.78V to 0.64V at 300mA/cm^2. Operating the cell with thinner membranes (86 vs 170µm) also resulted in an improved overall cell performance, while the catalyst loading (1 vs 0.5mgPt/cm^2) had a negligible effect on the operating voltage. SEM images and EDX analysis were performed on the best performing MEA (N1135) which showed that no degradation of the MEA had occurred.

Keywords: *SO_2 solubility, Sulfuric acid, Hybrid Sulfur Process, SO_2 electrolysis, Membrane electrode assembly, Proton exchange membrane, Platinum catalyst.*

Opsomming

In die lig van die toename in die wêreld se energieverbruik word alternatiewe energie-bronne en-prosesse al hoe meer die onderwerp van vandag se navorsing. Binne die waterstofekonomie word die swawel-gebaseerde termochemiese prosesse wat suurstof en waterstof uit water vervaardig as die mees ekonomies vatbare prosesse beskou. Een so 'n proses, die Hibried Swawel (HyS) proses, gebruik eksterne energie (in die vorm van hitte) om H_2SO_4 termies te ontbind na SO_2, O_2 en H_2O. Nadat die suurstof verwyder is, kan die SO_2 en water oor 'n platinumgebaseerde katalisator, wat met 'n protongeleidende membraan bedek is, wat as 'n membraan elektrode samestelling bekend staan, chemies na H_2SO_4 protone (H^+) en elektrone (e^-) omgeskakel word. Die protone diffundeer deur die membraan om weer met die elektrone wat deur 'n eksterne elektriese baan verskaf word te verbind om H_2 te lewer. Die elektrolitiese proses het teoreties slegs 0.158V nodig om die reaksie te laat plaasvind wat beduidend laer is as konvensionele water elektrolise wat 1.23V benodig. Die aanvanklike- voersamestelling vir die elektroliesestap was 50% gewig H_2SO_4 wat met SO_2 gas versadig is.

Om die tegnologie in SA te ontwikkel, het die studie die i) ontwerp, bou en karakterisering van 'n eksperimentele opstelling om die oplosbaarheid van SO_2 gas in H_2SO_4 (50 gewig persentasie) eksperimenteel by verhoogde temperature en druk te bepaal en ii) die bou van 'n werkende SO_2 elektrolise opstelling en die toetsing van kommersieel beskikbare membraanelektrodesamestellings behels.

Die oplosbaarheid van SO_2 is as funksie van temperatuur (30^{o}C tot 80^{o}C) en druk (0 – 10 bar) is in 50% gewig H_2SO_4 gemeet. Dit het duidelik geword dat die SO_2 oplosbaarheid in H_2SO_4 gedaal het soos die temperatuur vanaf 30^{o}C (12g SO_2/100g H_2SO_4) na 80^{o}C (8g SO_2/100gH_2SO_4) verhoog is. 'n Verhoogde druk by 80^{o}C het geen noemenswaardige effek op die oplosbaarheid getoon nie

aangesien die SO_2 oplosbaarheid hoër was by 30°C, met 'n maksimum druk van 3 bar, teenoor die 10 bar druk wat bereik is by 80°C.

As 'n kontrole eksperiment is aparte oplosbaarheidmetings in water (by 40°C) gedoen, wat getoon het dat die opstelling genoegsame akkuraatheid het ten opsigte van die meting van SO_2 gas oplosbaarheid in vloeistowwe.

Die SO_2 elektrolise is uitgevoer deur SO_2 gas, aan die anode van die membraanelektrodesamestelling te voorsien terwyl water aan die katode m.b.v. grafietvloeivelde voorsien is. Die sel is eers by atmosferiese druk bedryf waarby verskeie aspekte, o.a. temperatuur, membraandikte en die hoeveelheid katalisator geevalueer is. Deur die seltemperatuur te verhoog van 50°C na 80°C het die spanning (V) verlaag van0.78V na 0.64V by 300mA/cm^2. Dunner membrane (86µm) het ook beter effektiwiteit getoon as dikker membrane (170µm). Die hoeveelheid katalisator is (tussen 1mgPt/cm^2 tot 0.5mgPt/cm^2) gevarieer by 80°C en membraandikte van122.5µm, maar geen noemenswaardige verskil kon gemeet word nie. SEM foto's en EDX- analises is op die membraan met die beste effektiwiteit (N1135) uitgevoer. Geen degradasie van die membraan was sigbaar na SO_2 elektrolise nie.

Kernwoorde: *SO_2 oplosbaarheid, Swaelsuur, Hibried Swael Proses, SO_2 elektrolise, Membraanelektrodesamestelling, Protongeleidende membraan, Platinum katalisator.*

Table of Content

Chapter 2 – SO_2 Solubility in Sulfuric acid

Chapter 3 – SO_2 Electrolyser research and development for the HyS Process

Chapter 4 – Evaluation

Appendix A – Hazard and operatibility study on the SO_2 solubility in conc. H_2SO_4 setup

Appendix B – Hazard and operatibility study on the SO_2 Electrolyser setup

List of Tables

Chapter 3 – SO_2 Electrolyser research and development for the HyS process

Appendix A – Hazard and operatibility study on the SO_2 solubility in conc. H_2SO_4 setup

List of Figures

Chapter 1 – Introduction

Chapter 2 – SO_2 solubility in Sulfuric acid

Chapter 3 – SO_2 Electrolyser research and development for the HyS Process

CHAPTER 4 – Evaluation

Appendix A – Hazard and operatibility study on the SO_2 solubility in conc. H_2SO_4 setup

Appendix B – Hazard and operatibility study on the SO_2 Electrolyser setup

Nomenclature

LIST OF ABBREVIATIONS

EDX	Energy-dispersive X-ray
HyS	Hybrid Sulfur Process
H_2SO_4	Sulfuric Acid
SO_2	Sulfur Dioxide / Sulphur Dioxide
SO_3^{2-}	Sulphite Ion
PEM	Proton Exchange Membrane
MEA	Membrane Electrode Assembly
GDL	Gas Diffusion Layer
UV	Ultra – Violet Light
Wt%	Weight percentage between H_2SO_4 and water
SS316	Stainless Steel 316
HaZop	Hazard and Operatibility Study
PTFE	Polytetrafluoroethylene / Teflon
EPDM	Ethylene Propylene Diene Monomer
sPEEK	Sulfonated Polyetheretherketone
N**11**7	Nafion membrane (**11**00 EW, and 7 mils thick)
EW	Equivalent Weight
Mils	Thickness of membrane (1 mils = 24.5µm)
SEM	Scanning Electron Microscopy

LIST OF SYMBOLS

n_{SO_2}	Molar amount of SO_2	(mol)
n_i	Initial amount of N_2 and vapour pressure of liquid	(mol)
n_{eq}	SO_2 Molar amount at equilibrium	(mol)
n_{abs}	Molar amount of SO_2 absorbed by H_2SO_4	(mol)
P_{B2}	Pressure in SO_2 compartment (B2)	(bar)
P_{eq}	Pressure at equilibrium	(bar)
P_{B3}	Pressure in H_2SO_4 compartment (B3)	(bar)
V_{B2}	Volume occupied by SO_2 (B2)	(m^3)
$V_{B2}+V_{B3}$	Volume of entire system	(m^3)
V_{B3}	Volume of H_2SO_4 compartment (B3)	(m^3)
$z_{T,P}$	Compressibility factor	(-)
B	Compressibility coefficient	($m^3.mol^{-1}$)
R	Ideal gas law constant	(8.314 $J.K^{-1}.mol^{-1}$)
T	Temperature	(Kelvin)
P_{eq}^{calc}	Pressure drop calculated	(bar)
P_{eq}^{exp}	Pressure drop experimentally observed	(bar)

CHAPTER 1

Introduction and problem statement

1.1 Background

Traditional energy sources such as natural gas, coal and oil are non renewable and currently supply the majority of the world's energy demands. The processing of these sources (natural gas reforming, coal gasification and oil refining), to yield energy, produces various known pollutants and with global pollution awareness increasing each year, alternative renewable clean fuels are actively sought. A wide range of clean (no carbon footprint) and/or renewable alternative energy sources have been suggested to replace these traditional sources, which include wind, solar, hydro-electrical, biomass and, although they are not processes that use a renewable source, water electrolysis and thermo-chemical processes. Although water electrolysis and thermo-chemical processes both use a non-renewable energy source (H_2O) to produce hydrogen fuel, the water based processes are generally seen as alternative clean energy processes. In thermo-chemical processes, both thermal energy and chemical reactions are used in a cyclic system to produce hydrogen and oxygen from water, while all other reactants are recycled. The Hybrid Sulfur (HyS) thermo-chemical process for the production of hydrogen fuel was chosen as research area for this study. This process entails a common (to all sulfur based thermo-chemical processes) sulfuric acid decomposition step, with subsequent separation of oxygen from the products and feeding of sulfuric acid saturated with SO_2 gas over the anode of a SO_2 electrolyser to produce hydrogen. The electrolyser efficiency is partly a function of the amount of SO_2, i.e. the amount dissolved in the acid (available for the reaction). While some research, especially in the US, has been conducted on SO_2 electrolysis, much information is still required for the optimisation and evaluation of the process.

1.1.1 Traditional Energy Sources

As the world's focus shifts from the traditional energy sources like fossil fuels (carbon containing materials) to clean renewable energy sources due to pollution and future availability concerns; new inventive ways for energy supply are being investigated. Popular traditional fossil fuel energy production methods include natural gas reforming, coal gasification and oil refining. These methods all require a fuel, which is non renewable, to be processed into usable products.

1.1.1.1 Natural gas reforming

Even though pollution is of great concern, natural gas reforming (or steam methane reforming, SRM) is still the preferred method for energy generation, producing some 50% of the worlds energy demand[1]. During this process, natural gas (hydrocarbons) is burned with oxygen in the presence of steam. It is for this reason that the process is also referred to as steam reforming. Equation *(1.1)* shows the generalized stoichiometric equation.

$$C_nH_m + nH_2O \rightarrow nCO + \left(\frac{n+m}{2}\right)H_2 \qquad (1.1)$$

Highly poisonous CO gas is produced along with the H_2 product. The water-shift reaction *(1.2)* is introduced into the cycle to lower the CO gas concentration to produce CO_2 and more H_2.

$$CO + H_2O \rightarrow CO_2 + H_2 \qquad (1.2)$$

While this step is necessary to avoid high concentrations of CO gas, CO_2 a well-known pollutant, is produced. It is this fact that makes natural gas reforming a temporary energy solution, in spite of the fact that this process with its 86% efficiency remains highly cost-effective[2].

1.1.1.2 Coal Gasification

A similar process is coal gasification *(1.3)*, which produces some 20% of the world's energy demands by burning coal with oxygen in the presence of steam[1]. In the second step the water-shift reaction *(1.2)* is once again used to convert the CO to CO_2 with the subsequent production of H_2. This process therefore also produces the syn gas *(1.2)* mixture found in natural gas reforming while using only a different fuel. It should be noted that when comparing *(1.1)* and *(1.3)*, natural gas reforming produces a H_2:CO_2 ratio of 1:2, whereas coal gasification produces a ratio of 1:1.

$$C + H_2O \rightarrow CO + H_2 \qquad (1.3)$$

The raw coal with varying moisture content is initially dried to a moisture content of 2%. This dried coal is then gasified in the presence of O_2 and steam producing a mixture of gasses including CO, H_2, H_2S, SO_x and NO_x. The product gas is then cleaned to extract only CO and H_2. The water shift reaction is used to convert the CO to CO_2. Although this process is effective, it does not remove all the CO

from the stream. Methanation processes, such as the Fischer-Tropsch process, are used to convert the remaining CO into usable fuels as shown in equation *(1.4)*.

$$(2n+1)H_2 + nCO \rightarrow C_nH_{2n+1} + H_2O \qquad (1.4)$$

Thermodynamic studies showed that the overall efficiency for the coal gasification process can reach 59%[4]. The coal gasification process might be practically easier than natural gas reforming, but lower efficiency keeps it at the second place in terms of world energy supplies.

1.1.1.3 Oil refining

Oil refining supplies about 30% of the energy used in the global market[2]. While the process of converting crude oil into usable products doesn't directly add to pollution, the use of these products does. Typical products formed with oil refining are gasoline, kerosene, diesel oil and fuel oils. These products (Figure 1.1) are obtained by sending the crude oil through a furnace and separating the obtained products. All these gas products have different boiling points which can easily be separated by fractional distillation as shown in Figure 1.1. The separated products, for example gasoline can then be catalytically converted into different grades such as high and low octane gasoline. With the constant increase in oil prices and political issues decreasing the stability of supply of this energy source for the future, it is however advisable to find suitable alternatives.

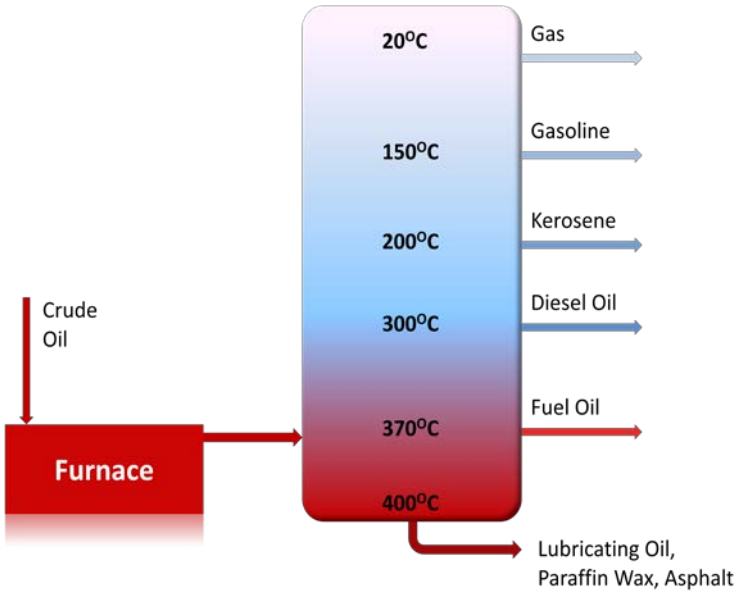

Figure 1.1 : Oil refining via a fractional distillation process.

Although these traditional methods of energy production are well-established and researched, they provide "pollutant" energy which makes them temporary solutions for the future. Factors such as climate change, CO_2 emissions, supply security and increasing world energy demands will force a shift towards clean and renewable energy sources. However, in spite of the disadvantages of these fossil fuel energy sources, they remain well established and cost effective, while developing competitive pollutant free energy source will be difficult and expensive. One such route, which might be both efficient and cost effective, entails the use of thermo-chemical processes to produce hydrogen as energy source.

1.1.2 Thermo-chemical Processes

Hydrogen is thought to be one of the most important energy carriers for the future[3]. Unfortunately, H_2, unlike coal, is a secondary energy source meaning that H_2 must be produced as it is not naturally occurring in adequate quantities. Research is thus needed to evaluate all possible hydrogen production methods, past and present to ensure that the most suitable production method is chosen for the future. This will entail evaluating all parameters including cost, practicality, efficiency and materials.

Apart from the methods described in Section 1.1, some of the established clean methods for the production of hydrogen include water electrolysis, wind, solar or hydro-electrical energy. Although water electrolysis requires water, which, while abundant, is not a renewable energy supply, it produces highly pure hydrogen without producing pollutants. Furthermore, it is a well-established process which has been studied extensively[4].

The electrolysis of liquid water[5] is achieved by splitting water into gaseous oxygen, protons and electrons over a precious metal catalyst (Pt) according to equation *(1.5)*. The protons diffuse through a proton exchange membrane (PEM) to recombine with the produced electrons over another catalyst, which migrates through an external circuit, to produce hydrogen *(1.6).* The theoretical voltage input for this conversion is 1.229V but due to ohmic resistance of the electrolyser the operational voltage varies between 1.5 – 2V for single cells.

$$H_2O \rightarrow 0.5O_2 + 2H^+ + 2e^- \qquad (1.5)$$

$$2H^+ + 2e^- \rightarrow H_2 \qquad (1.6)$$

Water electrolysis can be achieved under various conditions, for example low temperature water electrolysis versus high temperature and pressure electrolysis. Although low temperature water electrolysis produces high purity hydrogen, it has a lower efficiency compared to other production methods such as high temperature steam electrolysis and thermo-chemical processes. Other components can be added to the water electrolysis to improve efficiency, for example by adding SO_2 in the hybrid sulfur process (HyS) the reaction potential is reduced[6].

The U.S. Department of Energy (DOE) launched a Nuclear Hydrogen Initiative (NHI) under the Department of Nuclear Energy (DOE-NE) to research hydrogen production methods. This programme was established to improve the economic viability of hydrogen production technologies. A number of possible technologies were identified and after a screening process, the most probable technologies were identified. One of the front-runner technologies entailed using a thermo-chemical production process. Thermo-chemical processes chemically convert a hydrogen source to pure hydrogen using an external heat source[7]. Similar to normal water electrolysis, hydrogen and oxygen are produced from water, while any additional chemicals used are recycled.

A thermo-chemical hydrogen production method that exceeds the efficiency, or reduces the cost, of previous methods, must meet specific requirements. These include, for example, cost and availability of reactants. Non-toxic materials will facilitate disposal and decrease the overall risk factor. Similarly, any cycle with low or controllable side reactions, which will simplify the overall process, will be beneficial. Low maintenance and the durability of materials will increase effectiveness, while lowering maintenance costs. In the next section the two favored thermo-chemical processes i.e. the sulfur iodine cycle and the hybrid sulfur process, will briefly be illustrated.

1.1.2.1 Sulfur iodine process

While the sulfur iodine (SI) process does not contain an electrochemical step in the cycle, it has the potential to produce low-cost and clean hydrogen. In this process, hydrogen is produced via the Bunsen reaction where sulfur dioxide is reacted with water in the presence of iodine to produce sulfuric acid (H_2SO_4) and hydroiodic acid (HI) via reaction *(1.7)* as shown in Figure 1.2.

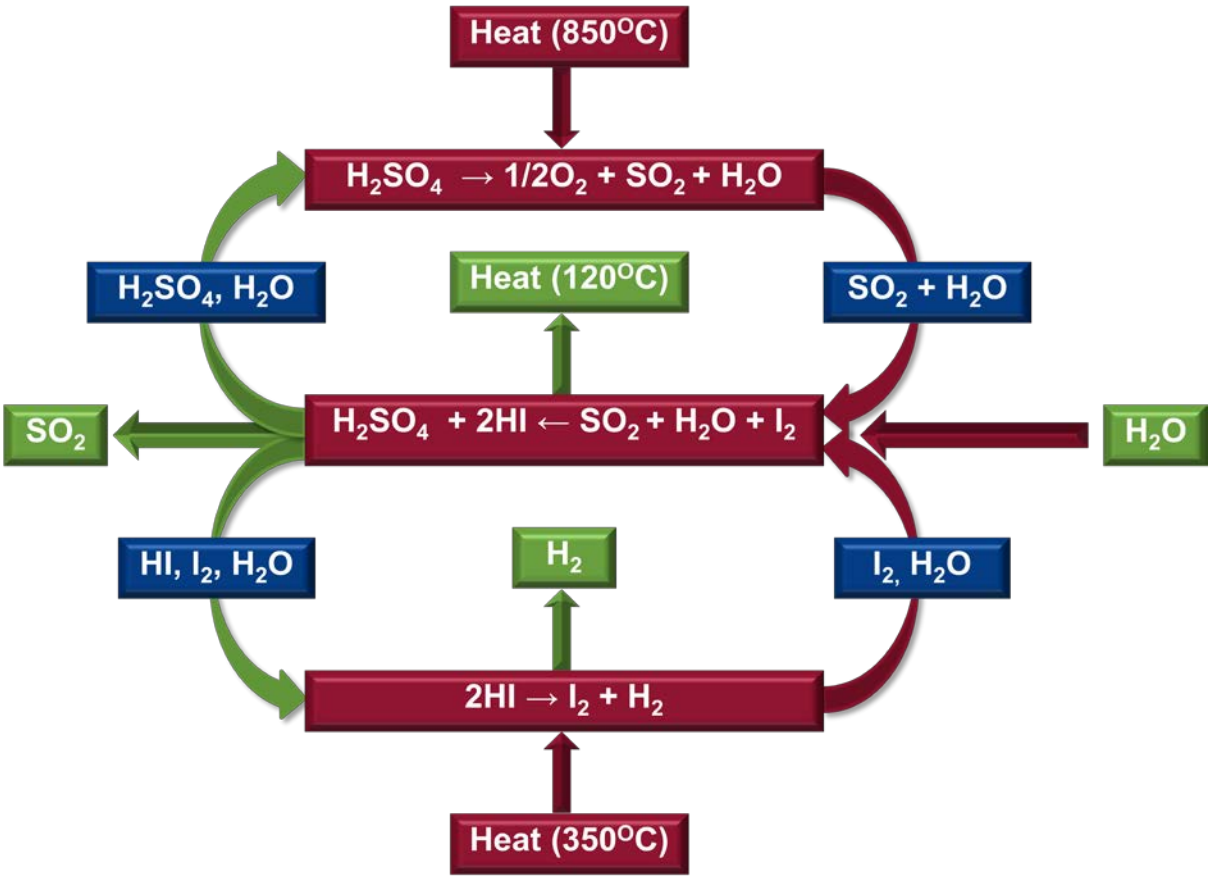

Figure 1.2 : SI thermo-chemical cycle for H_2 production[8].

After the sulfuric acid and hydroiodic acid have been separated, the sulfuric acid is decomposed over a catalyst to SO_2, O_2 and water *(1.8)* while the HI is converted to H_2 and I_2 via a second catalyst reaction *(1.9)*[9].

$$SO_2 + I_2 + H_2O \xrightarrow{120^oC} H_2SO_4 + 2HI \qquad (1.7)$$

$$H_2SO_4 \xrightarrow{850^oC} SO_2 + 0.5O_2 + H_2O \qquad (1.8)$$

$$2HI \xrightarrow{350-450^oC} H_2 + I_2 \qquad (1.9)$$

After oxygen is separated from the H_2SO_4 decomposition step, the water and SO_2 can be recycled back to the Bunsen reaction *(1.7)*. By separating the H_2 and I_2 from the HI decomposition step, I_2 can be recycled to the Bunsen reaction *(1.7)* and high purity H_2 is produced.

The separation of the sulfuric acid and HI components is achieved by adding additional I_2 to form a liquid-liquid phase that can be separated. This separation must be done in the temperature range of 120 – 350^{o}C to achieve maximum efficiency. For the acids to be recycled to the decomposition steps, they must be highly concentrated to increase the decomposition efficiency. Both polymeric and composite membranes have been tested for the separation of the acidic HI/H_2O systems. Polymeric membranes have the advantage of high water permeability, but the drawback of low thermal stability. Ceramic membranes on the other hand can withstand high temperatures, but are sensitive to acidic environments[10]. Pervaporation has been studied for the water separation of the H_2SO_4/HI/H_2O phase using a Nafion® 117 membrane with reasonable results on a low scale application[11]. If the H_2SO_4/HI separation, however, is not done effectively, the following side reactions can occur *(1.10, 1.11).*

$$H_2SO_4 + 6HI \rightarrow S + 3I_2 + 4H_2O \qquad (1.10)$$

$$H_2SO_4 + 8HI \rightarrow H_2S + 4I_2 + 4H_2O \qquad (1.11)$$

These side reactions are more prominent at higher temperatures and HI concentrations and it has been recommended to purify the contaminated phases with the reverse Bunsen reaction to remove the H_2SO_4 and HI[11]. For this reverse reaction to be possible the reaction temperature must be higher than the forward reaction (>120^{O}C), which results in a higher overall thermal energy input.

To ensure low energy consumption on the HI decomposition step of this cycle, a reactive column was suggested by Brown *et al.*[12], which facilitates I_2 removal during HI decomposition. The liquid-vapour equilibrium between the HI-I_2 and water phases leads to HI distillation at the top of the column, which subsequently decomposes over a suitable catalyst to I_2 and H_2. Liquid I_2 can then be separated from the bottom by continuously removing the I_2 from the phase which shifts the HI thermodynamically to the H_2 and I_2 products. A sweeping gas (N_2) can be used to increase the amount of HI present at the catalyst area.

The sulfuric acid decomposition step requires a high temperature source to decompose sulfuric acid over a suitable catalyst into the SO_2/H_2O/O_2 mixture. Oxygen must be removed from the stream before any SO_2/H_2O can be recycled to the Bunsen reaction *(1.7).* The SO_2 – O_2 separation must be achieved with high efficiency as oxygen is a highly oxidizing agent and will increase the possibility for

material corrosion[13]. Since the H_2SO_4 decomposition step is common to all sulfur based thermo-chemical processes, the issues surrounding this step will be addressed in detail in the next section.

Another separation must be performed to ensure that the product (H_2) is free of I_2. Although the product is formed at 350 – 450^{O}C, it can be cooled to about 300^{O}C where glassy polymeric membranes, such as Kevlar and Kapton, could be used for the separation. As this separation increases the overall technicality of the process, high temperature polyimides have also been suggested for this application. Low H_2/I_2 separation factors will discard I_2 from the system which would otherwise be use for the Bunsen reaction *(1.7)*, thus increasing the running costs of the SI cycle.

The above discussion clearly shows that the SI process has a set of challenges. Nevertheless, the SI process is one possible alternative technique for the production of clean hydrogen. However, the separation issues remain troublesome and solving this problem at the recommended temperatures necessary would be difficult with a membrane process as has been suggested.

1.1.2.2 Hybrid sulfur cycle

The Hybrid Sulfur (HyS) process, schematically depicted in Figure 1.3, which will be the focus of this study, is another attractive alternative thermo-chemical cycle that has received increased attention[5]. It also entails a sulfuric acid decomposition step described in the SI cycle *(1.8)* with a high temperature source, to produce the reactants needed for the chemical cycle. In the HyS cycle, the SO_2 from the decomposer is fed, with addition of water, to a proton exchange membrane (PEM) electrolyser where the SO_2 is catalytically converted to H_2SO_4, protons and electrons. This electrolysis step has a theoretical potential of 0.158V, which is subsequently lower and hence an advantage compared to normal water electrolysis (1.2V). The formed H_2SO_4 is subsequently decomposed again to SO_2 to complete the cycle. The net products produced from water in this cycle are H_2 and O_2, while the SO_2 and H_2SO_4 ideally remain within the cycle.

While SO_2 has previously been used to depolarize the anode of an electrolyser[14], the HyS process, which includes this electrolysis step, was developed by Westinghouse Electric Corporation[15] in the 1970's who did some research on the decomposition of sulfuric acid. In the electrolysis step, sulfuric acid saturated with SO_2 was fed to the anode side of the membrane electrode assembly (MEA), in an electrolyser. Using platinum as the electrode catalyst, the SO_2 is oxidized at the anode to produce protons and electrons *(1.12)* of which the protons migrate through the proton exchange membrane

(PEM) where they are converted to H_2 *(1.13)* at the cathode[16]. The overall reaction of the electrolyser can therefore be expressed as shown in *(1.14).*

$$SO_2 + 2H_2O \rightarrow H_2SO_4 + 2H^+ + 2e^- \quad (1.12)$$

$$2H^+ + 2e^- \rightarrow H_2 \quad (1.13)$$

$$SO_2 + 2H_2O \rightarrow H_2SO_4 + H_2 \quad (1.14)$$

Focusing on the electrolyser section of the HyS cycle, the primary challenges are the required operating conditions, which include elevated acid concentrations, pressure and temperature, and this poses a major challenge for most PEM's. Almost 40 different membrane types have been screened for use in these conditions, of which Neosepta and Nafion materials were shown to be the most suitable candidates[17].

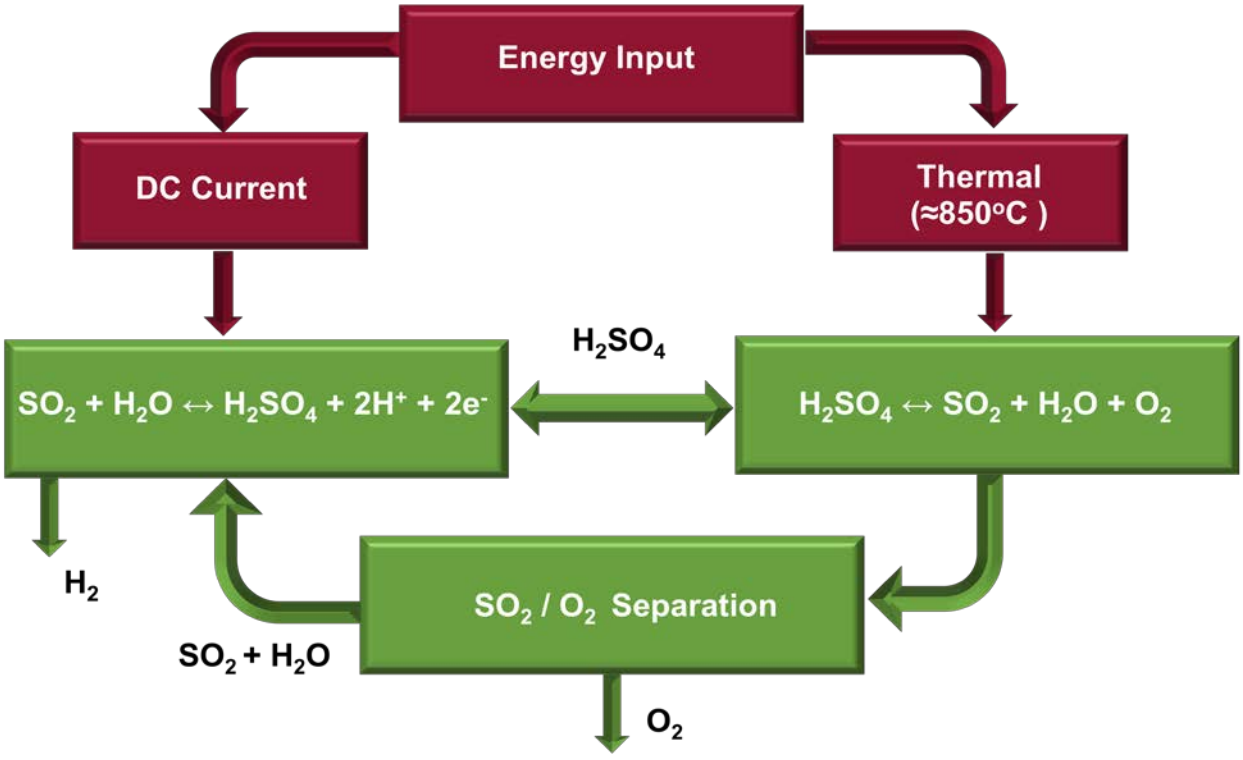

Figure 1.3: Schematic representation for the Hybrid Sulfur Process.

One of the attractive parts of this process is the manageable side reactions in the electrolysis step. An issue complicating the electrolyser operation is an elemental sulfur deposition between the membrane and cathode layer due to SO_2 transport through the membrane with subsequent reduction in efficiency. This sulfur formation can cause delamination of the catalyst layer, thereby

decreasing the contact area between the membrane and the catalyst significantly. SO_2 selective membranes are therefore needed to ensure that no SO_2 is transported through the membrane.

Brecher *et al.*[17] at Westinghouse suggested that the feed stream for the electrolyser should consist of sulfuric acid saturated with SO_2 gas, as this would lower the total electrical energy input of the entire cycle[18]. This implies that the conditions to maximize SO_2 solubility in sulfuric acid have to be known. Various parameters influence the amount of SO_2 soluble in H_2SO_4, including pressure, temperature and acid viscosity (wt %).

The concentration of the acid produced from the electrolyser is important as this influences the energy input for the decomposition reaction. The produced acid must either be of such high concentration that it can be sent directly to the decomposer, higher acid concentration lowers electrolyser efficiency[19], or the acid must be concentrated before being fed to the decomposer, which adds to the complexity and overall cost of this cycle[17]. Thermal decomposition (non-catalytic) of the sulfuric acid produces water and SO_3 in the 350^{o}C range. The gaseous SO_3 is then further decomposed over a platinum catalyst supported on metal oxides to produce steam and SO_2 at temperatures ranging from 700^{o}C to 850^{o}C. The decomposition step is a function of temperature, pressure and the feed rate. Due to platinum costs, Ginosar *et al.*[20] investigated other metal oxide catalysts for the decomposition reaction. The catalyst with the best performance with regards to stability and activity was shown to be $CuFe_2O_4$ although this catalyst had a lower life time than the rest.

1.2 Aim and objectives

Recently the Republic of South Africa committed to the partial funding of research to develop a SA hydrogen economy. Since a hydrogen economy requires platinum, the South African government estimates that it will be able to supply 25% of the global catalyst demand by 2020, as more than 70% of the world's platinum reserves are located in South Africa. Catalyst development will be jointly done by Mintek (a national mineral research organization) and the University of Cape Town (UCT). The University of the Western Cape (UWC) will be responsible for system integration and validation, while the hydrogen infrastructure centre of competence will be jointly hosted by the North-West University (NWU) and the Council for Scientific and Industrial Research (CSIR)[21]. These three centeres of competence have been established to develop an integrated SA hydrogen economy, thereby ensuring a successful partnership between universities and industry.

The aim of this study was to gather know-how as well as to establish expertise in the working of the SO_2 electrolyser for the production of hydrogen. To attain this there are two specific objectives i) Evaluate the SO_2 gas solubility in concentrated H_2SO_4 at elevated temperatures and pressures for the feed of an SO_2 electrolyser and ii) to construct a working SO_2 electrolyser in collaboration with Giner Electrochemical Systems (GES), with some initial membrane electrode assembly (MEA) testing to confirm the correctness of the setup hence, data produced.

1.3 Outline of dissertation

In this chapter an overview will be given of some traditional as well as clean (non renewable) energy sources, their production processes as well as their advantages and disadvantages; leading to the aim and objective of this study. The two objectives of this project, i.e. experimental evaluation of SO_2 gas solubility in concentrated sulfuric acid at elevated temperatures and pressures as well as the setup for SO_2 electrolysis and the testing of initial MEA's are presented in Chapter 2 and 3 respectively. In Chapter 4 an evaluation of the experimental results is presented including recommendations for future work. Appendix A and B contain technical information on design, material selection and the Hazard and Operatibility (Hazop) studies done for both setups used in Chapters 2 and 3.

1.4 References

[1] C. Koroneos, A. Dompros, G. Roumbas, N. Moussiopoulos, *Int. J. Hydrogen Energy*, **29**, 1443 – 1450 (2004).

[2] M.A. Rosen, Int. J. Hydrogen Energy, 21, 349-365 (1996).

[3] M. B. Gorensek, W. A. Summers, *Int. J. Hydrogen Energy*, doi:10.1016/ijhene.2008.06.049.

[4] C. Stone, A. E. Morrison, *Solid State Ionics*, **152-153**, 1-13 (2002).

[5] P. Millet, R. Ngameni, S. A. Grigoriev, N. Mbemba, F. Brisset, A. Ranjbari, C. Etievant, *Int. J. Hydrogen Energy*, **35,** 5043-5052 (2010).

[6] E. Varkaraki, N. Lymberopoulos, E. Zoulias, D. Guichardot, G. Poli, *Int. J. Hydrogen Energy*, **32**, 1589-1596 (2007).

[7] H. R. Colon-Mercado, M. C. Elvington, D. T. Hobbs, FY08 Membrane Characterization Report for the hybrid Sulfur Electrolyzer, Contract Number DE-AC09-08SR22470, (2008).

[8] B. J. Lee, H. C. Ho, H. J. Yoon, H. G. Jin, Y. S. Kim, J. I. Lee, *Int. J. Hydrogen Energy*, **34** 2133-2143 (2009).

[9] C. J. Orme, J. r. Klaehn, F. F. Stewart, *Int. J. Hydrogen Energy*, **34**, 4088-4096 (2009).

[10] F. F. Stewart, C. J. Orme, M. G. Jones, *Int. J. Hydrogen Energy*, **32**, 457-462 (2007).

[11] H. F. Guo, P. Zhang, Y. Bai, L. J. Wang, S. Z. Chen, J. M. Xen, *Int. J. Hydrogen Energy*, doi:10.1016/j.ijhydene.2009.05.009.

[12] L. Brown, J. Funk, S. Showalter, High efficiency generation of hydrogen fuels using nuclear power. GA, A23373, June, 2003.

[13] R. M. Spotnitz, J. Colucci, S. H. Langer, *J. Electrochem. Soc*., **130**, 2393 – 2395 (1983).

[14] W. Juda, D. M. Moulton, *Chem. Eng. Prog*., **63:4**, 59-60 (1967).

[15] L. E. Brecher, S. Spewock, C. J. Warde, *Int. J. Hydrogen Energy*, **2**, 7-15 (1977).

[16] M. B. Gorensek, W. A. Summers, *Int. J. Hydrogen Energy*, doi:10.1016/ijhene.2008.06.049.

[17] R. Junginger, B. D. Struck, *Int. J. Hydrogen Energy*, **7**, 331-340 (1982).

[18] L. E. Brecher, S. Spewock, C. J. Warde, *Int. J. Hydrogen Energy*, **2**, 7-15 (1977).

[19] J. A. Staser, M. B. Gorensek, J. W. Weidner, *J. Electrochem. Soc*., **157** (6), B952 – B958 (2010).

[20] D. M. Ginosar, H. W. Rollins, L. M. Petkovic, K. C. Burch, *Int. J. Hydrogen Energy*, **34**, 4065-4073 (2009).

[21] Fuel Cell Bulletin, November 2009, p 11. www.dst.gov.za/centres-of-excellence

CHAPTER 2

SO_2 Solubility in Sulfuric Acid

2.1 Introduction

In light of the worldwide increase in energy demand, existing clean energy processes have to be further improved and novel processes developed to meet these needs. Thermochemical processes which can be used to produce hydrogen, such as the Hybrid Sulfur Process (HyS) are currently receiving increased interest[1]. The HyS process entails a cyclical process where initially H_2SO_4 is converted to SO_2 in a decomposer. In the second step SO_2 is oxidized back to H_2SO_4 in an electrolyser. The electrolyser converts water, in the presence of SO_2 gas dissolved in sulfuric acid, at the anode to protons and electrons, while producing sulfuric acid. The protons migrate through a proton exchange membrane (PEM) to combine with the produced electrons, which travel through an external electrical circuit to the cathode, to produce pure hydrogen. While it is clear that the SO_2 concentration is vital for the efficiency of the process, as of yet no systematic and comprehensive experimental study has been done on the SO_2 gas solubility as a function of the most important parameters8, which include temperature, acid concentration and pressure. This chapter will firstly discuss research previously done on SO_2 solubility in i) common solutes and ii) sulfuric acid from diluted to concentrated solutions under ambient to high pressures (>250kPa), describing experimental methods and different reaction mechanisms[2,10]. The solubility of sulfur dioxide (SO_2) has been studied in numerous environments including water, hydrochloric acid, Na_2SO_4, acetic acid, sodium acetate, ammonia acetate, diluted H_2SO_4, concentrated H_2SO_4 and fuming H_2SO_4. Subsequently, an experimental setup is described that was used for solubility measurements at elevated temperatures and pressures in 50wt% H_2SO_4. The results for these measurements are then discussed leading to the selection of the most favourable conditions (maximum SO_2 dissolved) for the optimized electrolyser operation conditions.

2.1.1 SO_2 solubility at low pressures

The thermodynamics of SO_2 solubility in aqueous sulfuric acid have been studied for a specific set of parameters including acid concentration, temperature and pressure. When aqueous or dilute systems (< 22wt% H_2SO_4) are investigated, the ionization of both SO_2 and H_2SO_4 (dissolved in H_2O) must be taken into account. These ionization equations[2] can be written as

$$SO_2(g) \Leftrightarrow SO_2(aq) \qquad (2.1)$$

$$SO_2(ag) + H_2O \Leftrightarrow H^+(aq) + HSO_3^-(aq) \qquad (2.2)$$

$$H_2SO_4(aq) \Leftrightarrow H^+(aq) + HSO_4^- \qquad (2.3)$$

$$HSO_4^-(aq) \Leftrightarrow H^+(aq) + SO_4^-(aq) \qquad (2.4)$$

$$HSO_3^-(aq) \Leftrightarrow H^+(aq) + SO_3^{2-}(aq) \qquad (2.5)$$

For flue gas clean-up purposes, Krissmann *et al.*[2] studied the solubility of sulfur dioxide in both sulfuric acid and hydrochloric acid in the concentration range up to 0.5M (2.61wt %) sulfuric acid and 0.1M hydrochloric acid at 298K and 100kPa. By determining the concentration of the gaseous SO_2 phase, using an UV apparatus to measure the adsorption into the liquid, the solubility can be determined. They used the ionization reactions *(2.1 - 2.4)* to describe the equilibrium constants. It was shown by Goldberg *et al.*[3] that the first two equations describe the physical absorption and the hydrolysis of SO_2 respectively. Equations *(2.3)* and *(2.4)* relate to the dissociation of H_2SO_4 in water which is a function of the pH. In diluted systems (<22wt% H_2SO_4), the formation of the sulphite (SO_3^{2-}) *(equation 2.5)* must also be taken into account as it influences the ionization equations. However, at a pH below 2, sulphite formation can be neglected as the solution is too concentrated for this reaction to occur[4]. With these reactions, mass balances can be written to determine the solubility of the gas phase in the acid. The model of Krissmann *et al.*[2] showed good correlation with other authors[5] showing that these reaction equations reasonably explain the various species found in an aqueous environment.

Earlier SO_2 solubility measurements were done by Hunger *et al.*[6] using diluted SO_2 in Na_2SO_4 and H_2SO_4 with concentrations below 2M (10.45wt %) for both liquids and at constant temperatures (298K and 323K), while the overall pressure was kept constant at approximate 1 atm. They used the correlation of Kirchevsky and Kasarnovsky[7], that describes the vapour mole fraction and SO_2 fugacity as a function of the molality of species dissolved. They assumed that the molality of molecular SO_2

has a linear correlation with its partial pressure according to Henry's law. Measurements performed by Hunger *et al.*[6] showed that Henry's law is valid for pressures below 1 bar. The dissociation equations used for their study differ slightly from those used by Krissmann *et al.*[2]. In concentrated sulfuric acid, the protons formed (H^+ as in aqueous solutions) can only exist as H_3O^+. An additional equation *(2.7)* was introduced by Hunger *et al.*[5], describing the dissociation of dissolved sulfur dioxide, following the hydrolysis of adsorbed SO_2 in aqueous solutions *(2.2)*. Perhaps a more complete description of the sulfuric acid dissociation for concentrated sulfuric acid can therefore be given by *(2.6)* & *(2.7)*[6].

$$H_2SO_4 + H_2O \Leftrightarrow H_3O^+ + HSO_4^- \qquad (2.6)$$

$$HSO_4^- + H_2O \Leftrightarrow H_3O + SO_4^{2-} \qquad (2.7)$$

The first step of the dissociation of sulfuric acid, as described in equation *(2.6),* is regarded as complete at concentrations below 22wt % according to Hunger *et al.*[5], however at higher concentrations (above 22wt%), the molecular form of the acid (H_2SO_4) is dominant and the further dissociation into the sulfate *(2.7)* is negligible as the sulfate is present in very low concentrations. It was also shown that the partial pressures have an almost negligible effect on the system's pH for concentrations above 0.2M.

The model formulated by Govindarao *et al.*[8] showed the effect of the sulfuric acid on the SO_2 solubility in diluted systems (0-2.815mol/kg corresponding to <28wt %) by experimentally estimating Henry's law constant and using the equilibrium constant of the hydrolysis *(2.2)* of SO_2 for temperatures ranging from 30 – 80°C. Apart from the values determined for the Henry and equilibrium constants, the observation was made that the state of the SO_2 in sulfuric acid concentrations above approximately 22wt% can be assumed to remain unchanged, i.e. SO_2 is mainly present in its molecular form with a negligible percentage in any of its ionic forms described above. The reasoning is that an increase in the sulfuric acid content will increase the hydronium concentration which will push the equilibrium in eq. *(2.2)* to the left, therefore decreasing the hydrolysis of SO_2. Govindarao *et al.*[8] formulated equations relating equilibrium mole fraction of the total SO_2 to the partial pressure (190 – 1575 Pa) of the gas in the gas phase. From the assumption that SO_2 is mainly in its molecular form, they simplified the equation and could determine the Henry Constant for SO_2 dissolved in concentrated H_2SO_4. The results show that the dissolution *(2.1)* and hydrolysis *(2.2)* occur simultaneously and instantaneously. This model is specifically accurate when

diluted SO_2, low concentration H_2SO_4 (<22wt %) and high temperatures (≈80^0C) are used with small deviations between model and experimental values when higher acid concentration are used.

Knowing that the SO_2 is mostly in its molecular form above 22wt% and that the ionization of SO_2 is negligible for concentrated (>22wt %) systems, Zhang *et al.*[9] made the assumption that the concentration of molecular SO_2 in concentrated sulfuric acid may be approximated from its solubility in the acid. By doing this they were able to estimate Henry's constants more accurately for pressures above 1 bar than what could have been achieved using the method followed by Hunger *et al.*[6]. Using simpler equilibrium equations *(2.8 – 2.11)*, chemical equilibrium constants, equations and mass balances for SO_2 in the liquid phase, they formulated a correlation between the partial pressure of SO_2 and the solubility of SO_2 in concentrated sulfuric acid (>65wt %) and temperatures up to 393K.

$$HSO_4^- + H_2O \rightarrow H_3O + SO_4^{2-} \qquad (2.8)$$

$$H_2SO_3 \rightarrow HSO_3^- + H^+ \qquad (2.9)$$

$$HSO_3^- \rightarrow SO_3^{2-} + H^+ \qquad (2.10)$$

$$H_2O \rightarrow OH^- + H^+ \qquad (2.11)$$

By combining the equilibrium between the liquid and vapour phase, fugacity coefficient and SO_2 activity, equation *(2.12)* was formulated to express the SO_2 solubility in terms of pressure.

$$\ln P_{SO_2} + \frac{BP}{RT} = \ln H + \ln m_{SO_2} + 2\beta_{SO_2-SO_2} m_{SO_2} \qquad (2.12)$$

where P_{SO_2} is the partial pressure of SO_2 (kPa), $\frac{BP}{RT}$ the fugacity coefficient with B the second virial coefficient (mol/cm^3), H the Henry constant (mPa), $\ln m_{SO_2}$ the mass of molecular SO_2 in the liquid phase (g) and $2\beta_{SO_2-SO_2} m_{SO_2}$ corresponds to the SO_2 – SO_2 interactions. For systems with low partial pressures and high temperatures, the fugacity coefficient of SO_2 approaches unity and *(2.12)* can be further simplified to

$$\ln P_{SO_2} = \ln H + \ln m_{SO_2} + 2\beta_{SO_2-SO_2} m_{SO_2} \qquad (2.13)$$

The Henry Constants in both equations *2.12* & *2.13* can be determined using experimental solubility data. According to their model, at constant acid concentration increased temperature results in a decrease in SO_2 solubility while an increase in partial pressure shows an increase in solubility at higher temperatures. The values generated from this correlation were then used to compare the SO_2 solubility values in 97wt% H_2SO_4 determined by Hayduk *et al.*[10].

A paper from Gold and Tye[11], who studied the state of SO_2 in sulfuric acid at concentrations extending into the oleum region (fuming sulfuric acid - mixture of SO_2, H_2SO_4 and SO_3) supports the observation that SO_2 remains in its molecular form in concentrated sulfuric acid. Gold and Tye concluded that there is no evidence of the existence of the conjugate acid species HSO_2^+, which implies that the solubility of SO_2 is not due to a specific chemical interaction with the solvent. Oleum is indexed by its SO_3 percentage and the SO_2 solubility values produced by Gold and Tye unfortunately cannot be used for pure H_2SO_4/SO_2 systems, as the presence of the SO_3 species increase the SO_2 solubility with increasing SO_3 content as Miles and Carson[12] have shown.

2.1.2 SO_2 solubility at elevated pressures

Work done on the solubility of SO_2 at elevated pressures was presented in the paper by Hayduk *et al.*[10] who reported SO_2 solubility data in 97wt% H_2SO_4. The authors used mixtures of N_2 and SO_2 to increase the total pressure (>248kPa) in a gas reservoir cell. They observed that the rate at which SO_2 dissolves into the acid was a function of the acid viscosity and by mechanically stirring the acid solution the SO_2 solubility rate was higher in the starting minutes of the experiment than without a stirrer as was expected. They used a gas reservoir to calculate the amount of SO_2 and using a dissolution cell (containing the acid), the SO_2 was allowed to flow from the gas reservoir to the dissolution cell. After the pressure had stabilized over the two cells, equilibrium was achieved. From the equilibrium pressure and the known volumes of both cells, the solubility (loss of pressure) of SO_2 could be calculated using the ideal gas law to determine the amount of SO_2 before and after equilibrium. The gas reservoir was then pressurized again to higher pressures and released into the dissolution cell and the equilibrium pressure was again measured. Subtracting the second solubility measurement from the first, the higher pressure solubility was calculated. They observed a steady drop in SO_2 solubility up to 50 mol% acid with subsequent increasing solubility when more concentrated acids were used. They found that the maximum SO_2 soluble at 298.15K in 97wt% was 0.625g/100g H_2SO_4 with the partial pressure of SO_2 at 24.3kPa (total pressure = 514.2kPa).

In spite of the extent of the above discussed literature, no systematic experimental study has been performed on the SO_2 solubility over the entire temperature, pressure and sulfuric acid concentration ranges. Solubility measurements in the pressure range higher than the vapour pressure of SO_2 (≈2.8 bar) have been achieved by Hayduk *et al.*[10] when diluting the SO_2 with N_2. Due to thermodynamic boundaries of the SO_2, high pressures cannot be achieved without SO_2 becoming a liquid (see Appendix A.3).

Although the maximum amount of SO_2 soluble in sulfuric acid may be in the liquid SO_2 range, a paper from Gorensek *et al.*[13] showed, using computer modeling, that a liquid equilibrium is formed between the SO_2 liquid and sulfuric acid at higher pressures. Thus, a maximum pressure exists where any further pressure increase has a negligible effect on SO_2 solubility in sulfuric acid. The program used to evaluate the solubility was Aspen – Plus equipped with the Aspen – OLI interface to evaluate the activities of each species in *(2.14)*. The study aimed at predicting the SO_2 solubility in concentrations of sulfuric acid ranging from 30–60wt%, temperatures ranging from 30–80^{0}C and pressures from 0–20 bar for the electrolytic reduction of SO_2 used in the Hybrid Sulfur Process. From their model, the maximum amount of SO_2 soluble with regards to temperature (20 –100^{o}C), pressure (0–20 bar) and acid concentration (30–60wt %) corresponds to 40^{o}C, 5.3 bar and 30wt % H_2SO_4.

$$4H^+ + SO_4^{2-} + 2e^- \rightarrow SO_2 + H_2O \qquad (2.14)$$

In order to increase the vapour pressure of SO_2, the temperature of the gas/liquid mixture must be increased in accordance with the findings of Maass & Maass[14] who showed that the vapour pressure can be increased to ensure that SO_2 will remain a gas at pressures above 2.8 bar.

In this study, the aim was to experimentally evaluate SO_2 solubility in a 50wt% H_2SO_4 concentration at temperatures ranging from 30–80^{o}C and pressures ranging from 0–10 bar to provide a systematic study of SO_2 solubility as a function of pressure and temperature. To validate the suitability and accuracy of this experimental design and setup, SO_2 gas solubility values were also determined in water and compared to the available literature values. The acid concentration was kept constant at 50wt% H_2SO_4 as this was the acid concentration found to be favourable to be produced from the electrolyser step of the HyS process to ensure a 50% thermal to electrical conversion for the entire HyS process[15].

2.2 Materials and methods

2.2.1 Materials

Analytical grade 98% sulfuric acid (CJ Chemicals, South Africa) was used as received and a batch solution of 50wt % was prepared by diluting the 98 wt % with DI water (milli-pore). SO_2 gas (Afrox, SA) was used as received. A sampling cylinder (1Gal, 304SS) was used to contain the gas/liquid SO_2 for use in the laboratory. All piping and vessels where made from SS316.

2.2.2 Methods

2.2.2.1 System setup and calibration

The basic experimental setup (Figure 2. 1) was taken from Zhang *et al.*[16] with a few modifications for example to facilitate the high pressure conditions a stainless steel housing was machined containing a glass beaker. Similarly, SO_2 gas fed to the system was preheated to achieve the increased gas pressure. The sampling cylinder (A2) was fitted with a rupture disc to prevent excessive pressure build up in the sampling cylinder. A Hazard and Operatibility Study (Hazop – see Appendix A.2 & A.4) was performed on the experimental setup in view of the high sulfuric acid content, the SO_2 gas and the high pressures that were used.

The experimental setup mainly included a gas vessel B2 (102.60cm^3) containing only SO_2 gas and a solubility cell B3 (111.08cm^3) containing the liquid to be tested (See Appendix A.6.2). High accuracy UT-10 pressure transducers (PI1 & PI2, WIKA SA) were used to measure the pressure in both the gas vessel and the solubility cell. The temperature was measured using type K thermocouples (TI1 – TI5) connected to PID controllers (WIKA SA). Heating of the two vessels was achieved using a water bath (B1, Labotec SA, 14L capacity), while heating tape (A1, Hi-Tech elements) was used to heat the piping from the sampling cylinder to the gas vessel.

The volume of the system required for the SO_2 solubility measurements, including all piping from V1 to V4, was calculated to ensure that no experimental error existed due to the possible presence of dead volumes. A 0.37 **%** average deviation was found between the measured and the calculated volumes. Volumes were measured by filling the system with water and predicting the pressure drop with N_2 at different temperatures using the volumes measured by the water measurements. After the volume determinations, pressure tests were done to ensure that no gas leaks were present. The

complete system was pressurized to 15 bar with N_2 and left for 2 hours. Following this the entire system was flushed using N_2 at 15 bar for 10 minutes. The temperature of the sampling cylinder (A2) was kept at least 5^0C below the operating temperature of the water bath (B1) to avoid SO_2 condensation.

2.2.2.2 Calculations

The theory for determining the SO_2 solubility both in water and acid is in essence the same. The solubility for both was calculated in moles absorbed (n_{abs}) into the liquid, where the water solubility was expressed in molality (moles SO_2 per kg H_2O) and the solubility in the acid as grams of SO_2 per 100 grams of acid to facilitate the comparison with literature units used.

After successful pressure tests and system flushing, 70.00mL of either the milli-Q water or acid were added to B3 and connected to the rest of the setup. The entire system was placed under vacuum (GEC Machines LTD, BC2 212) after the desired temperature in both vessels (B2 & B3) had been reached. SO_2 gas was then supplied to B2. The initial amount of both SO_2 (n_{SO_2} in B2) and the trace amount of N_2 (n_i in B3) that had remained from the flushing step were calculated using equations *(2.15)* and *(2.16)* respectively. Although the trace amounts of N_2 present in B3 after vacuum was almost negligible it was added for completeness. Furthermore, the vapour pressure of the contained liquid, which is a function of the temperature, was included in the calculation as P_v which is included in the P_{B3} term.

$$n_{SO_2} = \frac{P_{B2} * V_{B2}}{z_{T,P} * R * T} \qquad (2.15)$$

$$n_i = \frac{P_{B3} * V_{B2}}{z_{T,P} * R * T} \qquad (2.16)$$

The initial amount of SO_2 gas in B2 was allowed to enter B3 and left to equilibrate over time. After equilibrium had been reached (approximately 500 minutes) the amount of SO_2 gas present in the entire system was calculated using the equilibrium pressure according to equation *(2.17)*[17].

$$n_{eq} = \frac{P_{eq} * \left(V_{B2} + V_{B3}\right)}{z_{T,P} * R * T} \qquad (2.17)$$

Once equilibrium had been reached it was possible to calculate the amount of SO_2 gas absorbed into the liquid using equation *(2.18)*.

$$n_{abs} = n_{So_2} + n_i - n_{eq} \qquad (2.18)$$

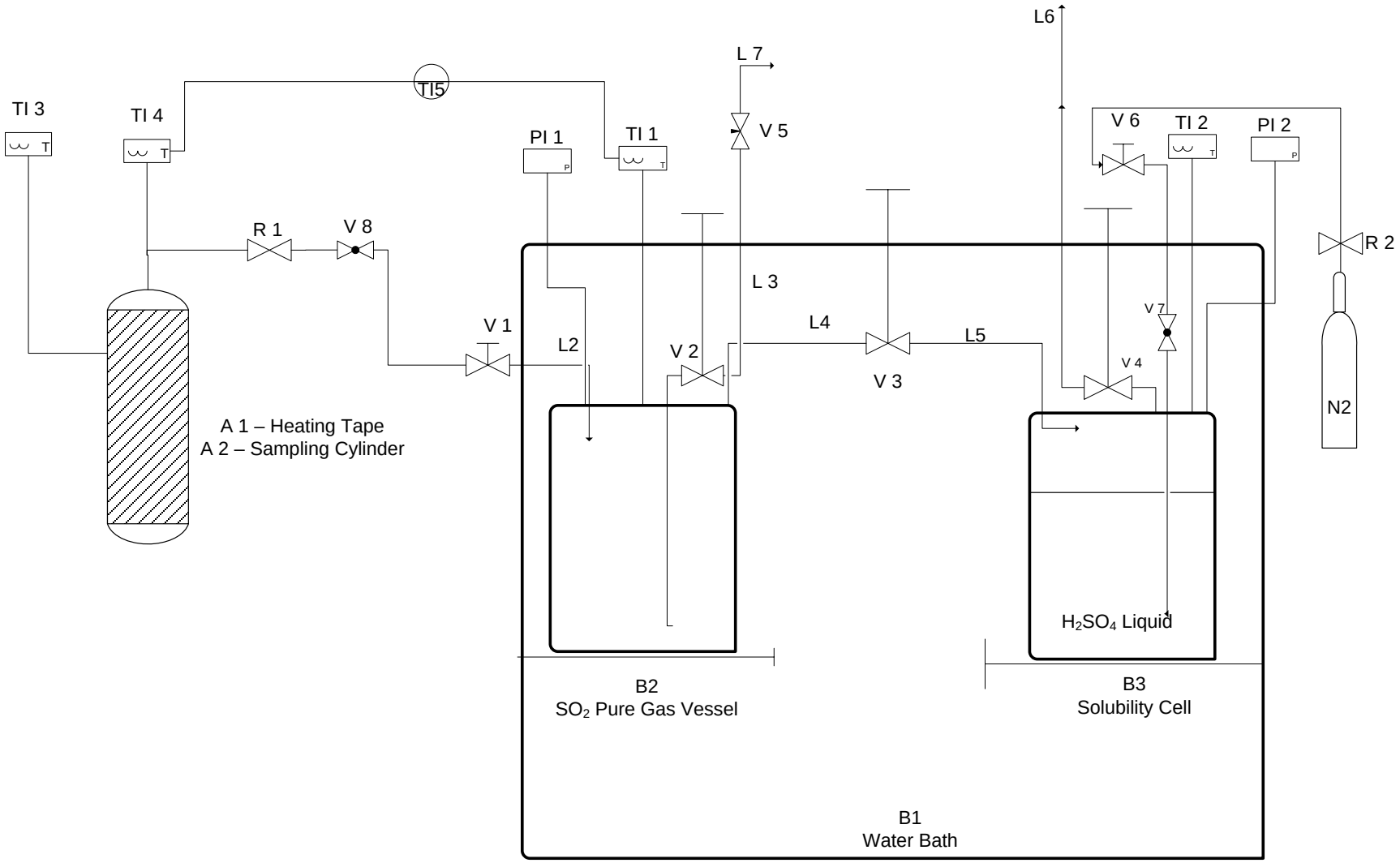

Figure 2. 1 : Setup for the SO_2 measurements in concentrated H_2SO_4

To determine the solubility in water, n_{abs}, was converted to molality using the density of the water used. To obtain the solubility in acid the n_{abs} term was first converted to g/mL and subsequently to g/100g H_2SO_4 using the acid density.

The above process described made it possible to measure the solubility of SO_2 gas in either water or acid liquid over a pressure range without having to change the liquid. The liquid was however replaced for each temperature measured. In Sections 2.2.2.3 and 2.2.2.4 the experimental procedures are described for determining the SO_2 solubility in water and H_2SO_4 respectively.

2.2.2.3 SO_2 Solubility in water at 40°C

SO_2 solubility in pure water has been studied by various authors including a recent paper by Shaw *et al.*[17] who studied the solubility of SO_2 at 25°C and 40°C over a pressure range of 0–5 bar. The same experimental work was used in this study for the same reason Shaw *et al.*[17] provided i.e., to show the experimental setup's ability to predict gas solubility in liquids. As this experimental validation work was easily incorporated into the experimental setup and design used in this study, it was included to verify the measuring accuracy when using this setup to measure SO_2 gas solubility in liquids. The milli-Q water used had a density of 0.9995g/mL, which was calculated by the average of three measurements. To be able to compare these results with those obtained by Shaw *et al.*[17], the calculations (as described in Section 2.2.2.2) were altered to show the SO_2 solubility in molality (mol S_{IV} per kg of water). The values were calculated with correction of water vapour pressure at 40°C (0.073 bar). The water solubility was measured twice at 40°C over a pressure range of 0–2 bar.

2.2.2.4 SO_2 Solubility in 50wt% H_2SO_4

The acid used in this study had a density of 1.3591g/mL, which was measured in the same way water density in the previous section. The vapour pressure (P_v from Section 2.2.2.2) of 50wt% H_2SO_4 as a function of temperature according to literature is 0.015, 0.047 and 0.196 for 30°C, 50°C and 80°C, respectively[16]. The compressibility factor ($z_{T,P}$) was obtained from Kang *et al.*[18] and interpolated for the 80°C measurements. A detailed description of the process used to evaluate the solubility is given in Figure A–2 (Appendix A.6.3.1), which was used for the solubility measurements over the 30–80°C temperature range, while operating in the 0–10 bar region.

2.3 Results and discussion

2.3.1 SO_2 solubility in water at 40°C

In Figure 2.2, a graph is shown comparing our repeated solubility results (Run 1 & 2) with those obtained by Shaw *et al.*[17] over the pressure range of 0 – 2 bar at 40°C. The SO_2 solubility in water study was repeated in the pressure range of 0.4–0.8 bar (Run 2) to determine internal repeatability.

According to Figure 2.2, it is clear that the solubility of SO_2 in water is proportional to the partial pressure of the SO_2 gas. This linear dependence on pressure is also seen by other authors for other acid concentrations[2,6,8,9,10] at constant temperature. From the close correlation obtained by our experimental work and that done by Shaw *et al.*[17], we can assume that the experimental setup proposed in this study is capable of predicting the SO_2 solubility in pure water with adequate accuracy. Following this it was assumed that the values obtained for the SO_2 solubility in 50wt% H_2SO_4 had a similar accuracy.

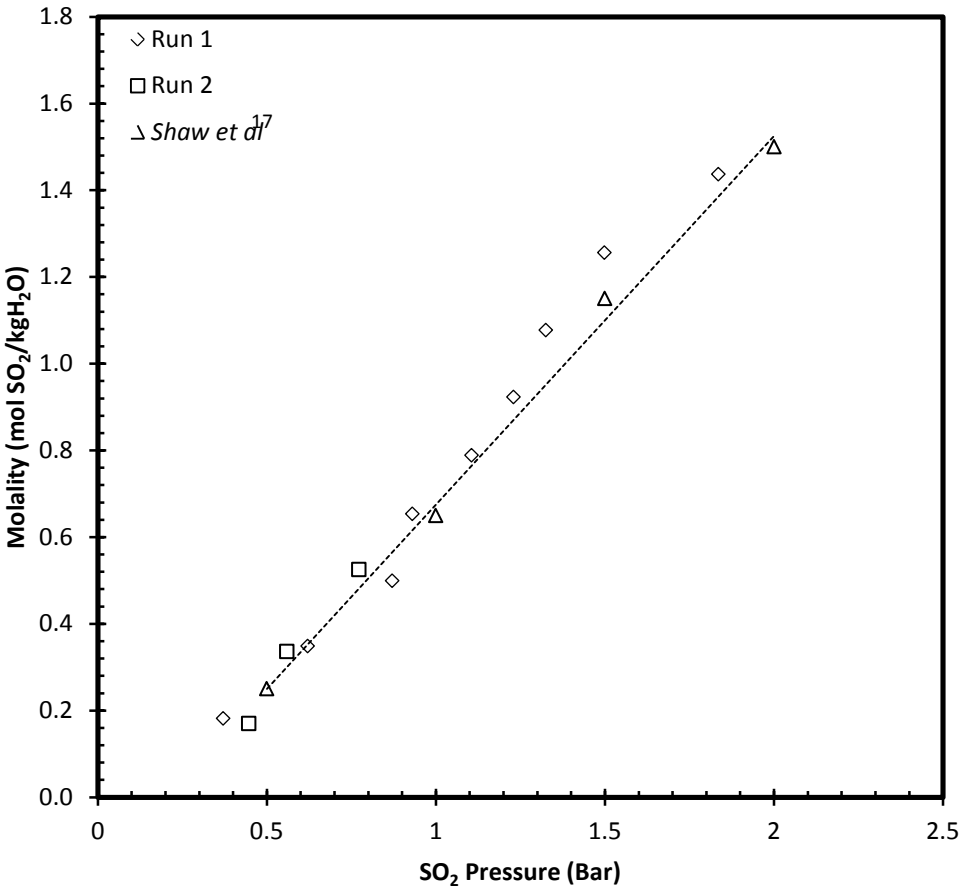

Figure 2.2: SO_2 solubility in water at 40°C.

2.3.2 SO_2 solubility in 50wt% H_2SO_4

It was previously discussed (Section 2.2.2.2) that the pressure drop of SO_2 over time (until equilibrium is reached) was measured to determine the amount of SO_2 soluble at a constant temperature. Figure 2.3 shows such pressure decay vs. time graph for a single pressure measurement at 30°C for both the SO_2 (B2) and H_2SO_4 (B3) compartments. A representative sample of these pressures vs. time measurements is given in Appendix A.6.3.3 (Figure A – 6) for the complete pressure range at 30°C. Since the same trend was observed for 50°C and 80°C runs, the graphs obtained for each pressure at each temperature is not shown in this section. It is clear that only the first two values (for SO_2 and H_2SO_4) are not equal (before V3 is opened). As soon as SO_2 had entered B3, the two values became superimposed due to the equilibrium between the SO_2 and H_2SO_4.

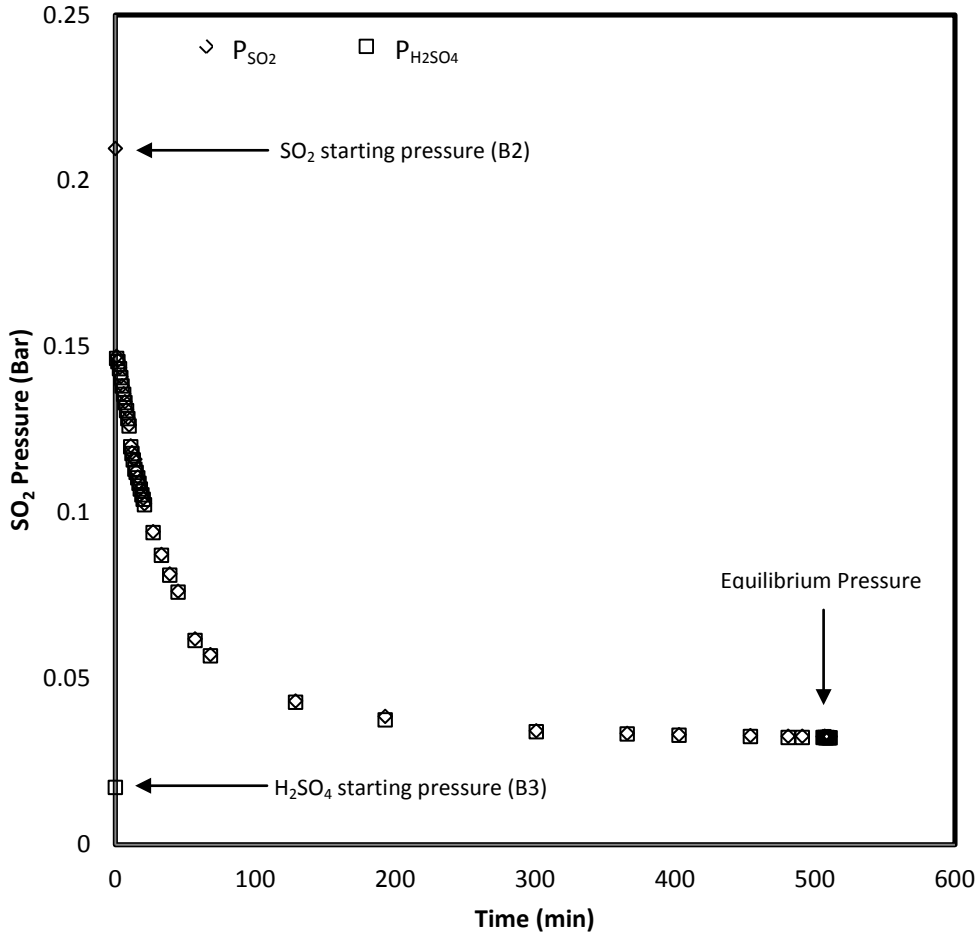

Figure 2.3 : Pressure decay as a function of time, 50wt% at 30°C.

The exponential decrease in pressure over time was observed for the entire pressure range tested in this study for all temperatures. From the starting conditions in Figure 2.3 (t =0, P_{SO2} = 209.7kPa & P_{H2SO4} = 2.5kPa), the total amount of SO_2 gas present in B2 (before solubility measurements started) was calculated as 0.576g. While the trace amount of N_2 (B3, from the flushing step) is negligible (9.8 x 10^{-3}g N_2 vs. 0.576g SO_2), it was included in the calculations before the SO_2 gas from B2 was bled to B3 and left to equilibrate. After 500 min (the average time required) to achieve equilibrium, the obtained equilibrium pressure (P_{eq} = 17.2kPa) was used to calculate the first solubility point of SO_2 which was 0.4605g of SO_2 per 100g of H_2SO_4. From these results, it became apparent that more time was needed to achieve equilibrium compared to what had been reported in literature9 (8–9 hours compared to the 1 hour used in literature). This is understandable since the acid solution in our study was not stirred during the equilibration period. Therefore, to attain a full pressure series, a total of 45 continuous measurements had to be taken.

The experimental solubility measurements at equilibrium for 30°C, 50°C and 80°C in 50wt% H_2SO_4 are presented in Figure 2.4. For comparison, the model predictions obtained from 40°C, 60°C and 80°C by Gorensek *et al.*[13] were also included.

When considering the experimental solubility at 30°C (◊ in Figure 2.4), it seems that initially the solubility increased linearly with increasing pressure up to approximately 2.5 bar, which implies adherence to Henry's law. When the pressure is however increased above the 2.5 bar region, an exponential increase in solubility seems to occur. The solubility measurements at 50°C (□) seem to follow the same solubility trend with a linear region up to 4.2 bar. Above 4.2 bar, an exponential pressure dependence (although very weak) seems to occur. The solubility at 80°C (+) showed an exponential dependence on the pressure, which was more prominent than what had been observed at 30°C and 50°C.

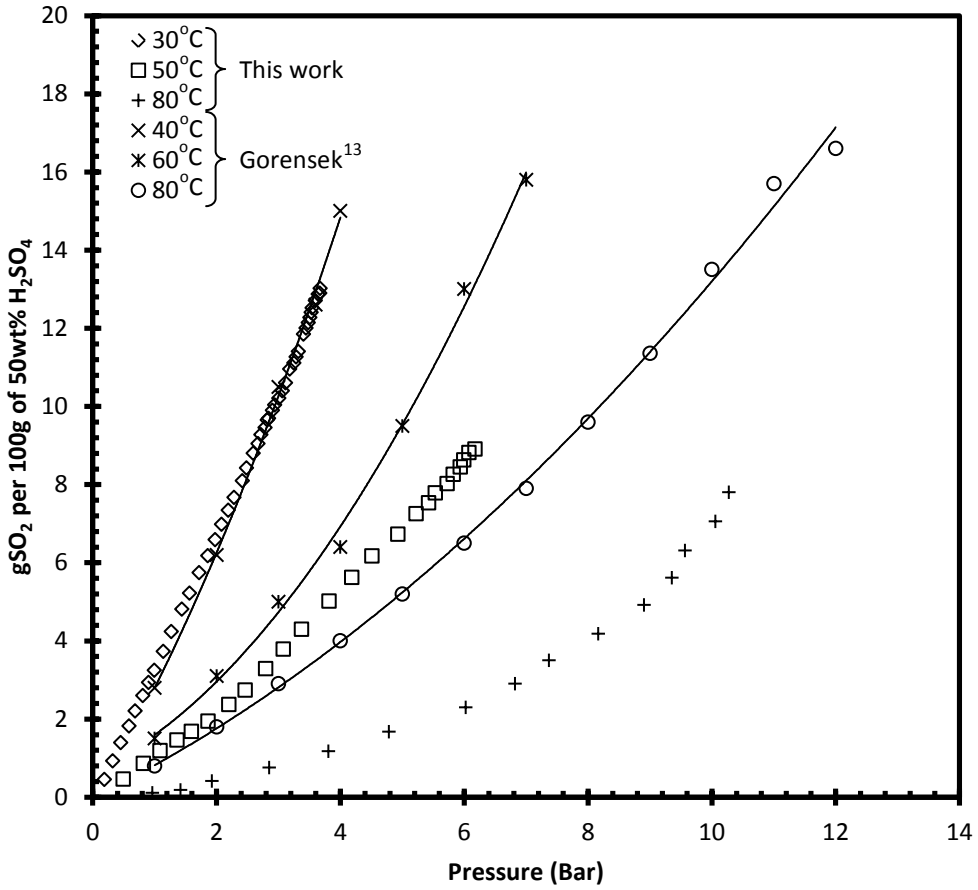

Figure 2.4 : Theoretical (Gorensek[13]) and experimental SO_2 solubility as a function of temperature and pressure in 50wt% H_2SO_4.

Zhang *et al.*[9] showed a similar linear pressure dependence of the solubility in concentrated H_2SO_4 (>65.71wt %) solutions at low pressures as was observed in this study. They found that above 65.71 wt% acid solution, a linear dependence was not valid for pressures above 100kPa.

A similar, but more prominent exponential trend is also visible for the modeled data obtained from Gorensek *et al.*[13] (x, ж and o in Figure 2.4). When comparing the modeling results from Gorensek *et al.*[13] at 40°C with our experimental data obtained at 30°C it is evident that the experimental solubility values obtained at 30°C were similar to the model predictions made by Gorensek *et al.*[13] at 40°C. In view of both the modelled as well as experimental trend observed, i.e. a decrease in SO_2 solubility with increasing temperature at a constant pressure, one would have expected that the modeled 40°C solubility should lie below the experimentally obtained data at 30°C. This discrepancy between the modelled and experimentally obtained data further increased with increasing temperature (50°C and 80°C).

It is clear from these results that in theory much higher solubility values were calculated than those obtained experimentally. To experimentally attain the high pressures predicted by the model, i.e. at pressures above the saturation pressures (as a function of temperature), the use of a compressor or external compression unit would have to be incorporated. In this study however only the gas pressure was used. If however the experimental values especially visible at 80°C, were to be extrapolated to higher pressures, the maximum solubility might come close to the modelled values again confirming the partial validity of both approaches.

Figure 2.4 also shows that the experimental maximum SO_2 solubility decreased with increasing temperature despite the fact that higher pressures were needed to achieve the same solubility (increasing from 3.2 (30°C) to 9.8 (80°C) bar). In Figure 2.5, a comparison is presented between the maximum solubilities obtained as a function of pressure and temperature both for the modeled[13] and experimental data. It is clear that the maximum SO_2 solubility in 50wt% H_2SO_4 is a function of pressure at constant temperature. The solubility was also significantly influenced by the system temperature. The maximum experimental solubility at 80°C is 7.8g SO_2 per 100g H_2SO_4 which is 30% lower compared to the maximum solubility reached at 30°C (13g SO_2 per 100g H_2SO_4), while a decrease of 8% was observed between the solubilities obtained at 50°C and 80°C.

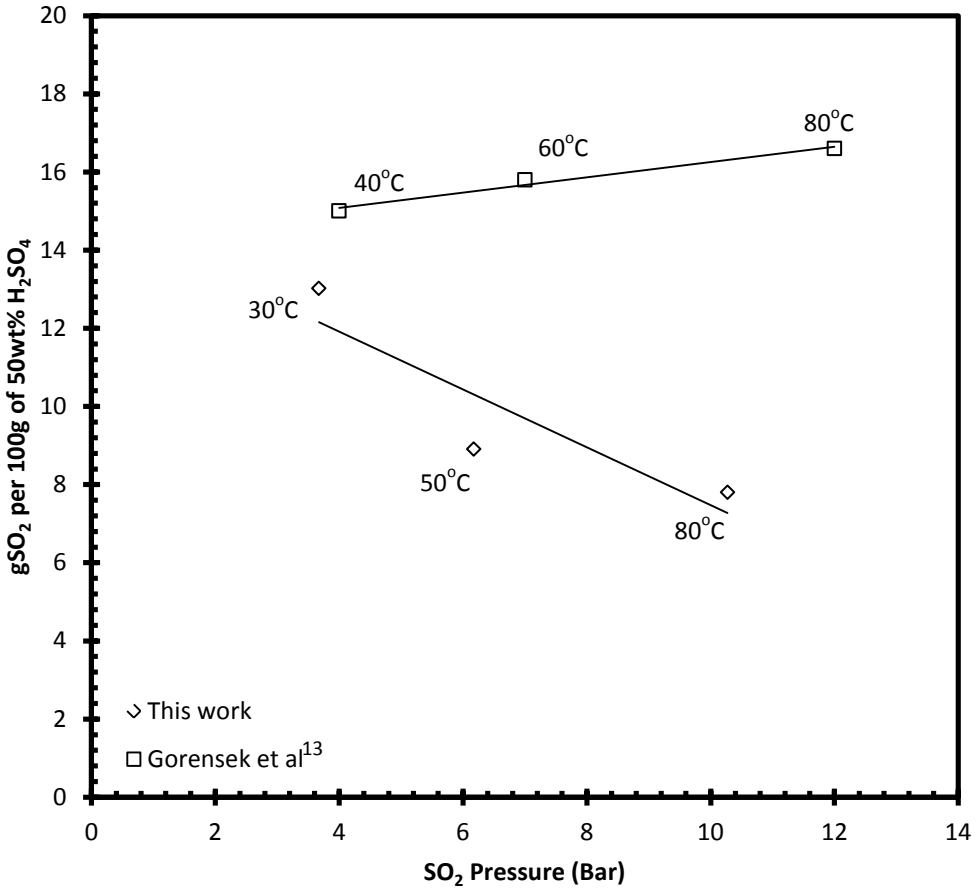

Figure 2.5 : Comparison between the experimental values and model predictions.

This decreasing experimental solubility with increasing temperature was however not observed for the model predictions, which shows an increase from 15 to 15.8 g SO_2/100g H_2SO_4 when the temperature was increased from 40°C to 60°C. This reverse in the trend of maximum solubility with increasing temperature for 50wt% could possibly be due to the assumptions made by the model predictions. One such assumption used by the model included the formation of the sulfate ion described previously (equation *(2.7)* – Section 2.1.1), which has however been shown to be negligible above 22wt% of acid6. A similar observation was observed by Gorensek *et al.*[13] when comparing their solubility trends as a function of H_2SO_4 concentration (40wt % and 50wt %), where a decrease in maximum solubility as temperature is increased (from 29.5g SO_2/100g H_2SO_4 at 40°C to 24g SO_2/100g H_2SO_4 at 100°C) was observed for 40wt% while an increase in solubility was observed for 50wt%. No explanation was, however, provided by Gorensek *et al.*[13] for their inversed solubility trend for 40wt %, and 50wt % respectively. The lower solubility with increased temperatures is also seen for other acid concentrations tested in literature6,8,9. Furthermore, the modelled solubility

values are for saturated systems and thus represent the maximum theoretical SO_2 solubility under ideal conditions.

From a maximum solubility point of view, in terms of the experimentally obtained data, it is thus clear that the most favourable conditions for solubility were attained at SO_2 gas pressures of 3.2 bar and 30°C (achieving 13 g SO_2 per 100g H_2SO_4). Comparing the solubility data from this study with the work done by Hayduk *et al.*[10] in 97wt % H_2SO_4, the maximum SO_2 solubility reached was 8.48g SO_2 per 100g H_2SO_4 at 25°C and 2.5 bar. This observation is also seen by Gorensek *et al.*[13] when comparing their solubility values at constant temperature (40°C) and varied acid concentration (30–60wt %) with the solubility decreasing from approximately 36.5 g SO_2 per 100g H_2SO_4 (30wt%) to 8.5 g SO_2 per 100g H_2SO_4 (60wt%).

2.4 Conclusion

To achieve an acceptable efficiency for the Hybrid Sulfur process (which includes an electrochemical step using SO_2 saturated H_2SO_4 as feed), a systematic study was done on the SO_2 solubility in 50wt% sulfuric acid as a function of temperature and pressure. A detailed Hazard and Operatibility Study was completed to determine setup design for increased temperatures and pressures. After the successful setup characterization, which included pressure tests, volume determinations and solubility measurements in water, was completed, the solubility in 50wt% sulfuric acid was determined at 30°C, 50°C and 80°C over a 0–10 bar range.

It was shown that the ability of the proposed experimental setup had adequate accuracy in measuring the SO_2 solubility in pure water. It was therefore assumed that the values obtained for SO_2 solubility in 50wt% H_2SO_4 were also accurate. Solubility values increased from 8 to 13 grams of SO_2 gas per 100 grams of sulfuric acid as temperatures were decreased from 80°C to 30°C. While the observed experimental trend (decreased solubility with increased temperature) was comparable with the computer modeling done at 40wt %, it was not comparable to the modelled 50wt% which was used to compare the data to our experimentally obtained solubility data at 50wt%.

Further experimental work could be done on other acid concentrations to determine the experimental influence of the acid concentration on SO_2 solubility. The maximum SO_2 solubility obtained for 50wt% H_2SO_4 was 13 grams per 100 grams of acid achieved at 30°C and 3.2 bar.

2.5 References

[1] M. B. Gorensek, W. A. Summers, *Int. J. Hydrogen Energy*, doi:10.1016/ijhene.2008.06.049.

[2] J. Krissmann, M. A. Siddiqi, K. Lucas. *Fluid Phase Equilib.*, 141, 221 – 233 (1997).

[3] R. N. Goldberg, V. B. Parker, *J. Res. Natl. Bur. Stand.*, 90, 341-358 (1985).

[4] M. A. Siddiqi, J. Krissmann, P. Peters-Gerth, M. Lucas, K. Lucas, *J. Chem. Thermodyn.,* **28**, 685-700 (1996).

[5] V. B. Parkinson, Tappi, 39, (1956) 517 – 519.

[6] T. Hunger, F. L. Lapicque, A. Storck, *J. Chem. Eng. Data.,* **35**, 453-463 (1990).

[7] I. R. Krichevsky, J. S. Kasarnovsky, *J. Am. Chem. Soc.,* **57**, 2168 -2171 (1935).

[8] V. M. H. Govindarao, K. V. Gopalakrishna, *Ind. Eng. Chem. Res.,* **32**, 2111-2117 (1993).

[9] Q. Zhang, H. Wang, I. G. Dalla Lana, K. T. Chuang, *Ind. Eng. Chem. Res.,* **3**, 1167 – 1172 (1998).

[10] W. Hayduk, H. Asanti, B. C. Storck, *J. Chem. Emg. Data.*, **33**, 506-509 (1998).

[11] V. Gold, F. L. Tye, *J. Chem. Soc.,* **571**, 2932-2934 (1950).

[12] F. D. Miles, T. Carson, *Ind. Eng. Chem. Res.,* **37,** 1167-1172 (1998).

[13] M. B. Gorensek, J. A. Staser, T. G. Stanford, J. W. Weidner, *Int. J. Hydrogen Energ.,* **34**, 6089 – 6095 (2009).

[14] C. E. Maass, O. Maass, *Am. Chem. Soc.,* **50**, 1352-1368 (1928).

[15] M. B. Gorensek, W. A. Summers, *Int. J. Hydrogen Energ.,* **34**, 4097-4114 (2009).

[16] Q. Zhang, H. Wang, I. G. Dalla Lanna, K. T. Chuang, *Ind. Eng. Chem. Res.,* **37**, 1167-1172 (1998).

[17] C. A. Shaw, M. A. Romero, R. H. Elder, B. C. R. Ewan, R. W. K. Allen, *Int. J. Hydrogen Energ*., (2011) doi: 10.1016/j.ihydene.2011.01.105.

[18] T. L. Kang, L. J. Hirth, K. A. Kobe, J. J. McKetta, J. Chem. Eng. Data, **2**, 220 – 226 (1961).

[17] P. Atkins, J. De Paula, Atkin's Physical Chemistry, 8th Edition, Oxford University Press, p.8.

CHAPTER 3

SO_2 Electrolyser research and development for the HyS Process

3.1 Introduction

As the search for clean renewable energy has been increased with increasing demand and pollution worldwide, alternative energy sources have to be evaluated. Largely, these alternative energy sources include solar energy, wind energy, water electrolysis, and thermochemical processes. Currently both wind and solar energy have efficiency as well as long-term stability issues. Although water electrolysis has a relative low efficiency, with an operating voltage of 1.5 to 2V, it is a well established technology and provides a clean source of highly pure hydrogen. In the Hybrid Sulfur (HyS) Process, one of the thermochemical processes, sulfur dioxide is added to the general electrolyser design, thereby reducing the total energy input (0.158V vs 1.229V) thus increasing the electrolysis efficiency[1]. This addition of SO_2 in the electrolysis step was first introduced by Westinghouse Corporation's attempt to supply a renewable energy alternative through the HyS process[2].

As previously explained (Figure 1.3), a heat source (≈850°C) is used in the HyS process to decompose H_2SO_4 to produce SO_2, O_2 and H_2O according to *(3.1)*. After SO_2 and H_2O have been separated from O_2, the electrolyser can be supplied with the SO_2 (saturated) in H_2SO_4 and H_2O. While the SO_2 is used to depolarize the anode of the electrolyser (Figure 3.1), sulfuric acid is produced according to *(3.2)*. The produced protons can then migrate through the proton exchange membrane (PEM) and recombine with electrons supplied by the external power supply to form hydrogen *(3.3)*. H_2SO_4 can be concentrated if necessary and re-circulated to the acid decomposer for SO_2, H_2O and O_2 production to close the HyS cycle.

$$H_2SO_4 \rightarrow SO_2 + 0.5O_2 + H_2O \qquad (3.1)$$

$$SO_2 + 2H_2O \rightarrow H_2SO_4 + 2H^+ + 2e^- \qquad (3.2)$$

$$2H^+ + 2e^- \rightarrow 2H_2 \qquad (3.3)$$

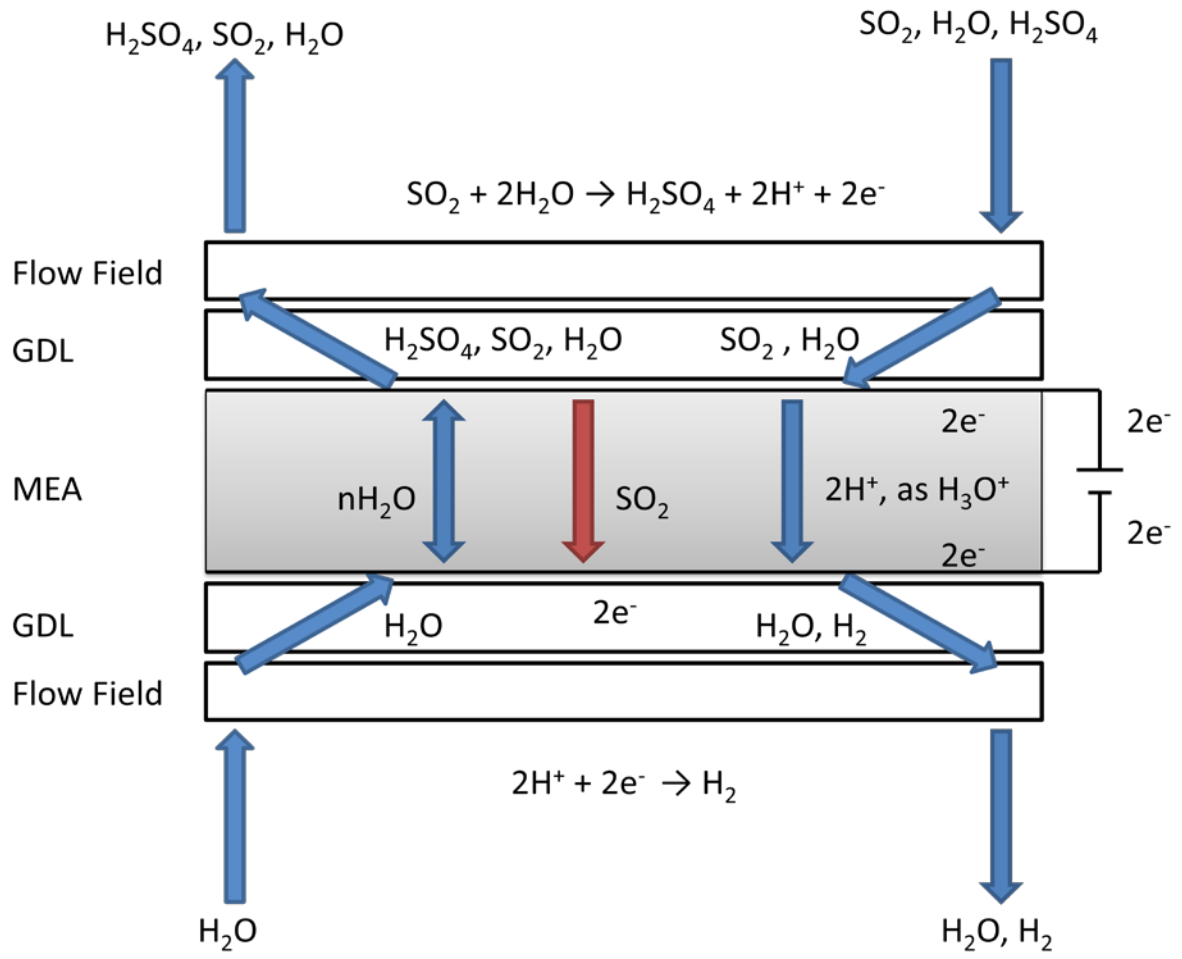

Figure 3.1 : Schematic representation of a gas-fed SO_2 electrolyser.

The SO_2 electrolyser consists of a proton exchange membrane (PEM) with a catalyst coating (usually Pt/C blends) on both sides, either attached to the membrane, which is known as a membrane electrode assembly (MEA), or attached to the gas diffusion layer (GDL), which is known as a gas diffusion electrode (GDE). Gas diffusion layers (GDL) are added to regulate the gas flow to and from the anode and cathode respectively, which are held in place by flow fields. Nafion® membranes, which are favoured in this highly corrosive environment, require the presence of water to transport the protons (H_3O^+) from the anode to the cathode side of the membrane[3].

The electrolyser performance is a function of a number of factors including membrane properties, material of construction, flow of reactants, properties of the electrocatalyst and applied voltages. The major challenges for the SO_2 electrolyser include:

i) producing acid resilient membranes with high proton conductivity,
ii) producing stable catalysts with high SO_2 kinetics in an acid environment for the SO_2 oxidation at the anode and the cathodic reduction of H^+ to H_2 *(eq3.3)*,
iii) producing highly concentrated H_2SO_4 to lower decomposition costs *(eq3.2)*,
iv) lowering possible side reactions while operating conditions are met and
v) solving issues pertaining to the materials of construction for long term operation.

The original Westinghouse electrolyser used a diaphragm to separate the anolyte from the catholyte[4]. However, operating voltages were significantly higher than the theoretical value (0.158V). A subsequent electrolyser was suggested by Struck *et al.*[5] replacing the diaphragm with a third liquid electrolyte to separate anolyte from catholyte. However, due to the difficulty of keeping the third electrolyte intact, alternative separators were investigated by Junginger *et al.*3. Nafion membranes showed the best performance and acceptable levels of chemical stability towards the sulfuric acid used[6].

A preliminary process flow-sheet analysis prepared by Gorensek *et al.*[7], determined that a thermal-to-hydrogen efficiency of 50% could be achieved when the desired operating conditions for the electrolyser were set at 500mA/cm^2 and 600mV. However, all previous saturated liquid electrolysers fall short of these criteria. Staser *et al.*[8] suggested a pure SO_2 gas-phase feed to the electrolyser instead of H_2SO_4 saturated with SO_2. This adjustment gave higher current densities than the liquid electrolyser; achieving 500mA/cm^2 @ 760mV, which complies with Gorensek's analysis for the optimum operating current density, in spite of the voltage which is still 160mV higher than recommended. The parameters identified that influence the gas fed electrolyser include the water transport, SO_2 crossover and the concentration of acid produced. The effect of water transport through the membrane was studied as a function of i) membrane thickness ii) H_2SO_4 concentration and iii) operating temperature[10]. The thinner Nafion® N212 membrane showed improved performance (reaching 1A/cm^2) than the thicker N115. A 1A/cm^2 will increase electrolyser effectiveness by 50% according to Gorensek *et al.*[9]. Membrane thickness also influences the acid concentration due to the lower water transport of thicker membranes. However by increasing the current density (A/cm^2 membrane), a more concentrated sulfuric acid product can also be achieved

with thinner membranes, which can then be decomposed at lower costs. They further found that an increased temperature resulted in better performance due to lower membrane ohmic resistance, which decreased from 0.584 Ω.cm^2 @ 50^{0}C to 0.265 Ω.cm^2 @ 90^{0}C.

Since the water transport across the membrane plays an important role in a gas-fed SO_2 electrolyser, a mathematical model was developed by Staser *et al.*[10] to predict the water transport due to diffusion, permeation and electro-osmotic drag. Using the net water flux, the authors could determine the sulfuric acid concentration produced as a function of membrane thickness, temperature and pressure differential across the membrane. They showed that the water flux increases with increasing H_2SO_4 concentration at low current densities due to an increasing concentration gradient across the membrane. Simultaneously, the water flux decreases when higher current densities are applied due to an increased electro-osmotic drag. At current densities above 500mA/cm^2, the water flux to the cathode due to the electro-osmotic drag is higher than the flux caused by the pressure differential and diffusion to the anode. Experimental studies, in conjunction with the model for water flux, showed that an increase in water flux will lead to a decrease in both the concentration of the produced acid and the cell voltage. A decrease in water flux on the other hand leads to a higher acid concentration which increases the cell voltage. It was shown from their study that the cell voltage increases with a decreasing pressure differential. Thus a thicker NR212 membrane will produce higher acid concentrations, at higher cell voltages, than a thinner N117 membrane due to lower water transport of the NR212[10].

Another aspect that influences the performance of the SO_2 electrolyser, is the SO_2 crossover from the anode to the cathode, resulting in possible side reactions (Table 3.1), which would both consume current needed for the maximum H_2 production as well as produce undesirable products at the cathode. Staser *et al.*[11] developed a model that quantifies the SO_2 crossover and shows how it is influenced by water transport across the membrane in a working electrolyser with an active area of 10cm^2.

Table 3.1 : Possible side reactions at the cathode[10,11,12]

Side Reaction	Equation	Catalyzed	Reference
$3H_2 + SO_2 \rightarrow H_2S + H_2O$	*(3.4)*	N	[12]
$3H_2S + SO_2 \rightarrow 4S + 2H_2O$	*(3.5)*	N	[11]
$SO_2 + 6H^+ + 6e^- \rightarrow H_2S + 2H_2O$	*(3.6)*	Y	[11]
$2SO_2 + 4H^+ + 4e^- \rightarrow H_2S_2O_3 + H_2O$	*(3.7)*	Y	[11]
$SO_2 + 4e^- \rightarrow S + O_2$	*(3.8)*	Y	[10]

The authors found that by controlling the current density, pressure differential and water transport across the membrane, the SO_2 crossover can be limited. At low current densities (<0.2A/cm^2), when no pressure differential is present, the water flux across the membrane is slow due to diffusion (water activity gradient). The SO_2 which is soluble in water can return to the cathode via convective flux, when the current density is increased and the electro-osmotic drag starts to dominate the water transport to the cathode.

Membranes other than Nafion have also been studied in terms of SO_2 transport. Elvington *et al.*[12] tested the SO_2 permeability and proton conductivity of a series of membranes and some of their results are shown in Table 3.2. From the data represented it seems that there exists a correlation between the current density and the SO_2 flux through the membrane despite the membrane characteristics.

Table 3.2 : Membranes tested for SO_2 crossover[12]

Membrane	SO_2 Flux (x 10^{-9}mol.s^{-1}.cm^{-2})	Conductivity (S.cm^{-1})	Current Density (mA.cm^{-2})
N115	5.23	0.0241	270
N211	21.8	0.0159	393
BPVE-6F	17.6	0.0109	335
BASF-Celtec-V	2.14	-	344
DuPont 1500 EW*	0.14	-	0.005

* Membrane with the lowest performance in terms of current density.

Kim *et al.*[13] performed similar tests on sPEEK (sulfonated polyetheretherketone) membranes for SO_2 permeability and ionic conductivity. While these membranes had higher SO_2 diffusion values at

higher temperatures (close to 75^{0}C) and sulfonation degrees (>60%), an advantage was achieved in terms of mechanical stability over the favourable Nafion membranes.

Selecting a catalyst for the best SO_2 reduction kinetics at the anode is also important in terms of overall effectiveness. While keeping in mind that the cathode catalyst must be inert to any corrosion/deposition by SO_2, its activity towards producing protons *(eq. 3.3)* have to be as high as possible. Colón-Mercado *et al.*[14] studied Pt supported on carbon (Pt/C, 45wt % Pt) and Pd supported on carbon (Pd/C, 40wt % Pd) for their activity and stability for the oxidation reaction *(eq. 3.2)*. Using cyclic voltammetry to determine overall stability and linear sweep voltammetry for activity measurements, they showed that the Pt blends had better activity and stability than the Pd blends. Catalyst loading was shown to have a negligible effect on electrolyser performance8.

So far a brief overview of the literature based research pertaining to SO_2 electrolysis was presented. In view of the South Africans Department of Science and Technology (DST) drive to establish this technology in SA, it was the aim of this study to develop and evaluate an electrolyser setup that can be used for further research on the SO_2 electrolysis for the HyS process in SA. To determine the efficiency of the setup, commercial MEA's (mainly Nafion® based) were purchased and evaluated in terms of SO_2 electrolysis.

3.2 Materials and methods

3.2.1 Materials

The electrolyser used in this study was manufactured and provided by Giner Electrochemical Systems LLC, and is based on previously developed direct methanol fuel cell hardware as shown in Figure 3.2. The cell plates were machined (serpentine flow fields) from non-porous graphite material provided by Electrochem, Inc. (Woburn, MA). End plates were used to achieve the necessary compression, which is attained with a torque wrench (6-8 in/lbs, RS Components). The electrolyser is heated by 40W Kapton heating pads connected to a temperature controller. A thermocouple can then be inserted in either of the holes provided on both the anode and cathode side of the non-porous carbon.

Figure 3.2 : SO_2 electrolyser cell based on direct methanol fuel cells supplied by Giner Electrochemical Systems.

The thermal expansion was corrected for by a silicon compression pad placed between the positive copper bus and the endplate. Pure SO_2 gas (Afrox, SA) was filled into a 1 gallon (3.785L) sampling cylinder (SS304, Swagelock SA) by lifting a 78kg SO_2 bottle (Afrox SA) to an angle of 45^0 and letting the liquid fill the sampling cylinder which had a SO_2 pressure ranging between 2.8–3 bar.

3.2.2 Methods

Figure 3.3 shows a schematic representation of the electrolysis setup used for the evaluation of different membrane electrode assemblies. N_2, H_2 or SO_2 can be supplied to the electrolyser via R1, R2 or R3 for flushing, testing and SO_2 operation respectively using V2 for SO_2 supply and V4 for N_2 or H_2 supply (the preliminary operational steps flushing & testing will be discussed in Section 3.2.2.1 followed by the SO_2 operation in Section 3.2.2.2). Water is fed from the catholyte vessel (GV3) to the electrolyser (cathode) using a peristaltic pump (WMB323, PP2). From the electrolyser the product water is sent to a water separator (GV2) to separate gasses and liquids. The separated gasses are then sent to a scrubber (GV4) to absorb all sulfur-containing species with hydrogen leaving the system through a flash back arrestor (V15). The separated water is returned to GV3 by means of a peristaltic pump (PP1), from where it can be returned to the cathode. When SO_2 gas is fed to the anode side of the cell via V5, the produced sulfuric acid and unreacted SO_2 is sent to a second separator (GV1).

A full Hazard and Operatibility (Hazop, Appendix B) study was done on the design to determine safety and operational procedures. This process was included to determine any hazards when using SO_2 and concentrated sulfuric acid and determine appropriate protocols for using the setup for each of the preliminary step discussed in Section 3.2.2.1 and 3.2.2.2.

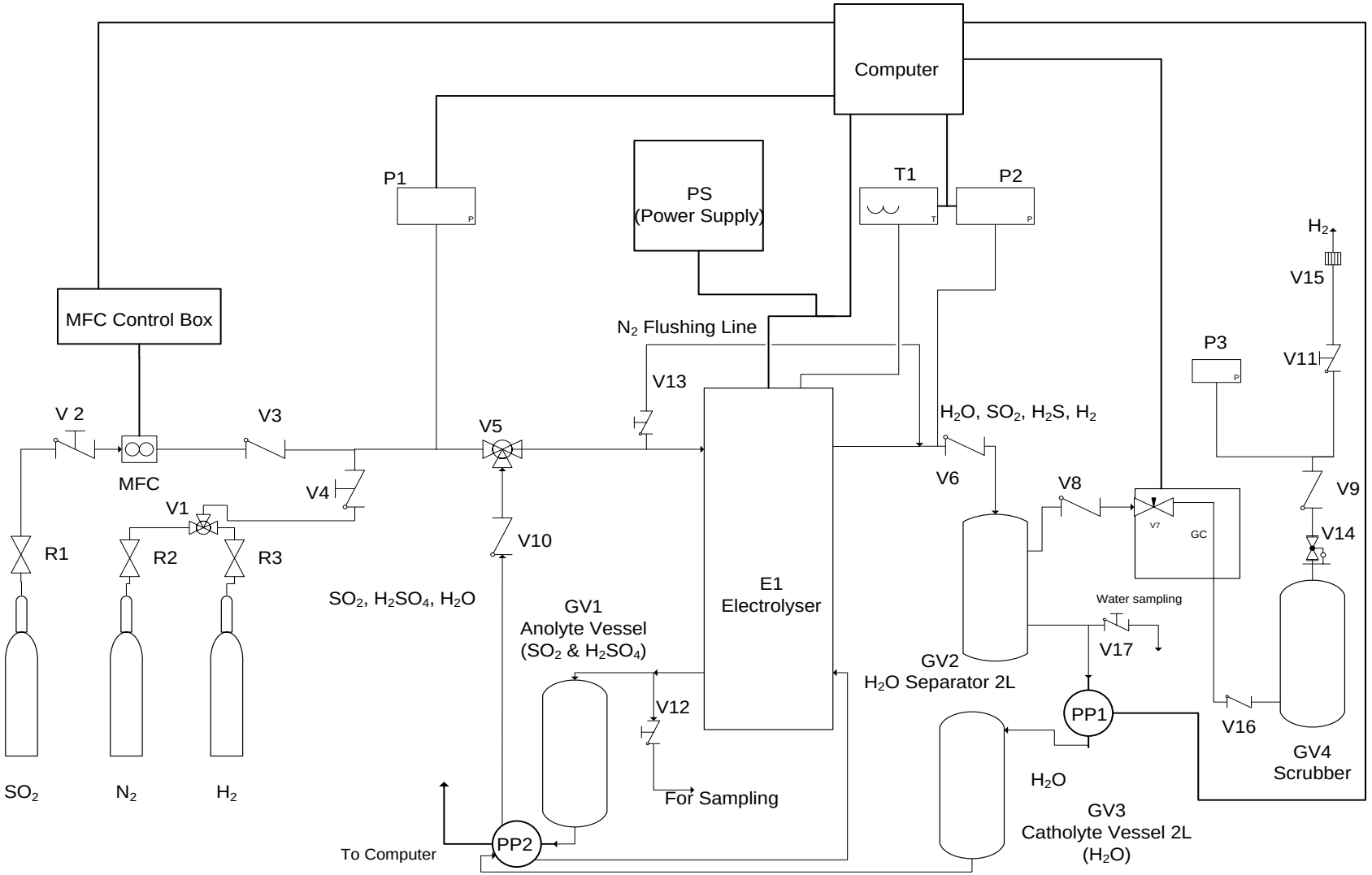

Figure 3.3 : Schematic representation of the SO_2 electrolyser setup.

The Hazop study included material design selections and for various areas of the setup as well as the development of appropriate protocols for each hazardous situation. These include for example a dripping tray for possible H_2SO_4 spillage and addition of PTFE non-return valves to prevent possible back pressure on the product stream which can damage the electrolyser cell. After the necessary changes recommended by the Hazop have been made to the initial setup, the following flushing, testing and SO_2 operation procedures were formulated for use with the SO_2 electrolysis setup. Appendix B also contains further information on assembling the MEA into the electrolyser cell.

3.2.2.1 Flushing and testing

Initially, the entire system must be pressure-tested as SO_2 gas is corrosive and poisonous. N_2 is used to pressurize the entire system (anode and cathode) to 150kPa. Subsequently, the system is left for 1 hour to detect any leaks by means of pressure drop. After a successful pressure test, N_2 is again used to flush the entire system at 1 bar for 15 minutes to ensure that no oxygen, which can cause corrosion, remains within the electrolyser system. With only N_2 gas present, the effectiveness of the MEA preparation can then be tested. For this, H_2 gas is used to flush the anode. After the H_2 had replaced all the N_2 and saturated the anode compartment, MEA operation was tested by supplying a current to the cell. For an effective MEA, a 1A/cm^2 should be achieved for H_2 oxidation (at the anode) and H^+ reduction (at the cathode) needing a maximum of 0.2V. This current density confirms that the protons migrate through the membrane and the electrons flow through the external electrical circuit without major resistance from the electrolysis cell. By connecting the SO_2 sampling cylinder to the setup via V2, the system can be supplied with SO_2 gas. DI water (pre-heated to 88^oC using a water bath, not shown in Figure 3.3) is then supplied (100mL/min) to the electrolysis cell using a peristaltic pump (PP1, WMB 323) while heating the end plates of the electrolyser cell to 80^oC using heating pads. SO_2 can then be introduced to the anode after the flushing and testing has been successfully concluded. The GC and computer were added to evaluate the product gas and control the automation of the electrolyser respectively.

3.2.2.2 SO_2 Operation

Before initiating SO_2 operation, the scrubber solution (GV4) is circulated (Pump not shown in Figure 3.3) to ensure total sulfur chemisorption. Subsequently, the contact between the SO_2 gas and the electrode must be ensured. By supplying a low flow of SO_2 (20cm^3/min) to the anode for 1 minute (removing any H_2 from the testing step and saturating the compartment) before a current density of 50mA/cm^2 (1.25A) is applied. When the voltage remained stable for 2 – 3 minutes, the current

density can be increased by 50mA/cm^2 increments to 650mA/cm^2. The applied voltage must be kept below 1.2V to prevent irreversible corrosion of the carbon based materials used in the electrolyser.

For this study Nafion® 1135, 117a & b, and 115a & b (Table 3.3) were tested for the SO_2 electrolysis at a constant ΔP=0 at 50^{o}C & 80^{o}C. The conversion rate of SO_2 was kept at 20% for all tests performed. Table 3.3 shows the different membranes tested with their respective properties.

Before doing the hydrogen pump test, the influence of temperature (10 – 80^{o}C) on ohmic cell resistance was determined for N117a, N115a and N1135 (Section 3 of Appendix B). The effect of membrane thickness was hence evaluated by comparing N117a, N115a and N1135 using polarization curves. The difference in catalyst loading was evaluated in terms of N115a (1mg/cm^2) vs N115b (0.5mg/cm^2) and N117a (0.3mg/cm^2 vs N117b (0.5mg/cm^2). The MEA with 1mg/cm^2 was supplied by Prof Vijay K Ramani (and students) from Illinois Institute of Technology through personal communication. Finally, the hydrogen production was measured for N115a, N117a and N1135. A SEM analysis (using a FEI Quanta 200 ESEM instrument) was also performed on N1135 to evaluate the MEA visually after SO_2 operation.

Table 3.3 : Membranes tested for SO_2 electrolysis.

Membrane	Thickness*	Catalyst Loading (mg/cm^2)	GDL	Supplier
N1135	3.5 mils (86 µm)	0.6	Hot pressed	Giner Electrochemical Systems
N117a	7 mils (171.5µm)	0.3	Separate layers	Ion-Power
N117b	7 mils (171.5µm)	0.5	Separate layers	Fuel Cell Store
N115a	5 mils (122.5µm)	1	Separate layers	Prof Vijay Ramani**
N115b	5 mils (122.5µm)	0.5	Separate layers	Fuel Cell Store

*Based on dry membrane, 1 mils equals 25.4µm.

** Prof Vijay K. Ramani, Illinois Institute of Technology, Chemical & Biological Engineering, Suite 127, Perlstein Hall, 10West 33rd Street, Chicago, IL 60616.

After successfully testing various membranes the influence of water pressure across the membrane i.e., cathode to anode, was investigated to determine the effect of pressure on the overall cell performance. The water pressure was increased to ΔP = 1 bar using a pinch valve at the exit of the cathode water. To maintain a constant pressure differential, the peristaltic pump (PP2) was replaced by a magnetic gear pump (Cole-Palmer). The cell temperature was kept constant at 80^{o}C with a water feed of 100mL/min. A Nafion® 115b membrane was used for this experiment.

3.3 Results and discussion

The overall performance of the gas-fed SO_2 electrolysis cell is a function of numerous variables including water transport, acid concentration produced, SO_2 transport, membrane thickness, operating temperature, equivalent weight of the membrane, electrical cell resistance of the cell and operating pressure differential as well as the catalyst and catalyst loading. Although all these factors contribute to the overall operating voltage, the water and SO_2 transport seem to contribute to the majority of the over-potential. The water transport across the membrane influences the acid concentration produced at the anode since more water results in a lower acid concentration and thus a lower operating voltage8. The water transport across the membrane is a function of the material, membrane thickness, pressure differential and acid concentration. Thicker membranes have a lower water permeability, which results in a decreased amount of water at the anode and thus a higher acid concentration8. Similarly, membrane resistance to SO_2 electrolysis decreases with increasing temperature due to an increase in the water transport8. The ability of proton exchange membranes to transport H^+ from the anode to the cathode is influenced by the equivalent weight, which is a measure of active (SO_3H) sites that facilitate this transport effect. A membrane with more active sites will therefore have a lower operating voltage. The electrical resistance across the membrane also influences the operating voltage of the cell according to ohms law. Thus, a higher electrical resistance will increase the over-potential of the system which will increase and add to the total over-potential. Although polymer membranes are known for their weak mechanical stability, an increased water pressure at the cathode reduces the operating voltage. Firstly, increased cathodic water pressure increases the amount of water present at the anode, which in turn decreases the acid concentration (lower operating voltage). Secondly, an increased water pressure decreases the SO_2 transport due to convective flux (SO_2 flow due to water transport)[10,11].

In Section 3.3.1 a comprehensive evaluation on the in-house built electrolyser and the variables influencing SO_2 electrolysis are presented. In this section all studies were done at no pressure differential ($\Delta P = 0$) across the membrane. In section 3.3.2, the effect of pressure differential of $\Delta P = 1$ is presented.

3.3.1 SO_2 Electrolysis

The effect of ohmic cell resistance as a function of temperature was first evaluated (3.3.1.1). Subsequently, a favourable temperature (80^oC) was chosen to test the MEAs using the H_2 pump test (3.3.1.2). Following the successful H_2 test, the effect of temperature on the SO_2 electrolysis was evaluated using polarization curves (3.3.1.3). Then, the influence of membrane thickness (3.3.1.4) and catalyst loading (3.3.1.5) on SO_2 electrolysis was tested. All above data were produced with no pressure differential over the membrane. Finally, we present the effect of membrane type and temperature on hydrogen production (3.3.1.6) determining prior to disassembly and SEM analysis of the N1135 MEA (3.3.1.7).

3.3.1.1 Cell resistance as a function of temperature

Staser *et al.*[10] showed in a previous study that a pressure differential had no measurable effect on the cell resistance8. Therefore the cell resistance was only determined at ΔP = 0. The 3 membranes tested were chosen based on thickness differences to determine the effect of membrane thickness on cell resistance as a function of temperature. After assembling an MEA into the electrolyser cell, the electrical resistance was measured to confirm correct assembly. Although the type and thickness of the membrane tested influences the electrical resistance, its influence should not exceed 40mΩ at 25^0C. It is further known that the AC resistance for PEM electrolysers should decrease with increased temperature8. Figure 3.4 show the AC resistance dependence of N117a, N115a and N1135 on the temperature of the cell.

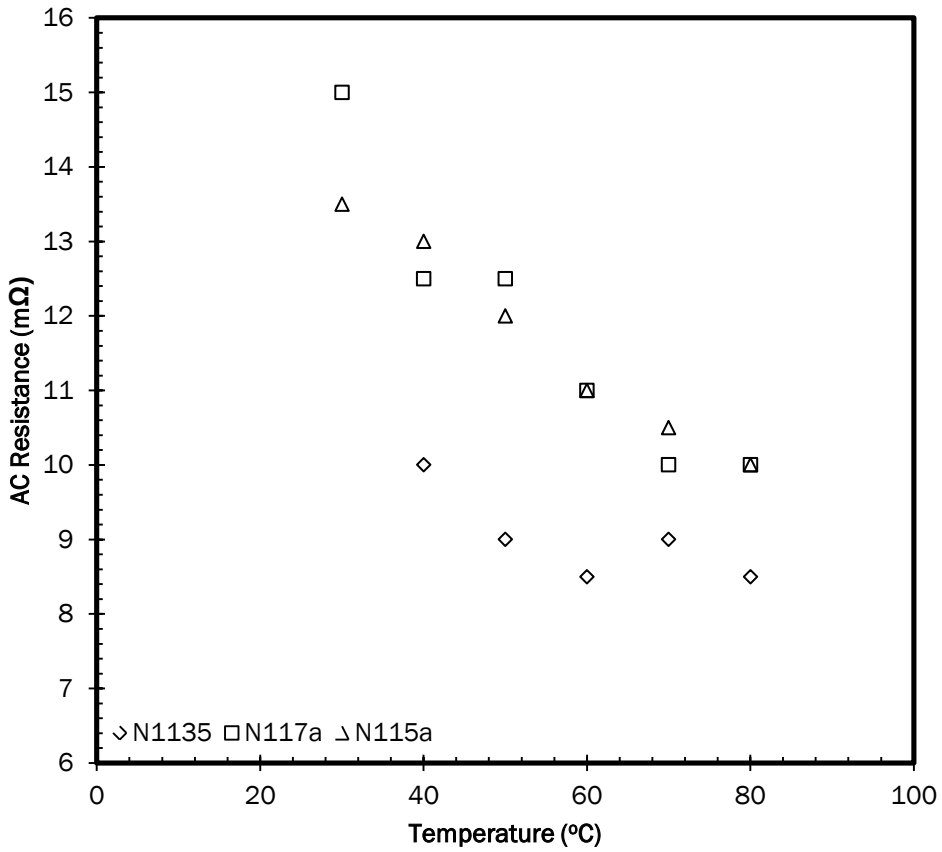

Figure 3.4 : AC resistance as a function of temperature for N1135, N115a and N117a.

From Figure 3.4, it can be concluded that the membrane thickness has a influence on the electrolysis efficiency. The thicker N117a membrane (on average) had a higher over-potential than the thinner N115a which in turn had a slightly higher over-potential than the thinnest N1135. The results also confirmed that a higher temperature decreases the ohmic cell resistance. For N1135, no significant decrease in resistance was, however, observed above 50°C. While increased temperatures seem advantageous, Nafion® membranes have the disadvantage of a significant decrease in mechanical stability at temperatures above 90°C due to water plasticization, although increased water pressure can reduce this effect up to a temperature of 130°C[15].

However, irrespective of the type of membrane or temperature, it was clearly demonstrated that the electrolyser cell and setup was correctly assembled and functioning properly with AC resistances varying between 8 and 15mΩ.

3.3.1.2 Hydrogen pump tests

To ensure correct MEA fabrication and cell assembly, the H_2 pump method was used to determine whether suitable contact between the MEA and the gas diffusion layers existed. The amount of volts needed to initiate the reaction should be low (≈30mV). Although the voltage should be 0.00V according to the table of standard reduction potentials but some resistance within the catalyst layer does exist. Figure 3.5 shows a polarization curve indicating the low voltages that were required (<0.2V) to attain 1A/cm^2 for N1135.

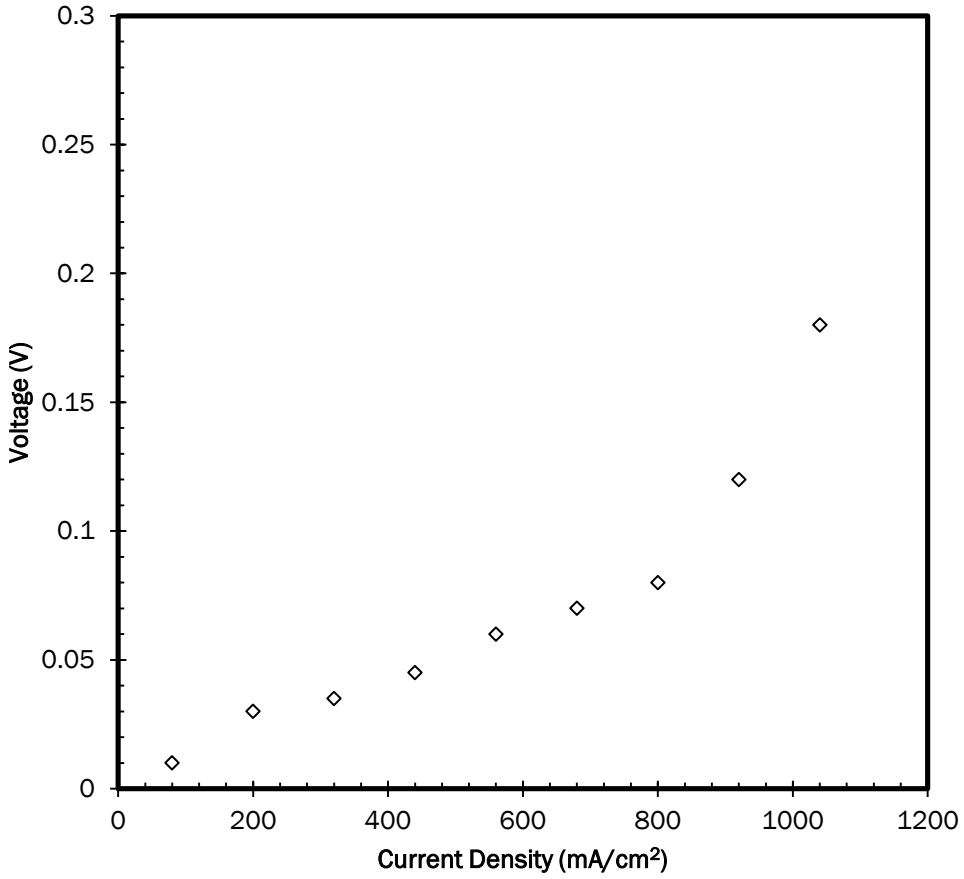

Figure 3.5 : H_2 pump test results for N1135 at 80^{o}C .

From the low voltage obtained (0.17V @ 1A/cm^2), it can be concluded that the contact between the GDL and MEA is sufficient for H^+ and electron transfer implying that the cell was ready for the introduction of SO_2. The H_2 pump tests were not performed for the other membranes tested, as the introduction of SO_2 (for N1135) compromises the graphite plates.

3.3.1.3 Temperature influence on SO_2 electrolysis

The effect of temperature (50°C & 80°C) on the overall performance is shown for the N117a, N115a and N1135 membranes in Figure 3.6, Figure 3.7 and Figure 3.8 respectively. The decrease in performance at lower temperatures for N117a (0.71V vs 0.93V @ 300mA/cm^2) is partly due to the higher electrical cell resistance discussed in Section *3.3.1*. Water transport and hence the amount of water at the anode also increases with increasing temperature which results in lower operating voltage as a result8. The water deficiency at the anode at low temperatures will result in the production of more concentrated sulfuric acid which increases the operating potential8.

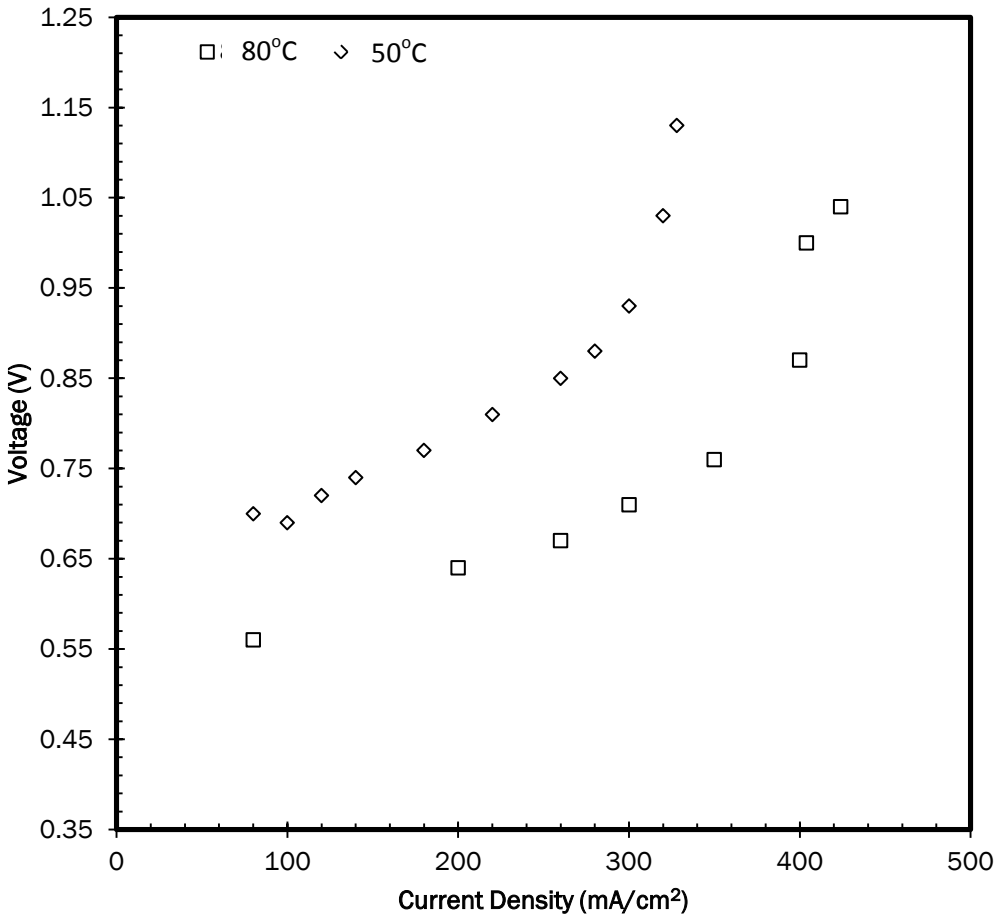

Figure 3.6 : Effect of temperature on SO_2 electrolysis for N117a

In Figure 3.7, the V-*i* curve of N115a is presented. When comparing these results to the data achieved for the N117a membrane (Figure 3.6), it becomes clear that the N115a membrane performed significantly better (0.78V @ 500mA/cm^2) than the N117a (0.76V @ 350mA/cm^2) at 80^{o}C, which for N115a is still 0.18V (N115a) above the required voltage (0.6V @ 500mA/cm^2) for a 50% thermal-to-electrical efficiency9. The same temperature trend was, however, observed for N115a, i.e. an increase in efficiency with increasing temperature.

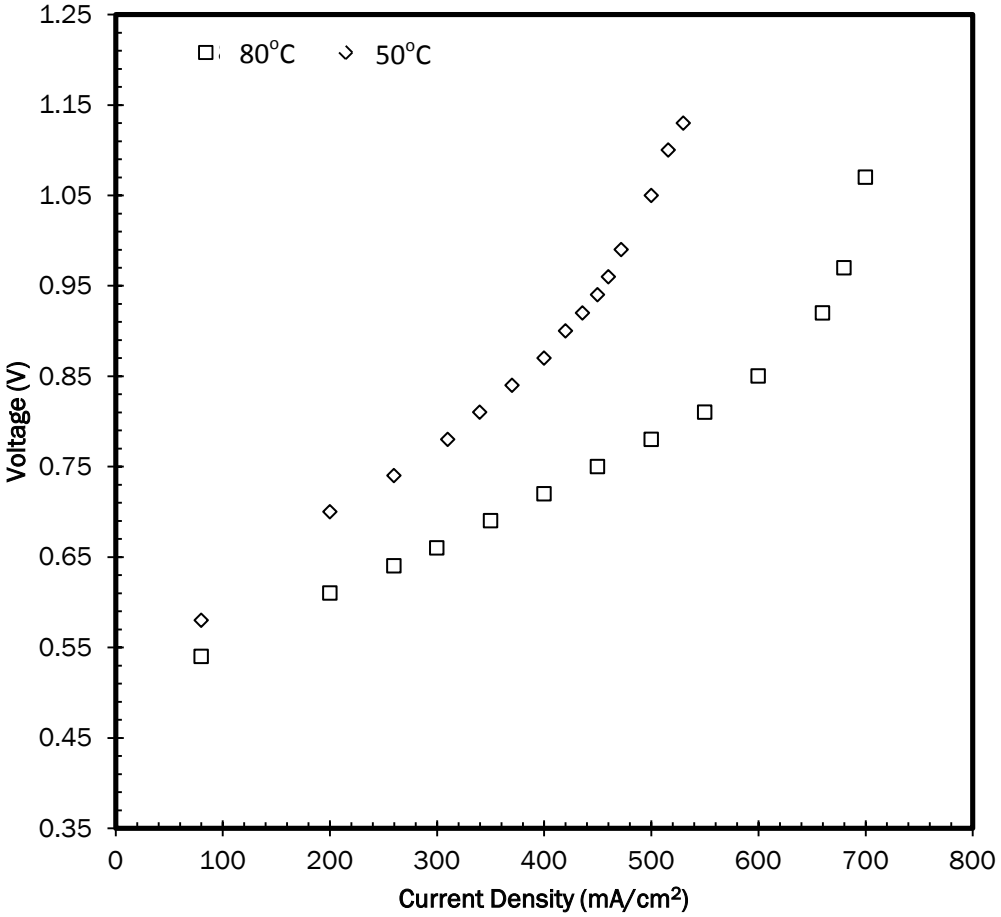

Figure 3.7 : Effect of temperature on SO_2 electrolysis for N115a

During the N115a testing, it was observed that the water recirculation at the cathode turned milky white. This observation was probably caused by SO_2 transported through the membrane to the cathode and dissolving in the water. By increasing the water pressure across the membrane on the cathode side, the SO_2 crossover would probably be decreased. Over time the dissolved SO_2 would initiate some of the side reactions presented in Table 3.1. However, for the short duration required to obtain these V-i curves (approximately 45minutes), no side-effects were observed in terms of cell performance.

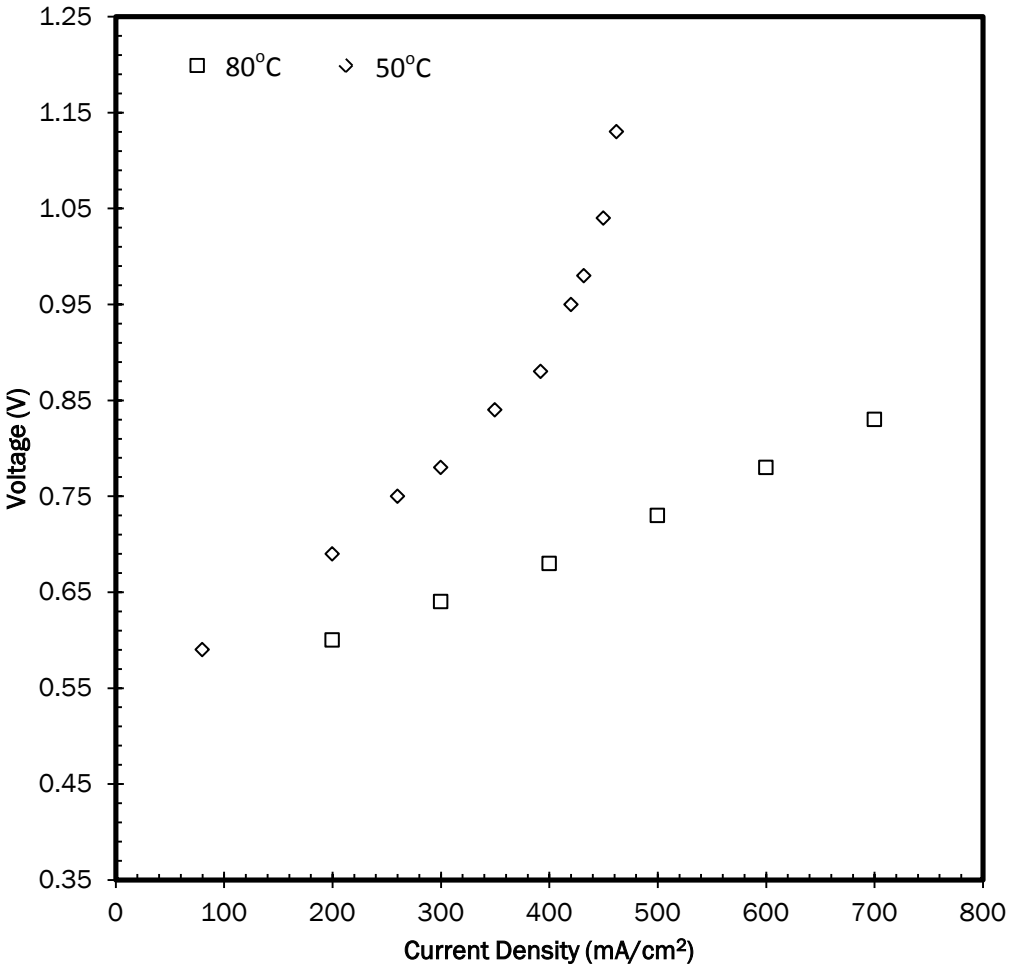

Figure 3.8 : Effect of temperature on SO_2 electrolysis for N1135.

In Figure 3.8 the V-*i* curves of N1135 are presented at 50°C and 80°C. The polarization curves for both N115a and N1135 are very similar at low voltages. However, at higher voltages it is still interesting to note that the N115a performed better at low temperatures, while the N1135 performed better at high temperatures. This implies that at higher temperature, which is where the best performances were observed for all the membranes, the efficiencies increased in the order N117a < N115a < N1135, showing that the thinnest membrane had the highest performance. Simultaneously however, an increase in SO_2 crossover was observed for the thinnest membrane (N1135) when compared to the thicker N115a and N117a.

It was previously shown that if the SO_2 transport could not be eliminated, the long term operation of the electrolyser will have a steady increase in over-potential as the side-reactions will decrease the

catalyst efficiency. This implies that at ΔP = 1 a balance has to be found between the inverse properties of cell efficiency and SO_2 crossover.

3.3.1.4 Effect of membrane thickness on cell efficiency

It has previously been shown that membrane thickness has a noticeable effect on the performance of SO_2 electrolysis8. Thinner membranes have higher water transport which decreases the acid concentration produced at the anode. This decreased acid concentration allows for lower operating voltages and improved cell stability[10]. In Figure 3.9, the V-i curves for N115b, N117b and N1135 at 80°C are combined for comparative purposes at 80°C. The figure clearly shows the effect that membrane thickness has on the operating voltages especially as the current density is increased. It must be noted that N1135 is compared to N115b and N117b and not to the membranes used in Section 3.3.1.3 as these membranes had different catalyst loadings (see Table 3.3). Although N1135 has more Pt catalyst (0.1mg/cm^2) than N115b and N117b, it did not influence the values significantly.

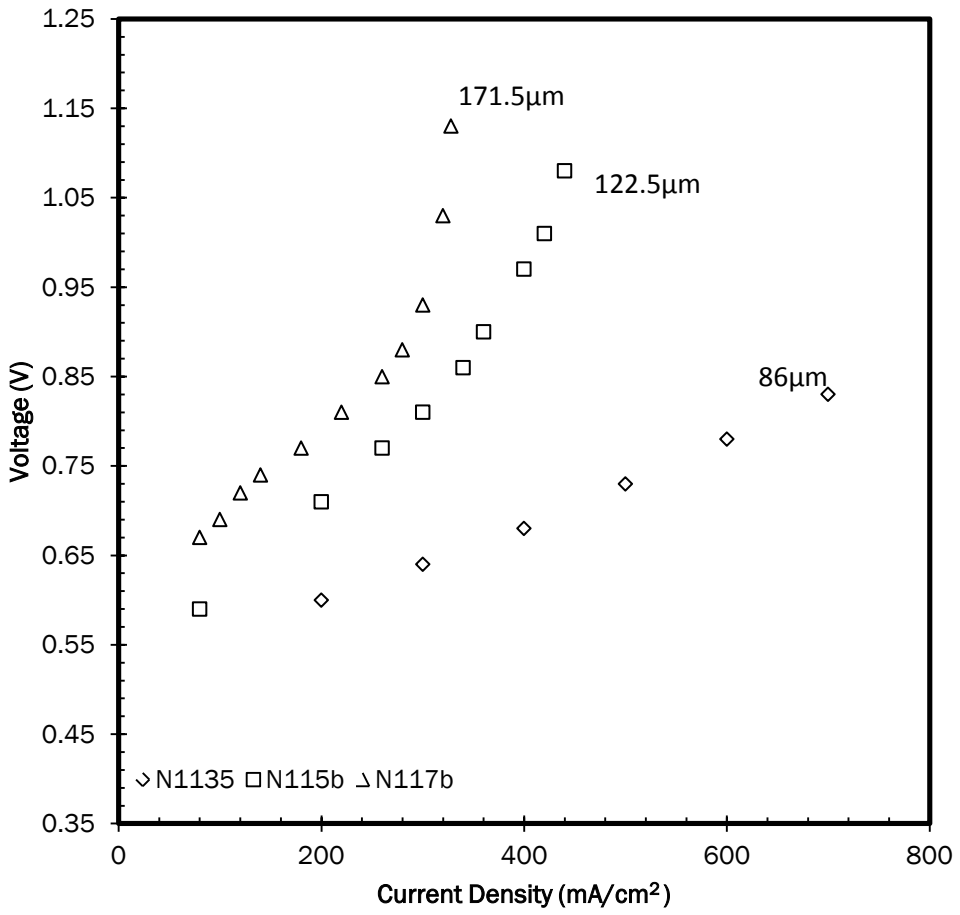

Figure 3.9 : Effect of membrane thickness on SO_2 electrolysis at 80°C.

The thickest N117b (170µm) produced more concentrated acid[10] (lower water transport) than the N1135 (86µm) and N115b (122.5µm), which resulted in a decreased cell performance (visible from the voltages reached by N115b and N1135) and N117b could therefore not reach 500mA/cm^2 (due to the increased over-potential) whereas the N115b and N1135 could. The best performance was obtained for the thinnest N1135, which reached 500mA/cm^2 at 0.73V.

In Section 3.3.1.3, it was also shown that the thinnest membrane yielded the highest efficiency. This confirms that this relationship between membrane thickness and cell performance holds irrespective of the catalyst loading which is the only difference between N117a and b and N115a and b.

3.3.1.5 Effect of catalyst loading on cell performance

Catalyst loading directly affects the cost of MEA fabrication and thus the cost of the entire process. Two N115 membranes with 1 mg/cm^2 (N115a) and 0.5mg/cm^2 (N115b) have been tested for SO_2 electrolysis (Figure 3.10). In previous studies, Staser *et al.*[8, 10, 11] showed that the catalyst loading had a negligible effect above 0.2mg/cm^2, while catalyst loadings below 0.2mg/cm^2 resulted in a significant increase in over-potential.

However, from Figure 3.10 it seems that the different catalyst loadings used in this study had a noticeable effect on the overall performance, with the higher catalyst loading yielding a lower voltage at similar current densities. Although the performance (for N115a) is comparable with that of Staser *et al.*[10], for short periods of time, the SO_2 transport in this study was observed to be significantly higher than what was achieved when operating the cell at increased water pressure[16].

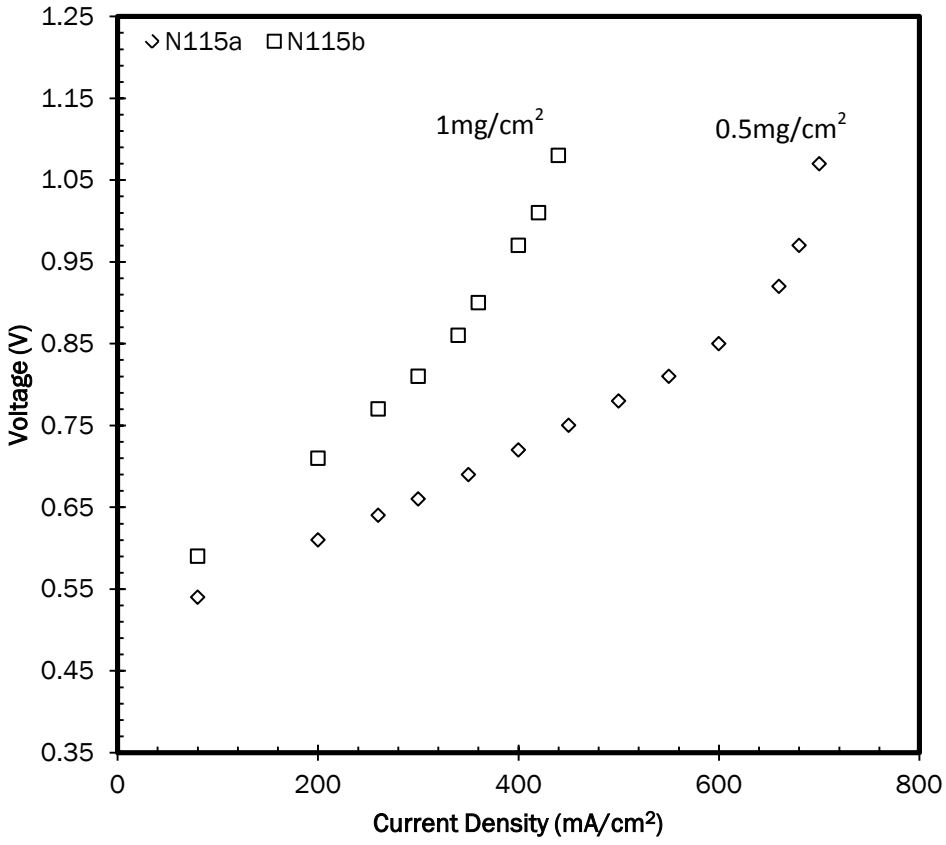

Figure 3.10 : Effect of catalyst loading on SO_2 electrolysis for N115a & b at 80^{o}C.

From literature it is clear that the cell assembly, specifically the GDL compression, could have had an influence on the cell operation[17]. The placement and compression of the GDLs directly influence the GDL's ability to transport electrons. Thus, the electrical resistance could have increased if the GDL's had not been fitted correctly or crushed between the graphite flow fields. This misalignment was confirmed when the electrical resistance of the cell was determined during SO_2 operation with the average cell resistance being 9 and 12 mΩ for N115a and N115b respectively. That the GDL of N115b had probably been damaged was confirmed when comparing the effect of catalyst loading for N117a and b (Figure 3.11).

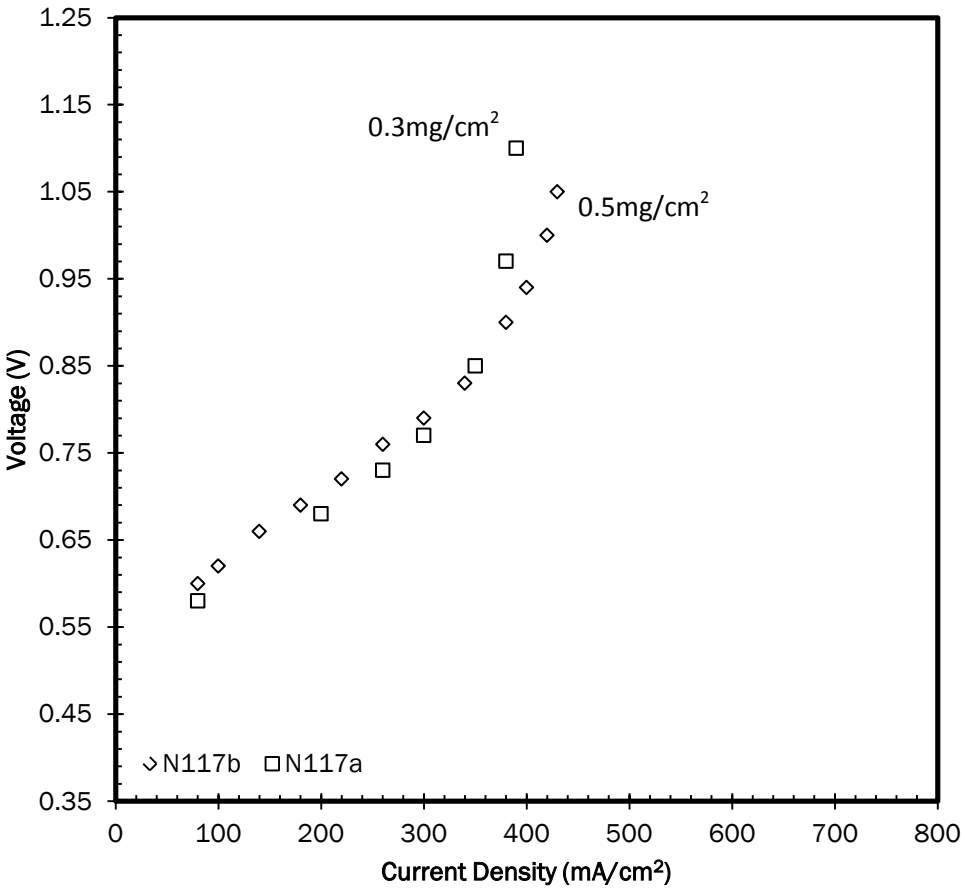

Figure 3.11 : Effect of catalyst loading for N117a & b at 80°C.

It is clear from Figure 3.11 that for N117 the effect of catalyst loading was negligible. This was also evident from the ohmic resistance for both catalyst loadings differing by 1mΩ (13mΩ for N117a and 12mΩ for N117b). From Figure 3.10 and 3.11 the effect of cell assembly is clearly an important factor in cell operation.

3.3.1.6 Hydrogen production

For adequate efficiency (Figure 1.3, *Section 1.2.2*), the hydrogen production must be maximized at the optimum voltage of 0.6V. In Figure 3.12 the H_2 production as a function of voltage at 80°C is presented for N1135, N115a and N117a. Hydrogen production for both the N117a and N115a are in the 80mL/min range at 0.7V, while N1135 achieved 125mL/min at the same voltage. Similar trends were observed for N115b and N117b (not shown) when compared to N115a and b. In Fig 3.12 the

direct relation between voltage and H_2 production is clearly illustrated, i.e. hydrogen production increased linearly with increasing voltage.

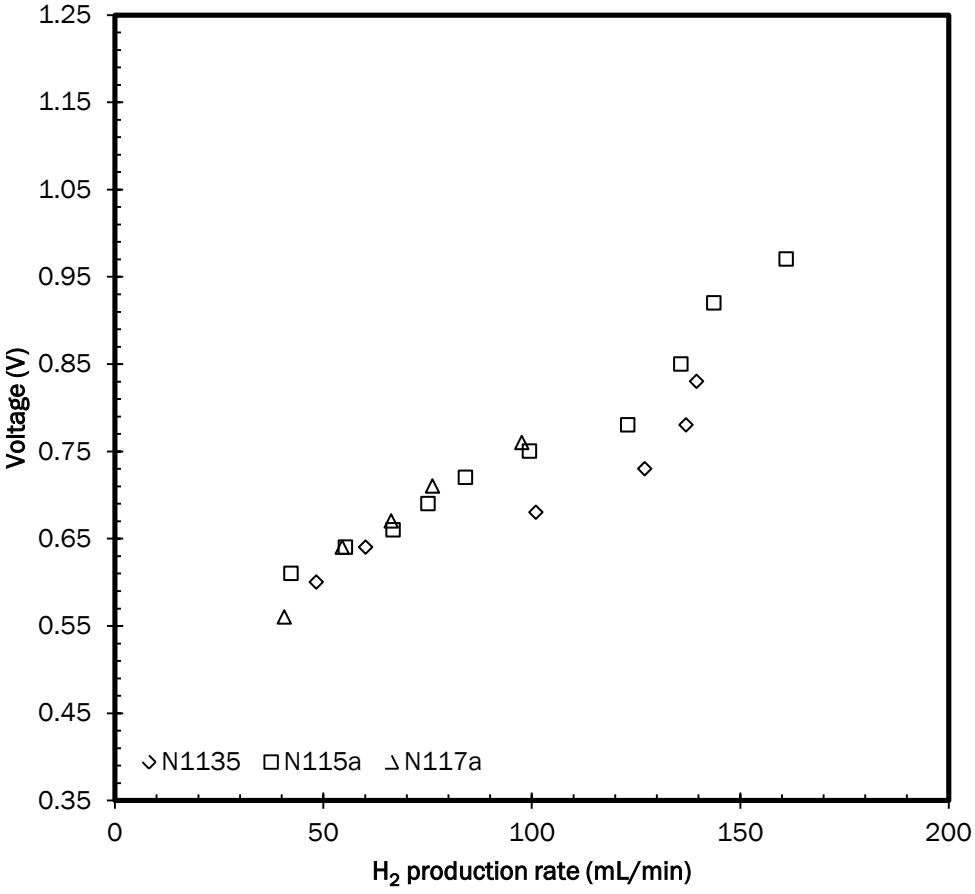

Figure 3.12 : H_2 production rate as a function of voltage at 80^{o}C.

As discussed in Section 3.3.1.3 Temperature influence on SO_2 electrolysis, temperature significantly influences the operating cell voltage of SO_2 electrolysis. In Figure 3.13, the influence temperature had on the hydrogen production rate is clearly illustrated where the higher temperature yielded higher H_2 production rates than the lower temperature irrespective of voltage. This further supports the previously mentioned need for higher operating temperatures. Similar trends were observed for the other membranes (N1135, N117a) tested (results not shown).

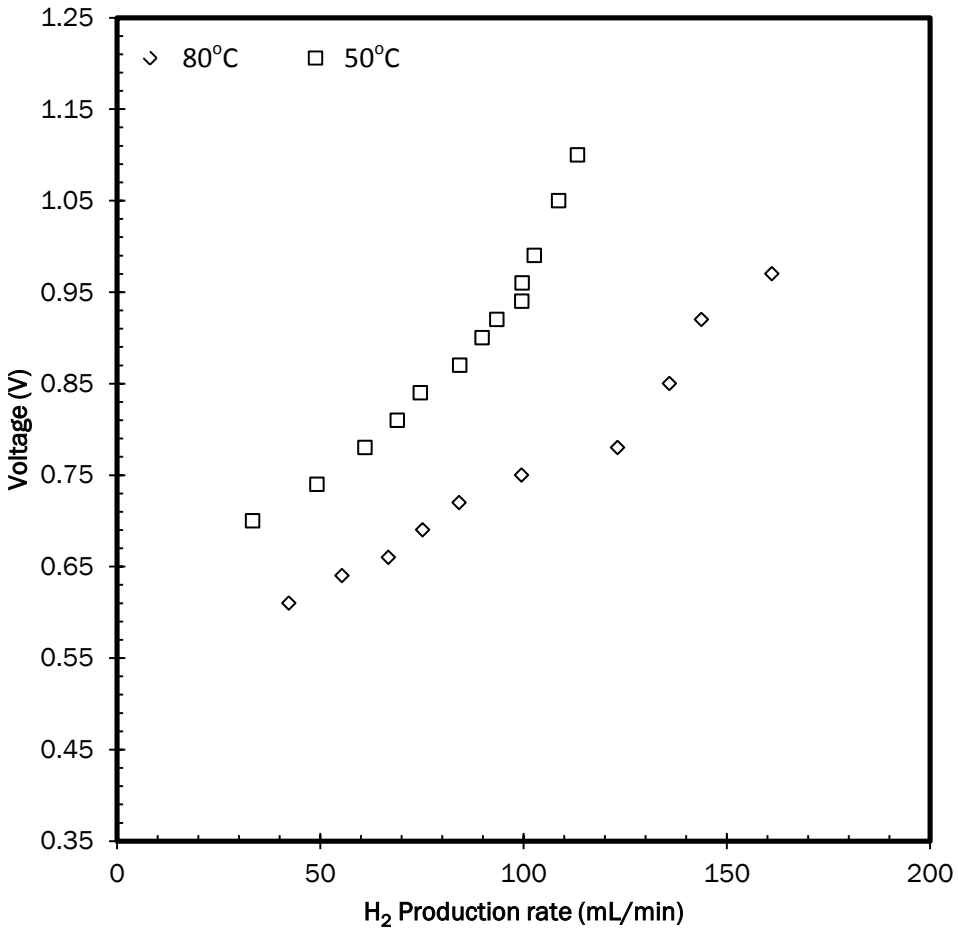

Figure 3.13 : Temperature dependence on H_2 production rate for N115a.

The increased performance at elevated temperatures has been ascribed to the increased water content of Nafion® type membranes, which facilitates proton conductivity across the membrane resulting in an increased H_2 production rate.

3.3.1.7 SEM analysis of N1135

SEM images were taken of the best performing N1135 membrane in terms of polarization curves and hydrogen production, to evaluate the MEA after SO_2 operation. Although no control images were taken (before SO_2 operation) the images can be used to evaluate if any elemental sulfur was formed between the membrane and cathode GDL.

As can be seen from Figure 3.14 : Cross sectional view of a N1135 MEA. the catalyst coated Nafion® membrane is centered between two carbon papers which make up the MEA. It can also be seen that the membrane thickness can be roughly estimated to be between the 80-90µm as Table 3.3 showed earlier. The lighter parts on both sides of the membrane indicate the Pt catalyst particles.

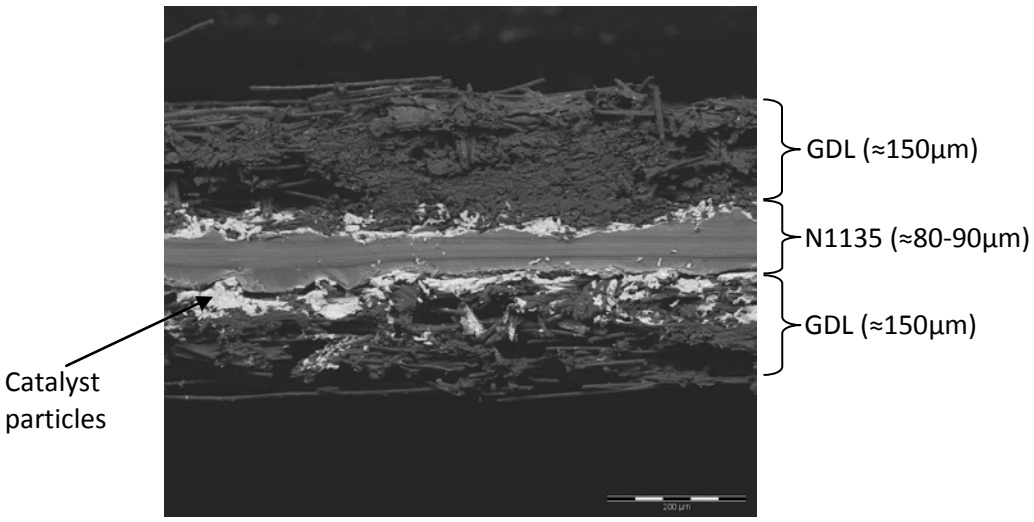

Figure 3.14 : Cross sectional view of a N1135 MEA.

A line-scan was performed across the cross-section of the N1135 membrane after 4 hours of operation using EDX (Figure 3.15). Figure 3.15a shows clearly the carbon distribution of the N1135 membrane between 150µm and 210µm and the areas of the GDLs on both sides of the membrane, i.e. above 210µm (anode GDL) and below 150µm (cathode GDL).

The fluorine distribution (Figure 3.15b) is added for completeness and shows clearly the area where the fluorine containing Nafion® membrane is present, i.e. between 150 and 210µm, with little fluorine having migrated into the GDL layers.

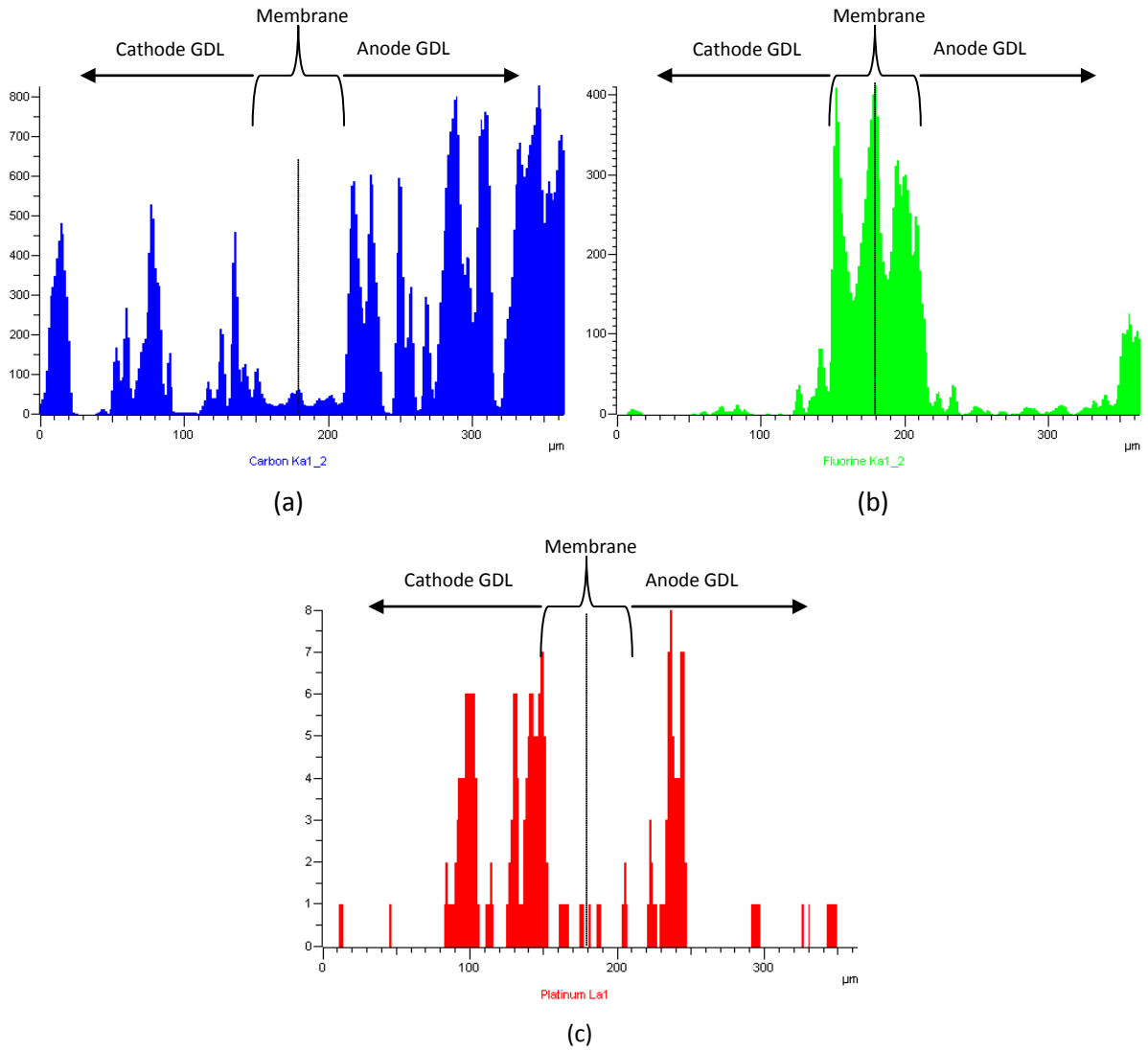

Figure 3.15 : EDX line scan through the cross section of N1135 and GDL in terms of (a) carbon, (b) fluorine and (c) platinum.

It is clear that in order to achieve long term operation of the MEA efficiency; the catalyst must remain between the membrane and GDL material. Catalyst migration through the membrane would decrease the active area and thus decrease operation efficiency of the electrolyser. From Figure 3.15c, it is clear that some platinum particles (at the cathode) have moved away from the membrane into the GDL. This movement of platinum particles was first suspected to be due to migration as a result of electro-osmotic drag (electron flow from the anode to cathode) and SO_2 transport via convective flux which could force the Pt away from the membrane and into the GDL. However, sample preparation could have influenced the line scan analysis in terms of the Pt particles. It is suspected that due to incorrect sample preparation some Pt particles could have been forced (by the scalpel used to cut the membrane) into the GDL material as the MEA was cut from the anode to the cathode. It has further been shown that electro-osmotic drag has a negligible effect at current

densities greater than 200mA/cm^{2,} 8. The sample preparation could also have contributed to the small amounts of Pt observed within the membrane (150µm-210µm). It is hence not possible to give conclusive evidence of Pt migration. Further work is thus necessary to optimize the sample preparation for membrane electrode assemblies.

3.3.2 Cathode water pressure increased to 100kPa

It was shown by Staser *et al.*[10] that increased cathode water pressure has a significant effect on the cell performance. This increased performance was ascribed to i) increased water at the anode to reduce the acid concentration produced and ii) reduced SO_2 transport to the anode. In our study this effect was investigated with a pressure differential of 100kPa cathode to the ambient gas pressure at the anode, which was the maximum pressure differential possible for this cell design. Although this pressure is not entirely representative of the pressure differential used by Staser *et al.*[10] which was 700kPa at the cathode and 100kPa at the anode, it was possible to obtain some idea of the effect of water pressure.

Both the N115a and N1135 membranes were tested at these elevated pressures. Although these membranes had good performance with no pressure differential across the membrane, they showed significant increase in over-potential at a ΔP of 100kPa. The N115a achieved a poor 0.74V @ 200mA/cm^2, while the N1135 gave 0.77V @ 80mA/cm^2. This performance decrease could be due to water saturation of the anode GDL, which would force the SO_2 gas to dissolve into the water and diffuse to the catalyst layer. This will increase the over-potential significantly due to the imposed mass transfer limitations. This explanation was confirmed when the cell was disassembled, where it was noticed that the hydrophobic GDL on the anode side was saturated with water.

The higher over-potential evident from the performance of N1135 could be assigned to higher amounts of water at the anode GDL interface than with the slightly thicker N115a. This would mean that the mass transfer limit was increased as the distance of SO_2 diffusion increased with more water present.

3.4 Conclusion

From the experimental data presented, it can be concluded that a working electrolyser setup was successfully constructed in spite of certain limitations which were presented with this setup. It was shown that membrane thickness had a significant influence on the operating voltage which will remain an important aspect for further electrolyser system optimizations. Even with an improvement on the operating voltages (0.73V at 500mA/cm^2) over those achieved in previous studies, the current performance would not be sustainable for long operation times as the higher SO_2 transport across the membrane will decrease the effectiveness of catalyst due to side reactions.

It has clearly been shown that thinner membranes and increased operating temperatures are of importance for decreasing the ohmic resistance which in turn will lower the SO_2 electrolysis operating cell voltage. Although lower ohmic cell resistance will improve cell performance, membranes for high temperature operation (>100^oC) must be developed and tested for both SO_2 transport and proton conductivity to maintain long term stability.

Future work will include an in-depth investigation on the effect of membrane thickness and equivalent weight on the overall performance of the electrolysis cell. The effect of a differential pressure across the membrane on membrane performance will be further investigated once a high-pressure setup has been developed. Reducing the SO_2 transport across the membrane remains a critical parameter, while maintaining high proton conductivity, as this will reduce the operating costs for long term operation.

3.5 References

[1] W. Juda, D. M. Moulton, *Chem. Eng. Prog*., **63**, 59-60 (1967).

[2] L. E. Brecher, S. Spewock, C. J. Warde, *Int. J. Hydrogen Energy*, **2**, 7-15 (1977).

[3] R. Junginger, B. D. Struck, *Int. J. Hydrogen Enegry*, **7**, 331-340 (1982).

[4] L. E. Brecher, S. Spewock, C. J. Warde, *Int. J. Hydrogen Energy*, **2**, 7-15 (1977).

[5] B. D. Struck, R. Junginger, H. Neumeister, B. Duka, *Int. J. Hydrogen Energy*, **7**, 43-49 (1982).

[6] R. Junginger, B. D. Struck, *Int. J. Hydrogen Enegry*, **7**, 331-340 (1982).

[7] M. B. Gorensek, W. A. Summers, M. R. Buckner, Z. H. Qureshi, AlChE 2005 Annual Meeting, Session 348, Paper 348c (2005).

[8] J. Staser, R. P. Ramasamy, P. Sivasubramanian, J. W. Weidner, *Electrochem. Solid-State Letters*, **10**, E17-E19 (2007).

[9] M. B. Gorensek, W. A. Summers, *Int. J. Hydrogen Energy*, doi:10.1016/ijhene.2008.06.049.

[10] J. Staser, J. W. Weidner, *J. Electrochem. Soc*., **156**, B16-B21 (2009).

[11] J. A. Staser, J. W. Weidner, *J. Electrochem. Soc*., **156**, B83 – B 841 (2009).

[12] M. C. Elvington, H. Colon-Mercado, S. McCatty, S. G. Stone, D. T. Hobbs, *J. Power Sources*, **195**, 2823 – 2829 (2010).

[13] N. Kim, D. Kim, *Int. J. Hydrogen Energy*, **34**, 7919 – 7926 (2009).

[14] H. R. Colón-Mercado, D. T. Hobbs, *Electrochem. Comm*., **9**, 2649-2653 (2007).

[15] Y. S. Kim, L. Dong, M. Hickner, T. E. Glass , J. E. McGrath, *Marcomolecules*, **38**, 5010 (2005).

[16] J. A. Staser, J. W. Weidner, *J. Electrochem. Soc.,* **156**, B836 – B841 (2009).

[17] J. Ge, A. Higier, H. Liu, *J. Power Sources*, **159**, 922 – 927 (2006).

CHAPTER 4

Evaluation

4.1 Introduction

The purpose of this study was i) to study the solubility of pure SO_2 gas in concentrated sulfuric acid at elevated temperatures and pressures and ii) to build and test an SO_2 electrolysis setup with performance validation. The solubility of SO_2 gas in sulfuric acid was determined to obtain important information regarding the possible composition of the feed of a SO_2 electrolyser used in the Hybrid Sulfur (HyS) Process[1]. Initial development by the Westinghouse Group suggested that SO_2 saturated sulfuric acid should be sent to the anode of such an electrolyser. The amount of SO_2 dissolved in sulfuric acid at different T & P therefore had to be determined in order to evaluate the operating conditions (where the maximum amount of SO_2 is dissolved in the acid) for the electrolyser.

The efficiency of the electrolyser is mostly determined by the reaction kinetics at the anode where a trade-off has to be reached between the maximum SO_2 dissolved and the reaction rate. Initial studies on the parameters that influence the efficiency of a SO_2 electrolysis cell were investigated. After an appropriate design was developed and a full Hazop study was completed the setup was used to benchmark and evaluate SO_2 electrolysis. The evaluation of the SO_2 electrolysis included i) the determination of the cell resistance as a function of cell temperature, ii) the effect of temperature on SO_2 electrolysis, iii) the influence of membrane thickness on cell performance iv) the effect of different catalyst loading on performance and v) the influence on increased cathode water pressure on the cell performance. SEM and EDX analysis was done on the best performing membrane in terms of polarization curves at 80^{o}C to determine the integrity of the membrane after SO_2 electrolysis.

4.2 SO_2 Solubility

After a detailed Hazard and Operatibility study (Hazop) was concluded on the proposed experimental setup, preliminary steps had to be followed before the actual SO_2 could be used. These included system pressure tests, volume determinations and the determination of the gas solubility in water prior to the actual acid solubility measurements. Subsequently, SO_2 gas solubility in 50wt% H_2SO_4 was evaluated at 30°C, 50°C and 80°C over a pressure range of 0–1000kPa. The results are summarized in Figure 4.1. Values obtained from this study showed some deviation from literature values based on computer modelling. However, since the water solubility values showed excellent correlation with experimental values obtained in literature, it is clear that the discrepancies observed for the solubility of SO_2 in acid between the experimental and modelled data is based on the differences in the various approaches and assumptions. A general trend of decreased solubility at higher temperatures, despite the increase in pressure at higher temperatures, was observed. It is clear from Chapter 2 that the rate of solubility decreased with temperature while the ultimate amount of SO_2 soluble also decreased with increasing temperature. The highest solubility, i.e. 13g SO_2/100g H_2SO_4 was attained at 30°C and 3.6 bar, while the lowest solubility (7.8g SO_2/100g H_2SO_4) was attained at 10.3 bar and 80°C. It can be concluded both from the SO_2 in water and SO_2 in H_2SO_4 results, that the design and building of the SO_2 solubility setup was achieved successfully and accurately in the 0–10 bar and 0–80°C operating range.

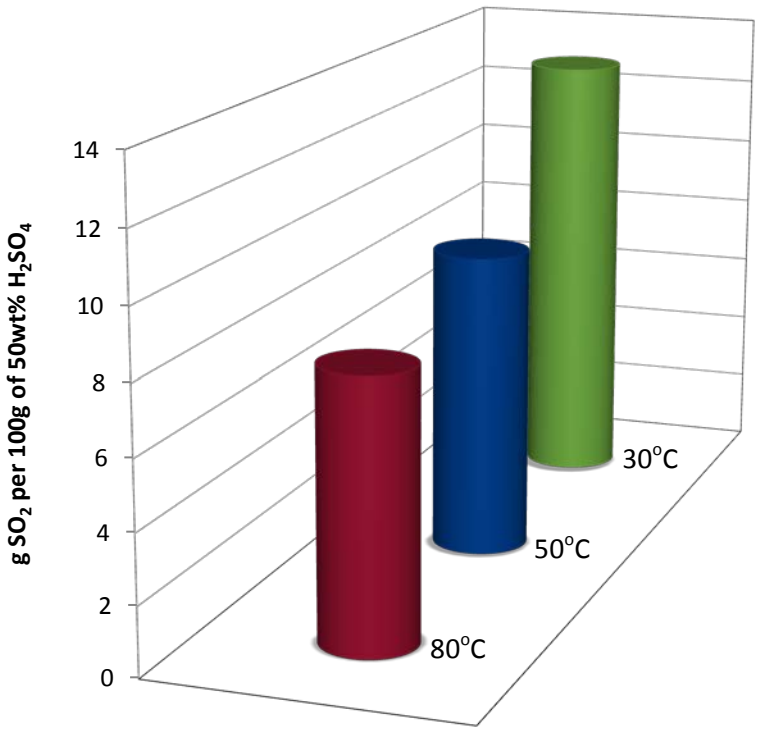

Figure 4.1 : SO_2 solubility in 50wt% as a function of temperature.

4.3 SO_2 Electrolyser setup

The second objective, i.e. the design and building of a SO_2 electrolysis setup as well as validating experimental data produced was shown in Chapter 3. The steps needed to achieve this included doing a Hazard and Operatibility Study (Hazop) on the proposed design. Subsequently, material selection had to be done to prevent corrosion due to sulfuric acid produced at the anode. From the experimental parameters tested in this study it was clearly shown that operating temperature directly influences cell efficiency significantly when increased from 50°C to 80°C achieving better cell performance at 80°C. Cell performance was further shown to be a function of the thickness of the membrane with the best performance achieved by the thinnest N1135 membrane at 80°C and atmospheric pressure, over the current density range tested although SO_2 crossover was higher than thicker membranes[2]. In the light of this cell performance, the catalyst loading was evaluated and it was shown that the loadings can be reduced from 0.5 to 0.3mgPt/cm^2 without any significant increase in the operating voltage.

Staser *et al.*[3] showed that by operating the SO_2 electrolyser with increased water pressure (dP = 6 bar) more stable voltages could be achieved with negligible SO_2 crossover. In this study an effort to reproduce the stable voltages (dP = 1 bar, cathode = 1 bar and anode at atmospheric) were not achieved, possibly due to flooding of the anode where no SO_2 pressure was imposed.

4.4 SO_2 Solubility vs. electrolyser performance

It was shown that the SO_2 solubility setup had adequate accuracy in measuring SO_2 solubility in both sulfuric acid and water. In light of the SO_2 electrolyser, initially using SO_2 saturated sulfuric acid as anode feed, the maximum SO_2 solubility was achieved at 30°C whereas the SO_2 gas fed electrolyser showed significant improved cell efficiency at temperatures in the 80°C range. During this study it became apparent that using SO_2 saturated sulfuric acid will not only limit the amount of SO_2 available for the reaction to take place at the anode of the electrolyser cell, but will impose an additional mass transfer limit which will further decrease the efficiency of the SO_2 reduction. In spite of the mass transfer limitations when an acid feed is used, a production rate of 0.27g H_2/min (calculated from maximum solubility at 80°C) could theoretically be produced at 80°C and 10 bar with no over-potential present from the cell itself.

It can thus be concluded that a SO_2 gas-fed electrolyser should be used, thus eliminating these limitations and the only factors influencing the cell efficiency include the SO_2 crossover, the water

transport to the anode and the concentration of sulfuric acid produced at the anode. Although these parameters are a function of various factors such as membrane thickness, water pressure, electro-osmotic drag, operating temperature and proton conductivity, a gas fed electrolyser does have more advantages than a SO_2 saturated sulfuric acid electrolyser.

4.5 Recommendation

For the solubility setup recommendation could be made.

- Reducing the corrosion observed for the pressure detectors to improve long term stability of the equipment.
- Introducing an external pump to increase the pressure and thus solubility attainable in the system.

Further work must be done on electrolyser cell and setup design to achieve increased performance and material life time. These changes include:

- Increased operating pressures for both water (cathode) and SO_2 (anode).
- Improved membranes to operate above 100^{o}C without the dependence on water for H^+ conductivity.
- Testing membranes with reduced SO_2 transport to decrease the negative side reactions at the cathode catalyst.
- Developing a more active catalyst which is acid-resistant at high temperatures.
- Development of the flow fields for improved reactant transport to the catalyst.
- Using either PFA-based materials (for T < 80^{o}C and P < 10 bar) or Tantaline-based materials (for T >100^{o}C and P > 30 bar) for the materials of construction of the setup.

4.6 References

[1] R. Junginger, B. D. Struck, Int. J. Hydrogen Energy, 7, 331-340 (1982).

[2] M. C. Elvington, H. Colon-Mercado, S. McCatty, S. G. Stone, D. T. Hobbs, *J. Power Sources*, **195**, 2823 – 2829 (2010).

[3] J. Staser, R. P. Ramasamy, P. Sivasubramanian, J. W. Weidner, *Electrochem. Solid-State Letters*, **10**, E17-E19 (2007).

Appendix A

Hazard and Operatibility Study on the SO_2 solubility in conc. H_2SO_4 setup

A.1 Introduction

A Hazard and Operability Study was done on the setup developed to determine the SO_2 solubility in sulfuric acid (Chapter2) to evaluate possible hazards when using high pressure SO_2 gas (0 – 1600 kPa) and concentrated sulfuric acid (50 wt %) at elevated temperatures (30 – 80^{o}C). High pressure equipment must be used by a qualified person with the necessary safety equipment and training. SO_2 gas is corrosive and harmful if inhaled or swallowed. Concentrated sulfuric acid is highly corrosive, which increases at elevated temperatures and can cause severe chemical burns. Material safety data sheets must be consulted for all chemicals before operating the apparatus or preparing any samples.

A.2 Material selection

Although stainless steel (SS) is a relatively corrosion-resistant material there are areas in the setup where it can't be used. On contact with sulfuric acid, stainless steel can corrode due to the reaction of the chromium with sulfuric acid. SO_2 gas on the other hand can be contained in a SS container as long as no excessive moisture is present, where the dissolved SO_2 will result in an increase in acidity of the moisture leading to the reaction of the chromium in the SS.

In view of this, a material was needed that could withstand the operating conditions used and still be resilient enough to withstand corrosion. PTFE was the material of choice according to the compatibility data consulted. A selection of available materials was immersed in 30wt% acid and heated to 120^{o}C and left for 24h while continually bubbling SO_2 gas through the acid. PTFE showed the best corrosion resistance in terms of material cost. Although PTFE showed excellent corrosion resistance it had to be replaced with a glass beaker as the SO_2 gas was absorbed by the polymeric material.

A.3 SO_2 P-V-T behaviour

The temperature–pressure behaviour of the SO_2 was important in the design of the overall setup to ensure that no SO_2 condensation in the gas pipes occur, which would create an undesired pressure drop in the system. ThermoSolver (Version 1), developed by C. Barnes and M. Korestsky from Oregon University, USA is freely available on the internet and was used to thermodynamically determine (using the Lee-Kesler equation) at which temperature – pressure ranges SO_2 would be in the gas form. In Figure A-1 attained plot of temperature vs. pressures of SO_2 is presented, showing the condensation profile of SO_2 as a function of pressure and temperature. From Figure A-1 : Phase diagram for SO2 as a function of T & P determined using Thermosolver (Version2). the T – P conditions for the experimental setup were chosen to ensure that the SO_2 remained in the gas phase. For example, a pressure above 100kPa cannot be achieved for an operating temperature (Figure 2.1, water bath B1) of 20°C. The experimentally determined values for the compressibility factors and vapour pressures, as reported by Kang *et al.*[1] have been used in the solubility calculations.

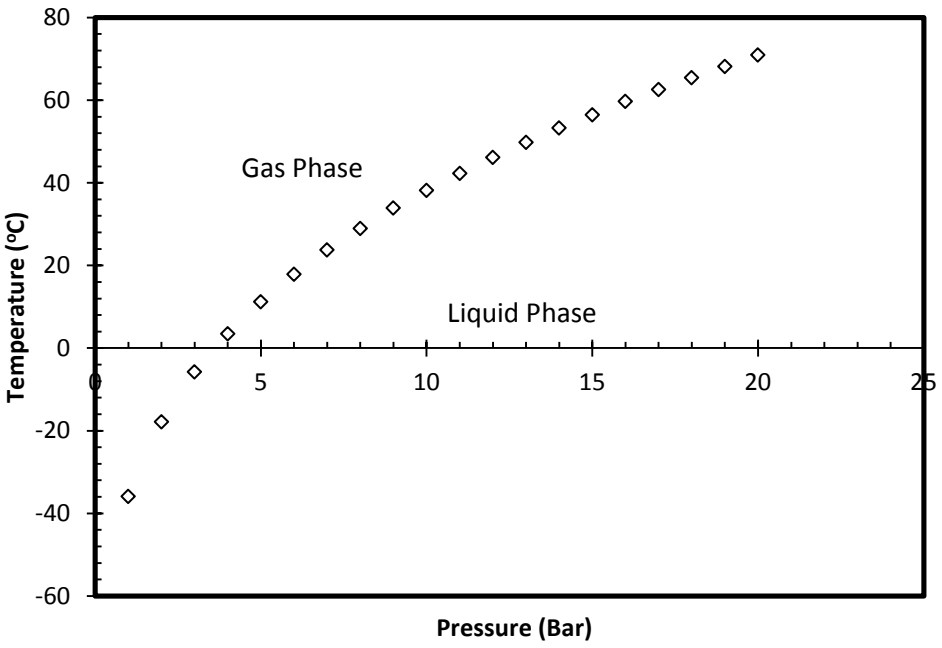

Figure A-1 : Phase diagram for SO_2 as a function of T & P determined using Thermosolver (Version2).

A.4 Setup considerations

While Teflon was selected as a suitable material for the sulfuric acid and SO_2 gas, the high operating pressures in the solubility cell (B3 in Fig. 2.1) can cause the PTFE to deform and containment of the acid can be lost. Thus B3 could not be made only from PTFE but by making a PTFE sleeve that could be placed into a carefully machined SS housing this issue was resolved. Thermal stability of PTFE should also be mentioned as all polymeric materials have a glass transition point at which the material looses significant mechanical strength. PTFE is stable up to 260^0C, and is therefore safe to use in this setup where temperatures will remain below 120^0C. All the fittings were purchased to withstand the operating conditions (T, P and acid conc.) in which they were to be used. Thus SS was used where SO_2 gas was present and Teflon was used where both sulfuric acid and SO_2 was present.

For the Hazop itself, the entire setup was divided into nodes and assessed for hazardous parameters. An example of one such node analysis is presented in Table 3 where the various aspects included for such a study are illustrated.

Table A-1 : Summary illustration of one node for the SO_2 solubility Hazop study

Node A	Deviation		Causes	Consequence or Hazard	Safeguards already provided	Recommendation and Actions
1	Flow	High			Add rotameter to L1	
2		Low	NA			
3		No	Valve not opened	No N_2 Flushing		No real hazard
4		Reverse	Wrong valves opened	Erroneous results		Add non return valve to L1
5	Pressure	High	A1 temperature to high	Rupture	Rupture disc T3 and T4	High pressure bottle training
6		Low	NA			
7	Temperature	High	See high pressure			
8		Low	NA			
9	High stress	High	See high pressure			
10		Low	NA			

The following process description is an example of the results obtained by the Hazop (Hazard and Operatibility) giving a detailed discussion on initial preparations and the actual experimental method.

A.5 Process Description

Figure A–2 shows a flow diagram of the method used to calculate the SO_2 solubility in concentrated sulfuric acid at elevated P & T. The diagram is designed to keep the concentration of sulfuric acid and temperature constant while varying the pressure over the range interested.

A.5.1 Initial preparations

A specific concentration of sulfuric acid was prepared by diluting a 98wt% batch solution to the desired wt % using DI water. Sufficient time must be left for all air bubbles to be removed from the solution so that erroneous dilution is avoided. The 70mL solution was added to the Teflon sleeve (inside SS housing B3, Figure 2.1) using a burette. The filled housing was placed into the water bath and all necessary connections were made. When the operating temperature (temperature of the water bath) was set, the sampling cylinder's temperature was set at 10^{o}C lower, to prevent any SO_2 condensation in the gas lines.

Next, the setup has to be pressure-tested to identify possible gas leaks. Using N_2, the system was pressurized to 1500kPa and left for 2 hours. If no pressure drop occurred, the vacuum test was done. If, however, a visible drop in pressure was observed, all fittings and connections had to be checked for leaks using diluted soap water. All water had to be removed with paper cloth before any SO_2 was introduced as this might cause corrosion.

Removing the remaining N_2 with a vacuum pump ensures that all gasses were removed and that SO_2 introduced to the setup was only gas present. With the vapour pressure of sulfuric acid determined[2] as 4.3x10^{-4} kPa, the sulfuric acid amount removed by vacuum can be regarded as negligible.

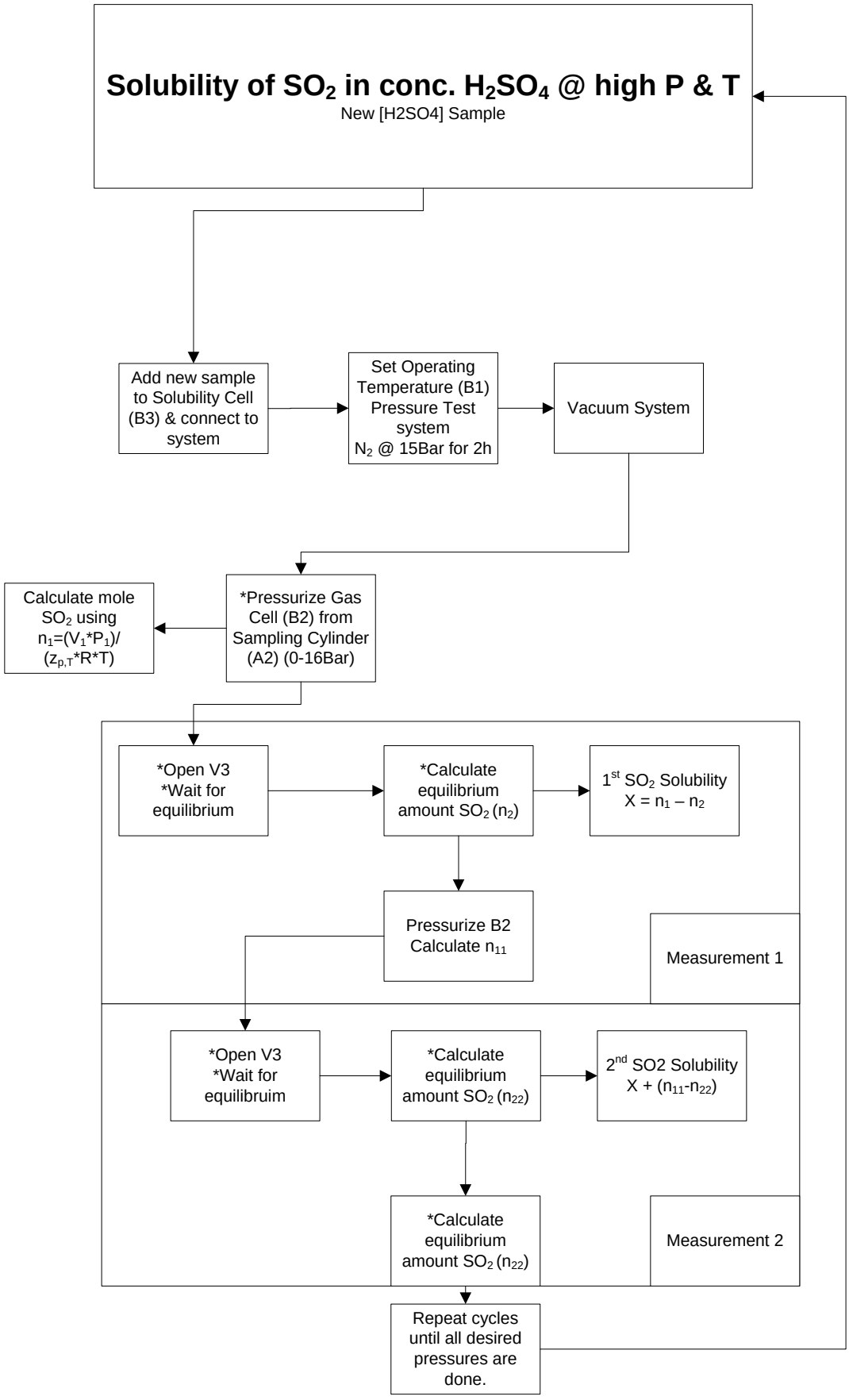

Figure A-2: Solubility cycle used to calculate the SO_2 solubility

A.5.2 SO_2 Solubility Testing

After all the initial preparations had been successfully completed the pressurized SO_2 (sampling cylinder, A1 Figure 2.1) could then be introduced to the SO_2 pure gas cell (B2) and reduced to the desired pressure. Using the initial pressure, the starting amount of SO_2 gas was calculated using the ideal gas law, compensating with the correct compensability factor. After the SO_2 had flowed to the solubility cell (B3) the system was equilibrated for one hour. The final pressure was used to calculate the remaining SO_2 gas. By subtracting the starting SO_2 pressure from the equilibrium SO_2 pressure the solubility was established.

The next pressure was prepared at the same temperature by charging B2 again with SO_2 at a higher pressure than the previous measurement. The solubility obtained from the second measurement then had to be added to the first solubility measurement. After all the desired pressures had been tested, the next temperature could be selected after the acid has been replaced with a clean sample. The same procedure was repeated for all the H_2SO_4 concentration experiments.

A.6 Data generation

A.6.1 Pressure tests

Initial pressure tests showed that the setup (which included the PTFE housing and seals at this stage) had significant pressure drops over the entire pressure range (0 – 1600kPa). A constant pressure drop of $5x10^{-4}$ and $3x10^{-4}$ was evident for both B2 & B3. The PTFE seals were thought to allow some permeation of SO_2 gas and were replaced with Viton O-rings. This configuration also showed a small pressure drop over a larger period of time. Subsequently the Viton O-rings were replaced by EPDM (peroxide cured) O-rings with the addition of another O-ring (larger than the previous one). The EPDM O-rings were specifically manufactured for use with SO_2 gas in an acid environment and is the industry standard for this combination (SO_2 & H_2SO_4). Nevertheless, pressure drop was present over a period of one day. With the sealing material replaced by known solutions; the pressure indicators were tested individually for possible gas leaks through the meter itself. Figure 3 shows the pressure decay when only the pressure transducers were tested (separate from the entire setup).

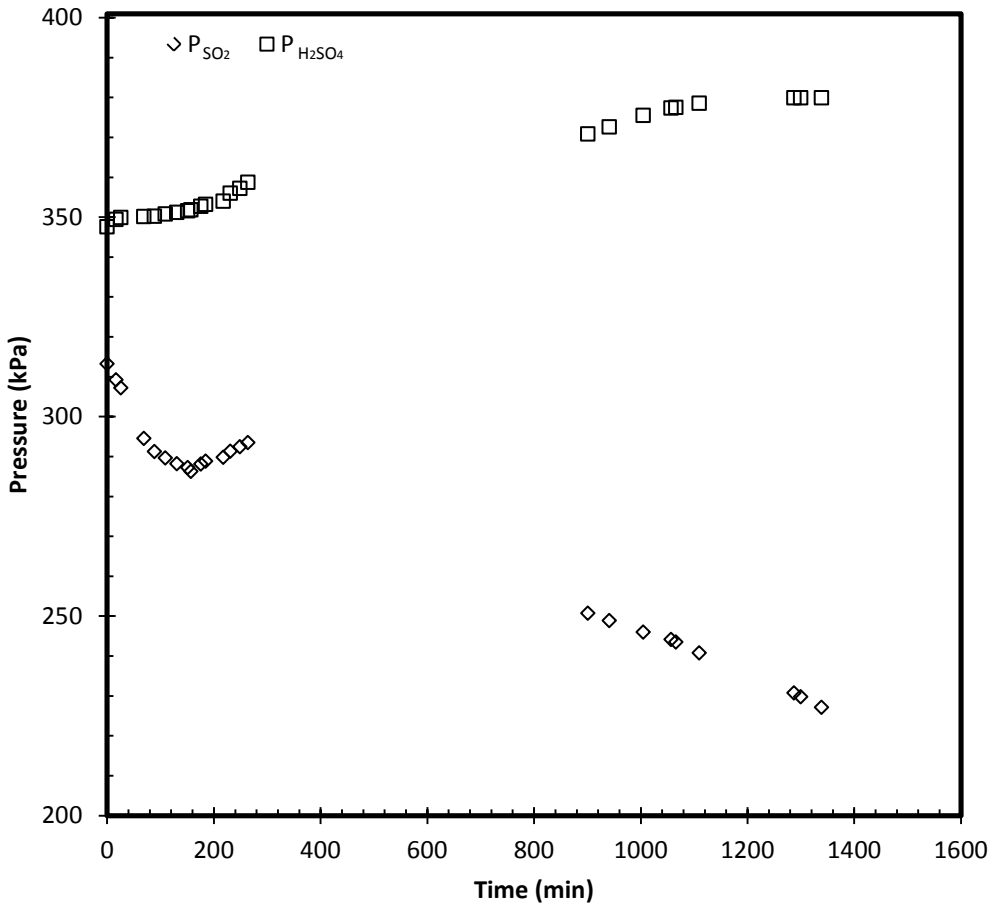

Figure A-3 : Pressure decay for both pressure indicators used where P_{SO2} is B2 and P_{H2SO4} is B3.

It can be concluded that the gas leaks were due to a small discrepancy within the pressure indicators. After re-calibration (done by supplier) of the instruments a successful pressure test was achieved for both N_2 & SO_2 gas over a period of 3 hours.

A.6.2 Setup calibration

The volume of the setup (B2 & B3 including piping) was determined by filling it entirely with water and using these values to determine the N_2 pressure drop from one vessel to another. These pressure drop tests were done at two temperatures over the pressure range for the solubility measurements. From the experimental water filling method, the calculated volumes, B2 and B3, were found to be 102.6cm^3 and 111.08cm^3 respectively. These values were used to predict the pressure drop from B2 to B3 using the ideal gas law (shown in Table A-2) with P_{eq}^{calc} the equilibrium pressure calculated and P_{eq}^{exp} the observed pressure.

Table A-2 : Pressure drop tests for SO_2 solubility setup.

T = 294.15 K		V_{B2} = 102.6 cm^3	V_{B3} = 111.08 cm^3	V_{TOTAL} = 213.68 cm^3
P_{B2} (kPa)	P_{B3} (kPa)	P_{eq}^{Calc} (kPa)	P_{eq}^{exp} (kPa)	Error %
87.9	1297.5	717.4	718.7	0.2
88	719.1	416.3	417.7	0.4
88	1304.5	721.1	723.2	0.3
88.1	723.4	418.5	420.2	0.5
88	420.3	260.7	261.5	0.4
1305.5	88.1	721.7	723.6	0.4
627.2	3.2	303	302.2	0.4
1307.5	3.1	628.1	623.7	0.8
T = 313.15 K		**V_{B2} = 102.6 cm^3**	**V_{B3} = 111.08 cm^3**	**V_{TOTAL} = 213.68 cm^3**
P_{B2} (kPa)	**P_{B3} (kPa)**	**P_{eq}^{Calc} (kPa)**	**P_{eq}^{exp} (kPa)**	**Error %**
87.7	1100.5	614.3	616	0.3
87.8	616.5	362.7	365	0.8
87.8	1309.5	725.4	723.9	0.2
87.8	727.6	421.3	422	0.2
87.8	1311.5	726.5	726.7	0.02
629.2	2.6	303.4	304.5	0.5
1305.5	1.2	627.7	626.9	0.2
626.9	1	301.6	302.8	0.5

A.6.3 SO_2 Solubility data

A.6.3.1 Equations used

The following equations where used (as described in Figure A-2 and Section 2.2.2.2) to determine the necessary values to obtain the SO_2 solubility in grams of SO_2 per 100 grams of H_2SO_4. After V1 is opened and the desired pressure (100kPa) is maintained for more than 10 minutes equation A-1 is used to calculate the amount of SO_2 gas that is to be sent to B3, at this stage V1 and 3 is closed.

$$n_{SO_2} = \frac{P_{B2} * V_{B2}}{z_{T,P} * R * T} \qquad (A-1)$$

Using equation A–2 the amount of N_2 (n_i) was calculated before any SO_2 is allowed to fill B3.

$$n_i = \frac{P_{B3} * V_{B2}}{z_{T,P} * R * T} \qquad (A-2)$$

Where $P_{B3} = P_{N2} + P_v$ to include the vapour pressure of the liquid. V3 was then opened and after equilibrium had been reached, pressure on both vessels remained stable within 0.001 bar over a 20minute period. Using this equilibrium pressure and the volume for the entire system ($V_{B2} + V_{B3}$), the amount of SO_2 gas could be calculated using equation A – 3.

$$n_{eq} = \frac{P_{eq} * \left(V_{B2} + V_{B3}\right)}{z_{T,P} * R * T} \qquad (A-3)$$

The amount of SO_2 moles could then be calculated according to equation A – 4.

$$n_{abs} = n_{So_2} + n_i - n_{eq} \qquad (A-4)$$

From this the solubility can be calculated for gas in liquids. As the water solubility needs to be in molality, for comparison reasons, the moles are converted to mol/kg of water using the density. The sulfuric acid solubility was converted to grams of gas per 100 grams of acid using acid density.

A.6.3.2 Compressibility factor

Although Figure A-1 was used for the planning of the experimental procedures, the values for the compressibility factor where obtained by mathematical equations and based on the Peng-Robinson equation of state. By using the virial equation an accurate value for the compressibility factor could be calculated.

$$z_{T,P} = 1 + \frac{B * P}{R * T} \qquad (A-5)$$

Figure A – 4 shows the correlation between the compressibility factors obtained from both the Peng-Robinson (theoretically based) and the virial equations (experimentally based).

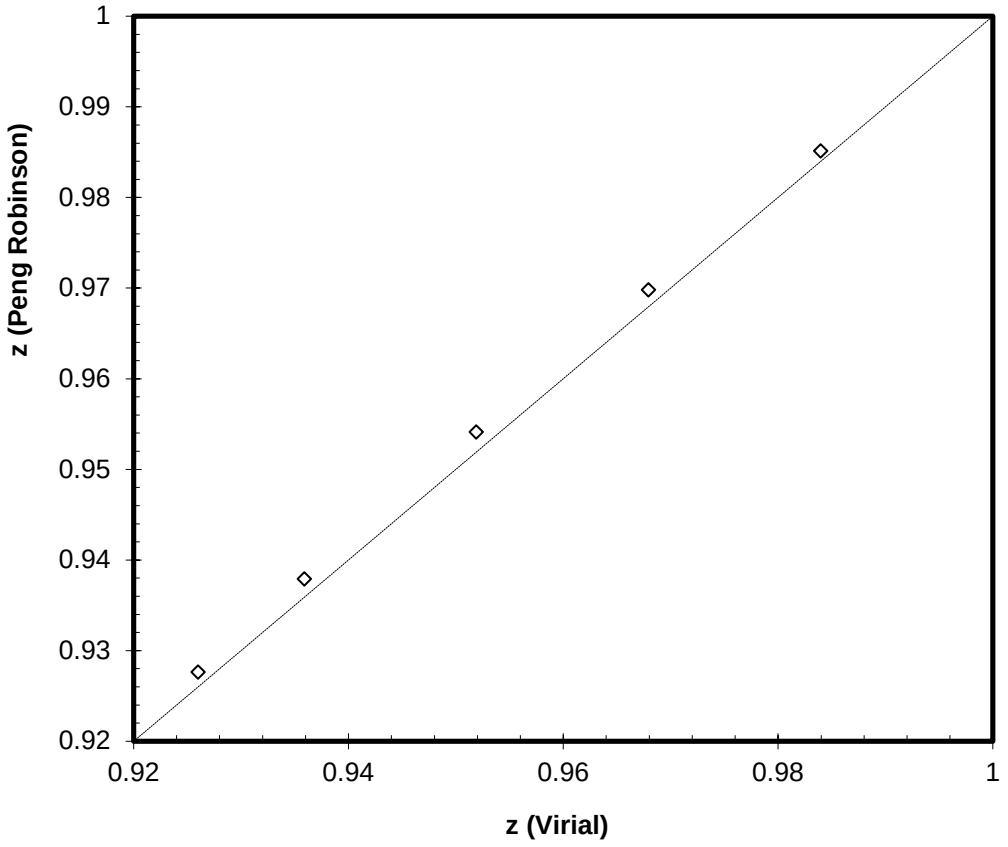

Figure A - 4 : Comparison between Peng-Robinson and Virial equations used to determine the compressibility factors of SO_2.

It can be deduced from Figure A - 4 that the difference between the two methods of determining the compressibility factor of SO_2 is nearly the same; nevertheless the difference in the values is enough to influence the overall solubility. It is for this reason that the virial equation was used to obtain the compressibility factor used for all calculations as it is based on actual experimental data.

Experimental values for the virial coefficient (B in equation A-5) could be obtained through the paper by Kang *et al.*[3] but had to be calculated as it was not measured for 80°C. Figure A–5 shows the equation used to calculate the B value at 80°C using the literature data cited.

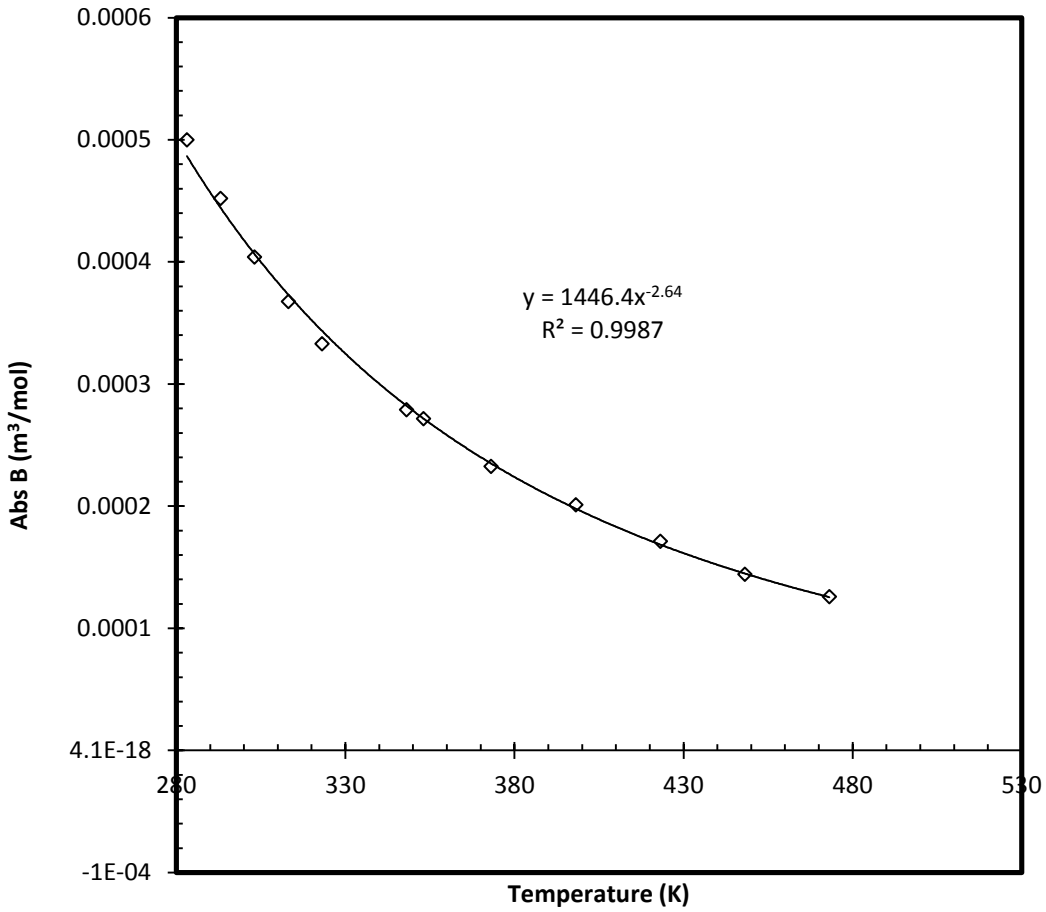

Figure A – 5 : Equation used to calculate the B value at 80°C.

A.6.3.3 SO_2 Solubility as a function of temperature.

Figure A - 6 shows a graph for the pressure decay (for B3, acid containing vessel, only) as a function of time (min) at 30°C. As can be seen from case 1 through 31 the equilibrium pressure increases steadily with each case. For simplicity all data point are not represented.

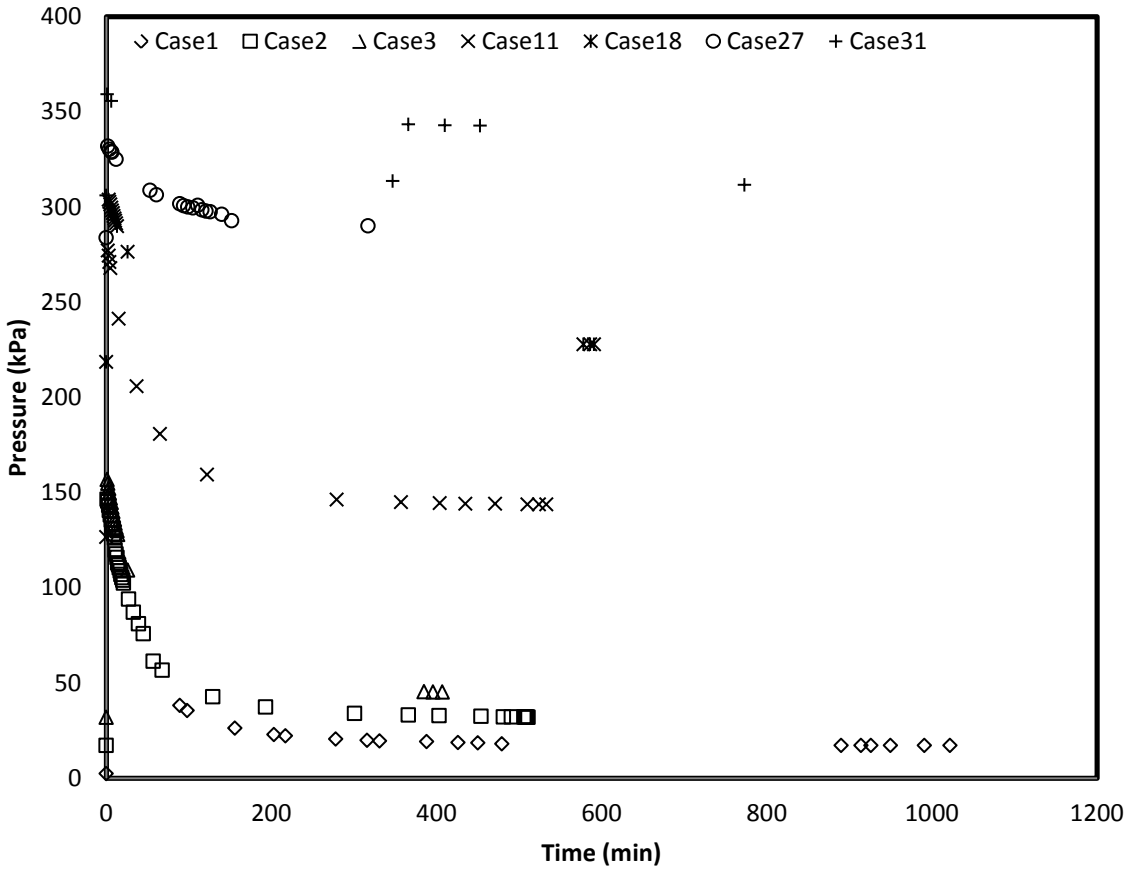

Figure A - 6 : Pressure decay due to solubility at 30^{o}C.

The actual values used for the construction of Figure 2.3 (Chapter 2) are given in Table A - 3. The solubility is ultimately given in grams of SO_2 gas dissolved in 100 grams of 50wt% sulfuric acid as this is the notation used literature. Table A–4 and A–5 are also represented for 50^{o}C and 80^{o}C respectively.

Table A - 3 : Actual data obtained for SO_2 solubility in 50wt% H_2SO_4 at 30^oC.

V_1 = 1.03 x 10^{-4} m^3		V_2 = 4.11 x 10^{-5} m^3		R = 8.3144J/mol.K		T = 303.15 K		B = -0.000404m^3/mol		
P_{SO2} (kPa)	z_{calc} (-)	n_{SO2} (mol)	P_{H2SO4} (kPa)	z_{calc} (-)	n_{H2SO4} (mol)	P_{eq} (kPa)	z_{calc} (-)	n_{eq} (mol)	n_{abs} (mol)	$gSO_2/100gH_2SO_4$
189.8	0.9696	0.0080	2.5	0.9996	0.0000	17.2	0.9972	0.0010	0.0070	0.4605
209.7	0.9664	0.0088	17.3	0.9972	0.0003	32.1	0.9949	0.0018	0.0143	0.9373
218.8	0.9649	0.0092	32	0.9949	0.0005	45.3	0.9927	0.0026	0.0215	1.4061
218.3	0.9650	0.0092	45.3	0.9927	0.0007	58.6	0.9906	0.0034	0.0280	1.8373
211.2	0.9661	0.0089	58.3	0.9907	0.0010	68.5	0.9890	0.0039	0.0339	2.2246
228.9	0.9633	0.0097	68.3	0.9891	0.0011	81	0.9870	0.0047	0.0401	2.6257
209.3	0.9665	0.0088	81	0.9870	0.0013	90.3	0.9855	0.0052	0.0450	2.9488
210.3	0.9663	0.0089	99.2	0.9841	0.0016	99.2	0.9841	0.0057	0.0498	3.2604
295.2	0.9527	0.0126	99.1	0.9841	0.0016	114	0.9817	0.0066	0.0574	3.7608
306.7	0.9508	0.0131	113.9	0.9817	0.0019	126.7	0.9797	0.0074	0.0650	4.2621
348.5	0.9441	0.0150	126.7	0.9797	0.0021	143.9	0.9769	0.0084	0.0738	4.8346
301	0.9518	0.0129	143.9	0.9769	0.0024	156.1	0.9750	0.0091	0.0799	5.2375
357.6	0.9427	0.0154	156.1	0.9750	0.0026	171.7	0.9725	0.0101	0.0879	5.7609
337.8	0.9459	0.0145	171.6	0.9725	0.0029	185.7	0.9702	0.0109	0.0944	6.1871
341.8	0.9452	0.0147	185.6	0.9703	0.0031	197.6	0.9683	0.0116	0.1006	6.5937
345.7	0.9446	0.0149	197.6	0.9683	0.0033	208	0.9667	0.0123	0.1066	6.9842
344.1	0.9448	0.0148	208	0.9667	0.0035	218.8	0.9649	0.0129	0.1120	7.3384
343.7	0.9449	0.0148	218.6	0.9650	0.0037	227.9	0.9635	0.0135	0.1170	7.6671
389.2	0.9376	0.0169	227.8	0.9635	0.0039	241.6	0.9613	0.0143	0.1234	8.0880
360.5	0.9422	0.0156	241	0.9614	0.0041	248.5	0.9602	0.0148	0.1283	8.4096
390.7	0.9374	0.0170	248.5	0.9602	0.0042	259.4	0.9584	0.0154	0.1341	8.7868
351.2	0.9437	0.0151	259.3	0.9584	0.0044	266.8	0.9572	0.0159	0.1377	9.0273
348.5	0.9441	0.0150	266.4	0.9573	0.0045	271.5	0.9565	0.0162	0.1411	9.2488
341.1	0.9453	0.0147	271.4	0.9565	0.0046	278.1	0.9554	0.0166	0.1438	9.4271
347.3	0.9443	0.0150	278.1	0.9554	0.0047	282	0.9548	0.0168	0.1467	9.6157

P_{SO2} (kPa)	z_{calc} (-)	n_{SO2} (mol)	P_{H2SO4} (kPa)	z_{calc} (-)	n_{H2SO4} (mol)	P_{eq} (kPa)	z_{calc} (-)	n_{eq} (mol)	n_{abs} (mol)	$gSO_2/100gH_2SO_4$
299.1	0.9521	0.0128	282	0.9548	0.0048	283.9	0.9545	0.0170	0.1474	9.6581
353.7	0.9433	0.0153	293.9	0.9529	0.0050	290	0.9535	0.0173	0.1503	9.8516
341.4	0.9453	0.0147	289.9	0.9535	0.0050	294	0.9529	0.0176	0.1524	9.9872
359.6	0.9424	0.0155	293.9	0.9529	0.0050	300.4	0.9519	0.0180	0.1550	10.1556
369.4	0.9408	0.0160	300.4	0.9519	0.0051	306.4	0.9509	0.0184	0.1577	10.3364
382.1	0.9388	0.0166	306.1	0.9509	0.0052	311.6	0.9501	0.0187	0.1608	10.5408
430.2	0.9310	0.0188	311.5	0.9501	0.0053	317.9	0.9490	0.0191	0.1659	10.8722
377.6	0.9395	0.0164	317.9	0.9490	0.0055	324.6	0.9480	0.0195	0.1682	11.0230
380.7	0.9390	0.0165	324.6	0.9480	0.0056	328.4	0.9474	0.0198	0.1705	11.1753
380.4	0.9390	0.0165	328.4	0.9474	0.0056	332.2	0.9468	0.0200	0.1727	11.3155
486.2	0.9221	0.0215	332.3	0.9467	0.0057	340.4	0.9454	0.0205	0.1793	11.7520
395	0.9367	0.0172	340.4	0.9454	0.0059	344.4	0.9448	0.0208	0.1816	11.8997
394.5	0.9368	0.0171	344.4	0.9448	0.0059	347.4	0.9443	0.0210	0.1837	12.0382
394.8	0.9367	0.0172	347.4	0.9443	0.0060	350.7	0.9438	0.0212	0.1857	12.1673
394.7	0.9367	0.0172	350.8	0.9438	0.0061	352.9	0.9434	0.0213	0.1875	12.2909
392.4	0.9371	0.0170	353	0.9434	0.0061	354.5	0.9432	0.0214	0.1893	12.4035
420.2	0.9326	0.0183	354.5	0.9432	0.0061	359.4	0.9424	0.0217	0.1920	12.5822
420.1	0.9327	0.0183	359.4	0.9424	0.0062	364.3	0.9416	0.0221	0.1945	12.7458
375.4	0.9398	0.0163	364.3	0.9416	0.0063	366.9	0.9412	0.0222	0.1948	12.7683
406.1	0.9349	0.0177	366.9	0.9412	0.0064	367.3	0.9411	0.0222	0.1966	12.8854

Table A - 4 : Actual data obtained for SO_2 solubility in 50wt% H_2SO_4 at 50^oC.

V_1 = 1.03 x 10^{-4} m^3		V_2 = 4.11 x 10^{-5} m^3		R = 8.3144J/mol.K		T = 303.15 K		B = -0.000404m^3/mol		
P_{SO2} (kPa)	z_{calc} (-)	n_{SO2} (mol)	P_{H2SO4} (kPa)	z_{calc} (-)	n_{H2SO4} (mol)	P_{eq} (kPa)	z_{calc} (-)	n_{eq} (mol)	n_{abs} (mol)	$gSO_2/100gH_2SO_4$
240.5	0.9702	0.0095	10.5	0.9987	0.0002	44.7	0.9945	0.0024	0.0072	0.4734
249.2	0.9691	0.0098	44.7	0.9945	0.0007	77.3	0.9904	0.0042	0.0136	0.8884
243.9	0.9698	0.0096	77.3	0.9904	0.0012	113.6	0.9859	0.0062	0.0182	1.1922
249.8	0.9691	0.0098	113.6	0.9859	0.0018	140.8	0.9826	0.0077	0.0221	1.4505
253.1	0.9686	0.0100	140.8	0.9826	0.0022	163.9	0.9797	0.0089	0.0254	1.6617
295	0.9635	0.0117	164	0.9797	0.0026	190.8	0.9764	0.0105	0.0292	1.9109
390.3	0.9517	0.0157	190.7	0.9764	0.0030	224.7	0.9722	0.0124	0.0354	2.3229
391.7	0.9515	0.0157	224.7	0.9722	0.0035	250.8	0.9689	0.0138	0.0409	2.6776
490.2	0.9393	0.0199	250.6	0.9690	0.0040	283.8	0.9648	0.0157	0.0490	3.2120
500.5	0.9380	0.0204	283.7	0.9649	0.0045	312.7	0.9613	0.0174	0.0565	3.7019
530.7	0.9343	0.0217	312.7	0.9613	0.0050	342.1	0.9576	0.0191	0.0640	4.1975
650	0.9195	0.0270	342.2	0.9576	0.0055	386.5	0.9521	0.0217	0.0748	4.9020
644	0.9202	0.0267	386.5	0.9521	0.0062	423	0.9476	0.0239	0.0839	5.4957
653.7	0.9190	0.0272	423	0.9476	0.0068	455.5	0.9436	0.0258	0.0920	6.0313
702.2	0.9130	0.0294	455.5	0.9436	0.0074	497.5	0.9384	0.0284	0.1004	6.5817
710.3	0.9120	0.0297	497.5	0.9384	0.0081	526.9	0.9347	0.0301	0.1081	7.0865
647.8	0.9198	0.0269	526.9	0.9347	0.0086	547	0.9322	0.0314	0.1123	7.3576
644.5	0.9202	0.0267	547.1	0.9322	0.0090	557.9	0.9309	0.0320	0.1159	7.5981
660.2	0.9182	0.0275	555.6	0.9312	0.0091	576.9	0.9285	0.0332	0.1193	7.8179
666.1	0.9175	0.0277	576.7	0.9286	0.0095	586.8	0.9273	0.0338	0.1227	8.0394
662.1	0.9180	0.0275	586	0.9274	0.0097	598.3	0.9259	0.0346	0.1253	8.2129
662.6	0.9179	0.0276	598.2	0.9259	0.0099	603.9	0.9252	0.0349	0.1279	8.3792
677.4	0.9161	0.0282	602.1	0.9254	0.0099	612.3	0.9242	0.0354	0.1306	8.5597
652.2	0.9192	0.0271	612.1	0.9242	0.0101	622.3	0.9229	0.0361	0.1318	8.6359

Table A - 5 : Actual data obtained for SO_2 solubility in 50wt% H_2SO_4 at 80^oC.

V_1 = 1.03 x 10^{-4} m^3		V_2 = 4.11 x 10^{-5} m^3		R = 8.3144J/mol.K		T = 303.15 K			B = -0.000404m^3/mol	
P_{SO2} (kPa)	z_{calc} (-)	n_{SO2} (mol)	P_{H2SO4} (kPa)	z_{calc} (-)	n_{H2SO4} (mol)	P_{eq} (kPa)	z_{calc} (-)	n_{eq} (mol)	n_{abs} (mol)	$gSO_2/100gH_2SO_4$
2.895	0.9688	0.0122	0.322	0.9965	0.0005	0.85	0.9908	0.0014	0.0113	0.1652
0.836	0.9910	0.0034	0.952	0.9897	0.0016	0.965	0.9896	0.0016	0.0147	0.2151
3.138	0.9662	0.0132	0.966	0.9896	0.0016	1.419	0.9847	0.0023	0.0272	0.3974
3.848	0.9586	0.0163	1.418	0.9847	0.0023	1.926	0.9793	0.0032	0.0426	0.6239
5.935	0.9361	0.0258	1.927	0.9792	0.0032	2.852	0.9693	0.0048	0.0669	0.9783
6.89	0.9258	0.0303	2.852	0.9693	0.0048	3.806	0.9590	0.0065	0.0955	1.3970
8.186	0.9118	0.0365	3.765	0.9594	0.0064	4.786	0.9485	0.0082	0.1302	1.9049
9.961	0.8927	0.0454	4.785	0.9485	0.0082	6.026	0.9351	0.0105	0.1733	2.5360
9.508	0.8976	0.0431	6.025	0.9351	0.0105	6.82	0.9265	0.0120	0.2150	3.1449
9.358	0.8992	0.0424	6.819	0.9266	0.0120	7.368	0.9206	0.0130	0.2563	3.7493
10.498	0.8869	0.0482	7.37	0.9206	0.0130	8.163	0.9121	0.0146	0.3029	4.4317
11.255	0.8788	0.0521	8.163	0.9121	0.0146	8.904	0.9041	0.0161	0.3536	5.1729
10.67	0.8851	0.0491	8.904	0.9041	0.0161	9.351	0.8993	0.0169	0.4018	5.8777
10.566	0.8862	0.0485	9.35	0.8993	0.0169	9.567	0.8970	0.0174	0.4499	6.5814
11.325	0.8780	0.0525	9.567	0.8970	0.0174	10.057	0.8917	0.0184	0.5014	7.3349
11.125	0.8802	0.0515	10.057	0.8917	0.0184	10.272	0.8894	0.0188	0.5524	8.0811

A.7 References

[1] T. L. Kang, L. J. Hirth, K. A. Kobe, J. J. McKetta, J. Chem. Eng. Data., **6**, 220-226 (1961).

[2] Perry, R. H.; Green, D., Eds. Chemical Engineers' Handbook, 6th ed.; McGraw-Hill: New York, 1984; pp 3-68, 3-85.

[3] T. L. Kang, L. J. Hirth, K. A. Kobe, J. J. Mcketta, J. Chem. Eng. Data, **2**, 220 – 226 (1961).

Appendix B

Hazard and Operatibility study on the SO_2 Electrolyser setup

B.1 Introduction

The Hybrid Sulfur (HyS) process includes a SO_2 electrolysis step that entails sending SO_2 gas to the anode while DI water is sent to the cathode side of an electrolyser. The products resulting from this electrochemical reaction include protons, electrons and sulfuric acid at the anode and hydrogen and possibly hydrogen sulfide at the cathode. In light of this, safety concerns, for example unidentified leaks in the electrolyser which can cause severe chemical burns must be taken into account due to the presence of the concentrated H_2SO_4.

B.2 Setup considerations

To deal with H_2SO_4 produced in the electrolyser, all materials were constructed either from glass, fluorel tubing or PTFE as needed. PTFE lift check valves were manufactured in-house (using the Swagelock template). Although the expected product gasses should only include H_2, other corrosive gasses such as SO_2 and H_2S can be present in the product stream. Thus all vessels (GV1–4, Figure 3.1) were constructed from glass and connected using fluorel tubing. Valves were replaced (V6, 7, 8, 10, 12, 13, 16, 17) by glass taps either with PTFE inserts or entirely made from glass.

B.3 Preliminary aspects

Before the electrolyser (shown in Figure B-1) can be supplied with pure SO_2 gas, initial steps must be followed to ensure that the correct operation is ensured. Although the membrane should have some gas permeability, the electrolyser must be checked for any cross-cell leakage ($\Delta P \neq 0$ over the membrane) and overall pressure ($\Delta P = 0$ over the membrane). Using N_2 gas to pressurize one side of the electrolyser and submersing it into DI water will show any cross-cell gas leaks (formation of bubbles due to membrane permeability) which could occur due to incorrect compressibility between the separate electrolyser components. Pressurizing both sides of the electrolyser can be used to ensure that no leaks are present for the entire electrolyser. The maximum pressure should be a function of the membrane mechanical durability, which is susceptible to gradient pressure damage when $\Delta P \neq 0$. The cell hardware supplied was designed for parameters up to 3atm with a 1atm pressure differential over the membrane.

Figure B-1 : SO_2 electrolyser based on direct methanol fuel cell hardware obtained from Giner Electrochemical Systems, LLC.

The electrical resistance in any electrolyser (or fuel cell) is a function of various factors, including MEA manufacture, compressibility of components and contact area between the MEA and the current collectors. It is therefore expected that the assembled electrolyser will show some "natural" electrical resistance. Thus the DC electrical resistance of the electrolyser should be tested with a DC multimeter. Low or no electrical resistance (<50Ω) is an indication of a possible electrical short due to wrong electrolyser assembly or excessive compression, while high electrical resistance can indicate low contact area between current collectors and MEA or that the MEA manufacturing process was not completely successful.

B.3.1 Electrolyser operation

The operation of the electrolyser entails supplying gaseous SO_2 to the anode to produce sulfuric acid, protons and electrons while the cathode is supplied with DI water that is needed for the oxidation reaction at the anode. Before proceeding to this step, the system must be pressure-tested, which differs from the cross cell leakage and overall pressure test discussed previously. This system pressure test is done to ensure that no hydrogen leaks into the atmosphere causing a fire hazard while SO_2 removed from the system will interfere with experimental values. Therefore, the system is pressurised with N_2 to 1 bar and left for a hour. The flushing step can be started after a successful system pressure test.

B.3.2 System flushing and testing

By initiating the pre-heated (88^{o}C) DI water feed at 0–100mL/min (using PP1) and heating the cell to 80^{o}C, the entire system (both anode and cathode) must be flushed with N_2 (at 20–80cm^3/min) for 15min at open circuit conditions (no applied potential), before any SO_2 gas can be introduced. This ensures that all other gas species are removed from the electrolyser to avoid possible side reactions and to ensure that the SO_2 sent to the anode is not diluted.

After sufficient flushing has been achieved and the scrubber solution (25wt % NaOH) is circulated at 150mL/min, the electrolyser can be supplied with a H_2 flow (20–80 cm^3/min) at open circuit for 1 min ensuring the anode compartment is fully saturated. Applying a low current density (≈60mA/m^2) the voltage can be monitored to ensure that it is stable. This step is to ensure correct operation of the electrolyser by converting H_2 into protons and electrons at the anode and recombining them at the cathode to form H_2; it can then be assumed that the electrolyser is fully operational and ready for SO_2 conversion. After the H_2 testing is done the system must again be purged with N_2 at open circuit. The electrolyser must be heated to the desired temperature before SO_2 is fed to the electrolyser. The AC resistance of the cell was measured at temperatures ranging from 30–80^{o}C.

B.3.3 SO_2 Operation

Low SO_2 flow (20cm^3/min) can then be supplied to the electrolyser for 1 minute before a low current density (50mA/cm^2 @ 500mV) can be supplied to establish if the SO_2 contact is sufficient (stable voltage) for further experimental work.

Once a stable voltage has been reached, the current density can be increased by 50mA/cm^2 every 2 minutes to 1A/cm^2 while recording the voltage received from the electrolyser in order to get a polarization curve; which is an indication of electrolyser performance.

The hydrogen production was also measured (using a bubble flow meter) at each stable voltage. Figure B-2 shows a schematic representation of the steps followed to ensure consistent and repeatability of the system.

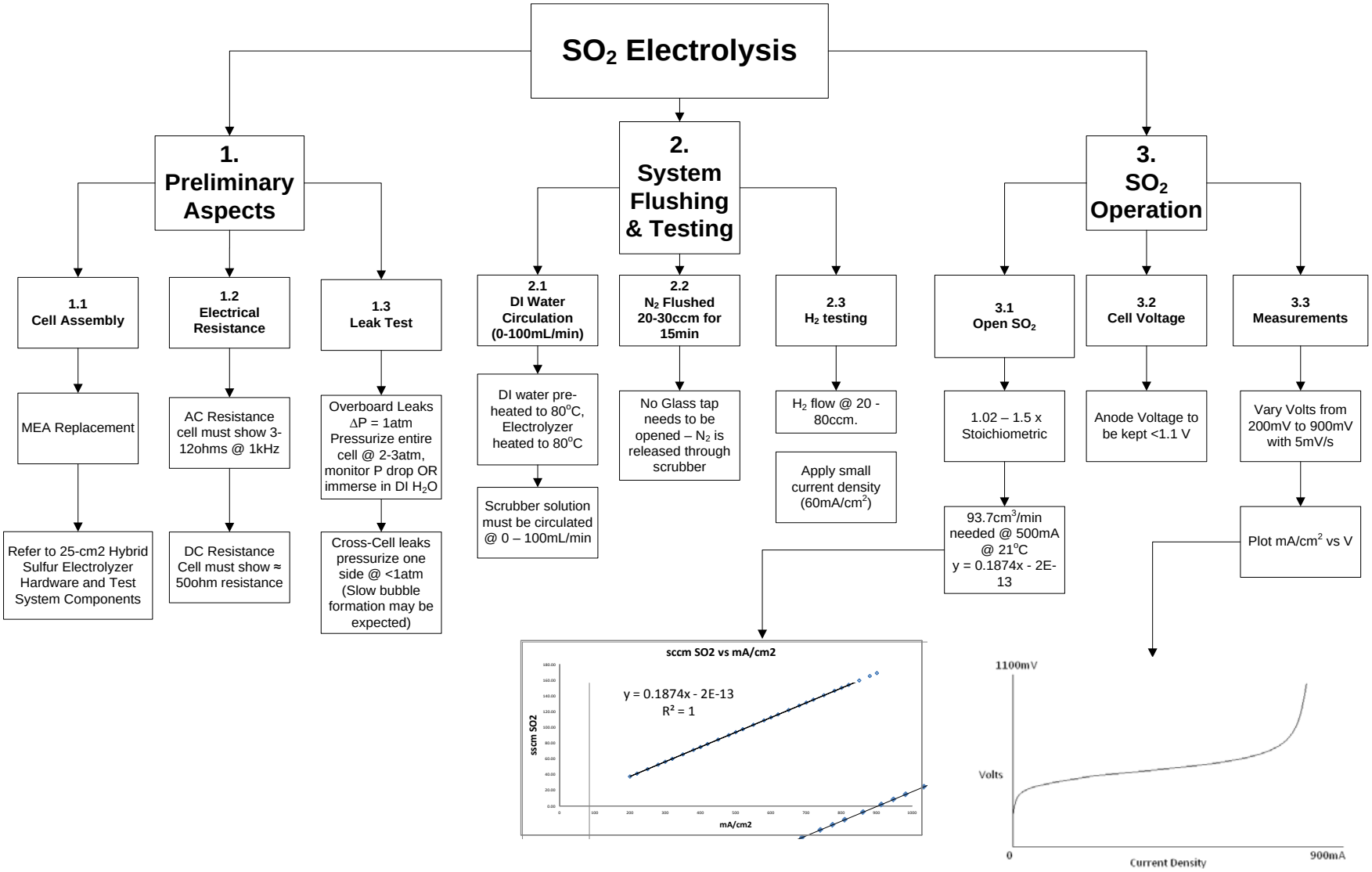

Figure B-2 : Operation cycle for SO_2 electrolysis